1-1-2015

The Role of AV integrins in Human Skin Tissue Homeostasis, Wound Healing and Squamous Cell Carcinoma

Elizabeth Kennedy Duperret
University of Pennsylvania, ekenne@mail.med.upenn.edu

The Role of AV integrins in Human Skin Tissue Homeostasis, Wound Healing and Squamous Cell Carcinoma

Abstract
Integrins play crucial roles in epithelial adhesion, proliferation, wound healing and cancer. In the epidermis, the roles of many integrin subunits are incompletely defined and mechanistic details regarding their functions are lacking. We performed a multiplexed shRNA screen to define roles for each subunit in human organotypic skin. This screen identified the integrin αv class of heterodimers as essential for generation of human skin tissue. We demonstrate that integrin αv loss drives a keratinocyte G1-S cell cycle checkpoint block. Surprisingly, αv integrins are not localized within keratinocyte focal adhesions and instead maintain proliferation by controlling c-myc translation through FAK, p38 and p90RSK signaling pathways. These phenotypes depend only on αv's binding partners β5 and β6, but not β1 or β8. Utilizing inducible genetic depletion of integrin αv, or blocking antibodies targeting αv heterodimers, we show that αv integrins are required for de novo tissue generation, but dispensable for epidermal maintenance. In an in vivo human xenograft skin model, we use blocking antibodies to show that integrin αv is required for epidermal proliferation during wound healing, but is dispensable for normal epidermal homeostasis.

In organotypic human neoplasias driven by Cdk4 R24C and oncogenic H-Ras G12V, we show that integrin αv is necessary for neoplastic tissue thickness and invasion through the basement membrane. This is dependent on expression of both binding partners β5 and β6. Blocking antibodies targeting αv heterodimers reduce tumor burden and proliferation in an inducible, orthotopic xenograft cutaneous squamous cell carcinoma tumor model. In conclusion, we demonstrate, for the first time, essential roles for αv integrins in human cutaneous wound re-epithelialization and tumorigenesis. We further determine a novel focal adhesion-independent signaling mechanism for αv's involvement in cell cycle progression.

Degree Type
Dissertation

Degree Name
Doctor of Philosophy (PhD)

Graduate Group
Cell & Molecular Biology

First Advisor
Todd W. Ridky

Keywords
C-myc, Focal Adhesion Kinase, Integrins, Signaling, Skin, Squamous Cell Carcinoma

Subject Categories
Cell Biology | Oncology

THE ROLE OF αv INTEGRINS IN HUMAN SKIN TISSUE HOMEOSTASIS, WOUND HEALING AND SQUAMOUS CELL CARCINOMA

Elizabeth K. Duperret

A DISSERTATION

in

Cell and Molecular Biology

Presented to the Faculties of the University of Pennsylvania

in

Partial Fulfillment of the Requirements for the

Degree of Doctor of Philosophy

2015

Supervisor of Dissertation

_____

Todd W. Ridky, M.D., Ph.D.

Assistant Professor of Dermatology

Graduate Group Chairperson

_____

Daniel S. Kessler, Ph.D.

Associate Professor of Cell and Developmental Biology

Dissertation Committee

M. Celeste Simon, Ph.D., Professor of Cell and Developmental Biology (Chair)

Richard K. Assoian, Ph.D., Professor of Pharmacology

John T. Seykora, M.D., Ph.D., Associate Professor of Dermatology

Andrei Thomas-Tikhonenko, Ph.D., Professor of Pathology and Laboratory Medicine

ACKNOWLEDGMENTS

First, I would like to thank my advisor Todd, who has constantly supported me and advocated for me. He is a whirlwind of energy and ideas, and has earned himself the nickname “Tornado Todd” among our lab members. Todd’s constant stream of energy, thoughtfulness and creativity has been highly motivating and has encouraged me to be a better scientist. I would like to thank all of the Ridky lab members, past and present, for their friendship and scientific support. Chris Natale, Christine Monteleon, Andrew McNeal and Seung Ja Oh have provided companionship and camaraderie, and have made the laboratory environment fun and enjoyable. I would also like to thank all of the undergraduate students who have worked in our lab throughout the years. Ankit, Kevin, Tanvir, Emily, Vihang, DJ and Jack have all brought energy and curiosity to the lab.

I am deeply grateful for the advice and guidance from my thesis committee members: Rick Assoian, Alan Diehl (former member), John Seykora, Celeste Simon and Andrei Thomas-Tikhonenko. They have provided valuable scientific insight and advice for furthering my career goals. I would also like to thank Brian Keith for giving me the opportunity to be a teaching assistant for his Cancer Biology course for two semesters, and for providing an excellent example of how to be an effective and approachable teacher.

I would like to thank Steve Prouty from the Dermatology department for processing all of my tissue samples and performing superb histological stains. I would like to thank Tzvete Dentchev from the Dermatology department for her impeccable job performing all of our immunohistochemistry. I would also like to thank Andrea Stout from the Cell and Developmental Biology Microscopy core for her training and assistance in confocal microscopy.

I am extremely grateful for funding support from the NIH/NIAMS Dermatology T32 training grant, an NIH/NCI NRSA F31 fellowship and the Patel Family Scholar Award. I acknowledge and greatly appreciate the help and support of the three CAMB coordinators: Kathy O’Connor-Cooley, Anna Kline, and Meagan Schofer. They have never left a single question of mine unanswered and work tirelessly to improve the CAMB graduate program.

I am very fortunate to have made strong friendships with many members of my CAMB cohort. I would like to thank all of these brilliant scientists for moral support, for encouraging one another to succeed and for making my time in graduate school so much fun!

Finally, I would like to thank my family for always pushing me to try my hardest and providing me with every opportunity for success. My brother, Chris Kennedy, and my parents, Tom and Diana Kennedy, have shown me how to be strong, resilient and independent. Most of all, I would like to thank my husband Jeff. His constant love and support over the last decade of my life have made it possible for me to pursue my PhD at Penn. I am incredibly proud of our journey together and I am forever grateful for his dedication and encouragement.

ABSTRACT

THE ROLE OF αv INTEGRINS IN HUMAN SKIN TISSUE HOMEOSTASIS, WOUND HEALING AND SQUAMOUS CELL CARCINOMA

Elizabeth K. Duperret

Todd W. Ridky

Integrins play crucial roles in epithelial adhesion, proliferation, wound healing and cancer. In the epidermis, the roles of many integrin subunits are incompletely defined and mechanistic details regarding their functions are lacking. We performed a multiplexed shRNA screen to define roles for each subunit in human organotypic skin. This screen identified the integrin αv class of heterodimers as essential for generation of human skin tissue. We demonstrate that integrin αv loss drives a keratinocyte G1-S cell cycle checkpoint block. Surprisingly, αv integrins are not localized within keratinocyte focal adhesions and instead maintain proliferation by controlling c-myc translation through FAK, p38 and p90RSK signaling pathways. These phenotypes depend only on αv's binding partners β5 and β6, but not β1 or β8. Utilizing inducible genetic depletion of integrin αv, or blocking antibodies targeting αv heterodimers, we show that αv integrins are required for de novo tissue generation, but dispensable for epidermal maintenance. In an *in vivo* human xenograft skin model, we use blocking antibodies to show that integrin αv is required for epidermal proliferation during wound healing, but is dispensable for normal epidermal homeostasis.

In organotypic human neoplasias driven by Cdk4 R24C and oncogenic H-Ras G12V, we show that integrin αv is necessary for neoplastic tissue thickness and invasion through the basement membrane. This is dependent on expression of both binding partners β5 and β6. Blocking antibodies targeting αv heterodimers reduce tumor burden and proliferation in an inducible, orthotopic xenograft cutaneous squamous cell carcinoma tumor model. In conclusion, we demonstrate, for the first time, essential roles for αv integrins in human cutaneous wound re-epithelialization and tumorigenesis. We further determine a novel focal adhesion-independent signaling mechanism for αv's involvement in cell cycle progression.

TABLE OF CONTENTS

LIST OF TABLES

LIST OF ILLUSTRATIONS

CHAPTER 1

Introduction: Integrins and focal adhesion proteins in skin and skin cancers

Parts of this chapter have been previously published in:

Duperret EK, Ridky TW. Focal adhesion complex proteins in epidermis and squamous cell carcinoma. *Cell Cycle*. 2013; Oct 15;12(20):3272-3285. Review.

Duperret EK, Dahal A, Ridky TW. Focal adhesion-independent integrin αv regulation of FAK and c-myc is necessary for 3D skin formation and tumor invasion. *J Cell Sci.* 2015; 128(21):3997-4013.

Duperret EK, Oh SJ, McNeal A, Prouty SM, Ridky TW. Activating FGFR3 mutations cause mild hyperplasia in human skin, but are insufficient to drive benign or malignant skin tumors. *Cell Cycle.* 2014;13(10):1551-1559.

Overview

The discovery of focal adhesions in the 1970's as highly conserved signal integrators that physically link the extracellular matrix (ECM) and the actin cytoskeleton suggested that these large protein complexes may be functionally necessary for tissue structure and the multicellularity of organisms (Hynes, 2004). Integrins, which function as αβ heterodimers, are catalytically inactive receptors within focal adhesions (FAs) that directly bind ECM ligands (such as Collagen, Fibronectin, and Vitronectin, among others) to initiate downstream signaling responses. There is a large number of integrin subunits (18 α subunits and 8 β subunits) and αβ heterodimers (24 total), all of which have some redundancy in ligand binding. Despite this, many individual integrin subunits are necessary for organismal viability (Bader et al., 1998; Fassler and Meyer, 1995; Gurtner et al., 1995; Stephens et al., 1995; Zhu et al., 2002). Relevant mouse models have

revealed that certain integrin subunits or focal adhesion proteins are necessary for embryonic development, while others are required only for development and homeostasis of certain tissue types. This is very apparent in skin, where loss of specific FA proteins can lead to defects in adhesion, wound healing and proliferation.

In pathological conditions such as squamous cell carcinoma, micro-environmental changes cause disorganization of the epidermis, degradation of the basement membrane, overexpression of specific integrin subunits and altered secretion and cleavage of ECM components. These micro-environmental changes lead to altered focal adhesion formation and downstream signaling, which has been shown to enhance the ability of tumor cells to proliferate, invade and metastasize. Functional studies defining the roles of specific focal adhesion complex proteins in both normal and tumor tissues has led to a better understanding of how individual members of these complexes can be targeted therapeutically.

Structure and organization of the skin

Similar to nearly every epithelial tissue in the body, the skin contains a stratified tissue layer lined with an extracellular matrix-rich basement membrane zone, and an underlying layer of dermis, immune cell infiltrates, fat and connective tissue (Watt and Fujiwara, 2011). Unlike many other tissues in the body, however, the epidermal portion of the skin is exposed to air and the environment, and thus comes in contact with heat, infectious agents, microbes, chemical carcinogens, ultraviolet radiation and physical abrasion. Thus, the epidermis of the skin must provide 1) a protective barrier to prevent excessive water loss and infection, 2) protection against UV- and chemical-induced carcinogenesis, and 3) a mechanism for rapid tissue regeneration upon injury. In addition to the inter-follicular epidermis, the epidermis contains several specialized appendages, including hair follicles, sweat glands and sebaceous glands. Unlike most other mammals, human skin consists primarily of inter-follicular epidermis, with thickness ranging from 0.05mm (on the eyelids) to 1.5mm (on the palms and soles). This is in contrast to mice, which have vastly more hair follicles, and much thinner, less protective epidermis that is <0.025mm

(only 2-3 cell layers) thick (Khavari, 2006). For this dissertation, I will focus specifically on the inter-follicular epidermis.

The human inter-follicular epidermis consists of several layers of keratinocytes (the epithelial cells of the skin). All of these cells contain fibrous structural intermediate filaments called keratins. The basal layer is a one-cell thick layer that lines the basement membrane and is highly proliferative (Blanpain and Fuchs, 2009). This layer is thought to contain inter-follicular epidermal stem cells, though the exact properties of these stem cells are highly contested (Fuchs, 2008; Hsu et al., 2014; Watt and Fujiwara, 2011). Melanocytes, pigment-producing cells of the epidermis, are interspersed throughout the basal layer at a ratio of approximately 1:5 (melanocyte:keratinocyte). Melanocytes produce pigment and transfer pigment to keratinocytes for protection against UV-induced carcinogenesis. Basal epidermal keratinocytes differentiate into the spinous layer. Spinous layer cells lose their proliferative capacity, and begin to express differentiation markers such as Keratin10, Keratin1 and Involucrin (Fuchs, 2008; Lopez-Pajares et al., 2012). Langerhans cells, specialized dendritic cells, are located within the spinous layer to help fight infection. In the granular layer, the keratinocytes undergo enucleation and contain cytoplasmic granules that hold keratin filaments together. Lamellar bodies, secretory organelles that release impermeable lipids via exocytosis, begin to form in the spinous and granular layers. The final stage of differentiation is in the formation of the stratum corneum at the skin surface (Fuchs, 2008). In the stratum corneum, keratinocytes are converted into a non-living, cornified keratin-rich layer which provides most of the protective barrier function of the skin (Fuchs, 2008).

In response to injury, human wounds heal through three major processes: re-epithelialization, deposition of granulation tissue (connective tissue) and contraction (Grinnell, 1994; Singer and Clark, 1999). Upon injury, fibroblasts migrate into the wound space and begin to proliferate and secrete extracellular matrix proteins such as Fibronectin, Vitronectin and Collagen—termed granulation tissue (Arwert et al., 2012; Schäfer and Werner, 2008; Singer and Clark, 1999). Angiogenesis into the granulation tissue occurs, and leukocytes migrate rapidly to the wound site to prevent infection (Shaw and Martin, 2009; Singer and Clark, 1999). Then,

epidermal keratinocytes migrate over the granulation tissue and proliferate to form full-thickness epidermis (Arwert et al., 2012; Singer and Clark, 1999). Both keratinocytes and fibroblasts synthesize key extracellular matrix components to re-form the basement membrane beneath the wound. Some contraction does occur during human wound healing, primarily due to pulling of fibroblasts on the extracellular matrix, which typically results in excess Collagen deposition and scarring (Penn et al., 2012; Shaw and Martin, 2009; Werner and Grose, 2003). Contraction and scarring are not essential for wound healing in humans, since scarless fetal wounds are observed (Penn et al., 2012). Disruption of any of the major phases of wound healing—re-epithelialization, granulation tissue formation, or contraction—can lead to complications such as chronic wounds or pathological scarring.

Squamous Cell Carcinoma (SCC): Current Therapy

Cutaneous squamous cell carcinoma (cSCC) is a generally under-appreciated public health concern, as non-melanoma skin malignancies cases are typically excluded from national cancer registries. The incidence of cSCC in the US is now estimated to be over 700,000 new cases/year, with a 4-12.5% risk of metastasis (Brantsch et al., 2008; Cherpelis et al., 2002; Rogers et al., 2010). Although this metastasis risk is lower than many other malignancies, the large burden of disease is such that in most regions of the U.S., total deaths due to cSCC may be as common as those from melanoma (Karia et al., 2013). While surgical excision is very effective treatment for local tumors, therapeutic options for disseminated disease are limited with few proven effective treatments. Clinical treatment regimens based on traditional chemotherapeutic agents including cisplatin, bleomycin, doxorubicin and fluoropyrimidines, radiation therapy, or newer targeted biologics including EGFR or general tyrosine kinases inhibitors do not result in long-term remissions in most cases (Cranmer et al., 2010; Maubec et al., 2011; Preneau et al., 2014). New therapeutic agents are needed to improve treatment outcomes for unresectable cSCC.

cSCC is primarily the consequence of chronic UV photodamage resulting in loss of p53 function, followed by activation of EGFR and its downstream pathways including Ras MAPK, PI3K/Akt, PLCγ/PKC, and Src kinases (Ratushny et al., 2012). Oncogenic signaling through these pathways in skin, as well as other epithelial tissues, is frequently associated with upregulation of integrin proteins. As activation of effector cascades initiating at integrin-containing focal adhesions appears to be necessary for the full malignant potential of some epithelial tumors, targeting integrins at the relatively accessible plasma membrane is an attractive option that may have clinical utility (Reuter et al., 2009).

Models for studying wound healing and squamous cell carcinoma

Historically, skin tissue homeostasis, wound healing and tumorigenesis have been studied primarily using *in vivo* mouse models. Important considerations for the study of wound healing in a laboratory setting are key differences between mouse and human wound healing. Mice have an additional muscle layer beneath the dermis called the panniculosus carnosus, which contributes significantly to the process of wound contraction, yet is not found in human skin (with the exception of certain portions of the head and neck region) (Wong et al., 2011). Rodents also have much looser skin, which results in rapid wound contraction with basically no residual scarring (Wong et al., 2011). This rapid wound contraction in murine models leads to little re-epithelialization, and thus contributions of epidermal keratinocytes to wound healing are difficult to study in these models. To prevent this rapid wound contraction, many groups have adopted a wound split protocol, in which the mouse skin is held in place during the course of wound healing (Galiano et al., 2004; Wang et al., 2013). Another approach is to graft human skin onto immunocompromised mice, and then wound the human skin tissue. This has been shown to significantly reduce the amount of contraction in the wound and re-capitulate the key features of human skin wounding *in vivo* (Escámez et al., 2004; Truong et al., 2005).

Chemical carcinogenesis protocols have been used for over 60 years for the study of cutaneous squamous cell carcinomas in mice. In a traditional protocol there are two stages: the

application of a chemical carcinogen, such as DMBA (7,12-Dimethylbenz(a)anthracene), which is known to cause activating mutations in the proto-oncogene H-Ras, followed by treatment with a tumor promoter such as TPA (12-O-tetradecanoylphorbol-13-acetate), which has a mitogenic function to accelerate tumor formation (Abel et al., 2009). Results from this model vary greatly with the mouse strain, which can impact the rate at which tumors form and the malignant potential of individual tumors (Abel et al., 2009). High levels of UVB exposure, over long periods of time, can also induce Squamous Cell Carcinoma formation in hairless mice (Tang et al., 2007). Transgenic mouse models driving expression of Src, Fyn, MEK-1, H-Ras G12V and ErbB2 in the epidermis develop cutaneous SCCs (Ratushny et al., 2012). While all of these mouse models for SCC formation provide an elegant way to study tumor progression in an *in vivo* setting, there are of course drawbacks. Transgenic models take a long time to develop, which makes it difficult to functionally interrogate signaling pathways that are deregulated during tumor progression. Additionally, there are key differences between mouse and human skin, as reviewed earlier in this chapter, which may result in differences between mouse and human tumorigenesis.

Additional models for studying human cSCC tumors *in vivo* include the use of human tumor cell lines, which can be injected subcutaneously and develop tumors rapidly (Ratushny et al., 2012). In this model, immunocompromised mice must be used, and thus the contribution of the immune system cannot be studied. Gene expression can be manipulated in 2D culture using lentiviruses to study functional roles for genes within the tumor cells. However, subcutaneous tumors do not reflect the proper tissue microenvironment and are not lined with basement membrane.

In our laboratory we have elected to utilize genetically engineered human skin xenografts for studying skin and skin cancers (Duperret et al., 2014; Duperret et al., 2015; Lazarov et al., 2002; Ridky et al., 2010). As a matrix scaffold we utilize intact human dermis containing a native, fully functional basement membrane. We isolate primary human keratinocytes, melanocytes and fibroblasts from human foreskins, culture these cells on plastic to manipulate gene expression, and then seed the cells onto a dermal matrix that is supported at the air-liquid interface using

metal support stands (Figure 1.1A). After only 2 weeks in culture, this tissue exhibits complete stratification and differentiation to form 3D skin in vitro (Figure 1.1C). This 3D skin contains proper expression of the differentiation marker Keratin10 in the suprabasal layers, and the proliferation marker Ki67 in basal epidermal cells (Figure 1.1C). We can incorporate melanocytes at the basement membrane to form pigmented skin, and can graft this skin onto immunocompromised mice (Figure 1.1B). We have the ability to transduce these keratinocytes with a physiologically relevant set of oncogenes—Cdk4 (R24C, resistant to cyclin dependent kinase inhibitors), dominant-negative p53 (dnp53, R248W) and oncogenic H-Ras (G12V)—to form squamous cell carcinoma *in vivo* (Figure 1.2). This SCC displays high levels of proliferation and ERK1/2 phosphorylation (Figure 1.2). This is an ideal model for studying integrin signaling, because it contains a physiologically relevant human extracellular matrix and basement membrane zone.

Focal adhesion structure and dynamics

Integrins are delivered to the cellular membrane as inactive, bent heterodimers. These heterodimers are initially partially activated through binding of cytoplasmic proteins (primarily Talin and Kindlin) to the intracellular integrin tails (“inside-out” signaling). Subsequent binding to extracellular matrix ligands (“outside-in” signaling), further extends the heterodimer and generates the fully-active receptor. These integrin receptors lack intrinsic catalytic activity, and execute their signaling and structural roles through recruitment of other proteins to adhesion complexes at the plasma membrane (Figure 1.3). Many of these focal adhesion proteins directly link integrins to the Actin cytoskeleton, thus allowing cells to directly sense their environment and exert forces that result in activation of signaling pathways—a process termed mechanotransduction.

Adhesion formation typically occurs at the leading edge of the cell, within the lamellipodium. Nascent adhesions are immobile and transient, and typically consist of Talin, Vinculin, FAK (Focal Adhesion Kinase) and p130CAS (CRK-associated substrate), among many others (Lo, 2006). Nascent adhesion formation is dependent on the Actin cytoskeleton, and maturation of nascent adhesions into mature adhesions is a Myosin II-dependent process

(Vicente-Manzanares and Horwitz, 2011; Zamir and Geiger, 2001). The process of adhesion maturation is dependent on the motility of the cells: more Actin cytoskeleton turnover leads to faster adhesion turnover and less adhesion maturation (Vicente-Manzanares and Horwitz, 2011; Zamir and Geiger, 2001). Mature adhesions are pulled towards the center/trailing edge of the cell, and form more stable interactions with bundled Actin filaments. These mature focal adhesions have a much longer half-life and are larger and more elongated (Vicente-Manzanares and Horwitz, 2011; Zamir and Geiger, 2001).

To date, mass spectrometry approaches have identified hundreds of proteins associated with focal adhesions (Byron et al., 2012; Humphries et al., 2009; Schiller et al., 2013). While many of these specific proteins are certainly integrin heterodimer, cell type and environment dependent, a putative core set of focal adhesion proteins has been identified across all cellular contexts (Humphries et al., 2009). This core set of adhesion proteins include structural proteins (α-Actinin, Parvin, Talin, Tensin, VASP, Vinculin, and Kindlin), kinases (FAK and Src) and adapters (p130Cas, Migfilin, Paxillin, PINCH and Zyxin) (Humphries et al., 2015; Kanchanawong et al., 2010). High resolution microscopy techniques have demonstrated that these proteins are organized in specialized layers: a membrane-proximal layer containing integrin tails, FAK and Paxillin, an intermediate layer containing Vinculin and Talin, and a membrane-distal layer that directly connects the adhesion to the actin cytoskeleton through Zyxin, VASP and α-Actinin (Kanchanawong et al., 2010). Because of the enormity of potential interactions within these complex adhesion structures, there is still active research ongoing to define 1) which specific adhesion components are required for adhesion formation and maturation, 2) which adhesion components are required for physiologic processes, including in vitro cellular phenotypes and *in vivo* morphologic processes, and 3) the role for focal adhesion proteins or focal adhesions in 3D tissues. It is recently becoming clear that focal adhesions have drastically different architecture in 3D environments; however, many focal adhesion proteins appear to maintain their 2D functions despite this different organization (Fraley et al., 2010).

Biological processes and signaling pathways regulated by integrins

The primary function of integrin adhesions is to promote cellular proliferation, adhesion, survival and migration. Many of the major biological processes regulated by integrins and focal adhesions are thought to be due to the action of the major kinases within these adhesions—FAK and Src—and their interactions with focal adhesion adaptor proteins (Moreno-Layseca and Streuli, 2014; Schwartz and Assoian, 2001).

FAK can directly bind to the p85 subunit of PI3K, thus initiating a PI3K-Akt downstream signaling pathway which blocks the action of several cyclin dependent kinase inhibitors and pro-apoptotic proteins (Reiske et al., 1999). This pathway ultimately leads to Skp2-dependent p27 degradation and down-regulation of p21 (Shanmugasundaram et al., 2013). FAK can also stimulate Ras-ERK signaling to promote Cyclin D1 transcription (Zhao et al., 2001). A FAK/Src/p130CAS complex is able to recruit Rac1 to the membrane to stimulate JNK signaling and subsequent cell cycle progression (Oktay et al., 1999). FAK also influences a major cell cycle checkpoint, p53, by binding to p53 or facilitating its degradation, to suppress its apoptotic and transcriptional activities (Golubovskaya et al., 2005; Lim et al., 2008). In addition to stimulation of FAK activity, integrins can also directly complex with growth factor receptors (such as EGFR and PDGFR) and mediate their activity to directly enhance PI3K and MAPK signaling pathways (Bill et al., 2004).

FAK, along with Paxillin, directly binds to GEFs and GAPs that control small GTPase activation (specifically, Rac activation) to ultimately promote cellular migration (Provenzano and Keely, 2011). Src binding to FAK through its SH2 domain is absolutely essential for cell migration (Yeo et al., 2006). The FAK-Src complex promotes both focal adhesion assembly and disassembly, and thus more rapid cell migration, through 1) phosphorylation of α-Actinin, to reduce crosslinking of stress fibers and release of these fibers from focal adhesions, 2) phosphorylation of N-WASP to promote Arp2/3-mediated Actin polymerization, and 3) phosphorylation of p190RhoGEF to promote stress fiber formation (Mitra et al., 2005). While FAK and Src play the major enzymatic roles in promoting these signaling pathways and cellular

phenotypes, other adaptor and structural focal adhesion proteins are key in coordinating the recruitment of major signaling players to these signaling hubs at the membrane.

Hemidesmosomes in skin

Integrin heterodimers are key components of two distinct types of adhesion complexes: FA complexes, which link the Actin cytoskeleton to the ECM, and hemidesmosomes, which structurally link intermediate filaments to the ECM. Through these complexes, integrin receptors play both a structural role mediating physical attachment of epithelial cells to underlying basement membrane, and also a signaling role promoting cellular proliferation and migration.

Hemidesmosomes play major structural role in the epidermis, but have also been shown to activate several intracellular signaling pathways, including Rac1, RhoA and Akt signaling (Marinkovich, 2007). Unlike focal adhesions, hemidesmosomes are not frequently recycled, and therefore serve to maintain keratinocyte anchorage to the basement membrane. Loss of the only hemidesmosomal integrin heterodimer, α6β4, leads to severe epidermal adhesion defects (Dowling et al., 1996; Georges-Labouesse et al., 1996). Integrin α6β4 and its ligand, Laminin-332, are also both required for squamous cell carcinoma formation in relevant epidermal *in vivo* models (Dajee et al., 2003). Because of the frequently severe skin blistering seen in patients lacking a number of different extracellular and intracellular hemidesmosomal proteins, targeting hemidesmosomal components was initially not considered to be a viable therapeutic strategy. However, it was later discovered that a specific domain of Laminin-332, G45, is present only in tumor tissue, and promotes tumor formation and progression (Tran et al., 2008). Blocking antibodies against G45 were shown in a pre-clinical model to be effective against SCC tumor formation through blockade of PI3K and ERK signaling, but to have no effect on normal skin homeostasis (Tran et al., 2008). This is one of the few examples of targeting specific ECM ligands for cancer therapy, but highlights the need for a deeper understanding of how the role of adhesion signaling and specific ECM ligands differ between various homeostatic and pathologic states.

Focal adhesion integrins in skin

Much effort has been focused on defining roles for individual integrin subunits in epidermal homeostasis. As integrin signaling requires an intact, structurally correct basement membrane zone lacking in traditional tissue culture, much of this work has employed mouse genetic models. Efforts have been made to generate knockout mice or conditional knockout mice for each of the 26 integrin subunits. Out of these 26 subunits, 18 are expressed at a detectable level in human or mouse skin, while the others are leukocyte-specific. Knockout mice have been generated for all of these 18 subunits, but many of these mice experience embryonic lethality and the skin specific null phenotypes have not been determined for some subunits (Table 1.1). Regardless, the available knockout mice have provided valuable insight into the roles of integrins in epidermal proliferation, hair follicle formation and turnover, wound healing and susceptibility to Squamous Cell Carcinoma (Janes and Watt, 2006; Margadant et al., 2010). In the next section, I provide a brief overview of these phenotypes.

β1 integrin and its phosphorylation

Severe phenotypes are seen in β1-null mouse skin. Loss of β1 during development leads to severe epidermal defects, including skin blistering and hair loss (Brakebusch et al., 2000; Raghavan et al., 2000). There are differences in these phenotypes depending on the promoter used for Cre-mediated recombination. K5-Cre induced β1 deletion leads to differentiation defects, skin thickening and mouse death at approximately 6 weeks after birth, potentially due to hypoproliferation in the esophagus (Brakebusch et al., 2000). K14-Cre induced β1 deletion results in normal differentiation, but significant epidermal hypoproliferation, and perinatal death within days after birth (Raghavan et al., 2000). Despite these severe developmental defects, β1 loss in adult mouse skin has no apparent deleterious phenotype (López-Rovira et al., 2005; Reuter et al., 2009). Using gene expression profiling and network topology analysis, integrin β1 was identified as a key oncogenic hub in a human skin graft model of squamous cell carcinoma (Reuter et al., 2009). Subsequently, antibody-mediated blockade of integrin β1 both prevented

tumor formation and slowed tumor progression, with no deleterious effects on normal human skin tissue or overall mouse health (Figure 1.3B) (Reuter et al., 2009).

Binding of Talin to β1 cytoplasmic tails disrupts a salt bridge between the α and β cytoplasmic tails, helping to separate the tails and enhance integrin binding affinity to ECM ligands. This is thought to be the first step in “inside-out” integrin activation. With subsequent integrin activation and clustering, Src phosphorylation of β1 tyrosines in the cytoplasmic NPxY motifs is thought to reduce binding of the adaptor proteins Talin and Kindlin (Anthis et al., 2009). This is consistent with the rounded morphology and loss of adhesion seen in v-Src transformed cells, which have high levels of β1 tyrosine phosphorylation (Sakai et al., 2001). In addition, focal adhesion kinase (FAK), which plays a role in promoting oncogenic transformation, is activated in response to β1 integrin phosphorylation (Figure 1.3) (Wennerberg and Armulik, 2000).

Complicating this understanding determined largely from cell culture systems are *in vivo* studies suggesting that the tyrosine residue itself, and not its phosphorylation, is most important for β1 function (Chen et al., 2006). Mutation of tyrosine to alanine in either the membrane proximal NPxY motif (Y783, Talin binding motif) or the membrane distal NPxY motif (Y795, Kindlin binding motif) results in embryonic lethality (Czuchra et al., 2006). However, mutation of either of these residues to phenylalanines, which contains the aromatic ring but is unable to be phosphorylated, results in viable, fertile mice with no apparent abnormalities (Chen et al., 2006; Czuchra et al., 2006).

Mice with keratinocyte-restricted expression of both Y783A and Y795A (YY/AA) using the K5-Cre promoter phenocopy mice with keratinocyte-restricted deletion of β1 (Czuchra et al., 2006). These mice experience impaired hair follicle morphogenesis, abnormal skin pigmentation, skin blistering and thickened epidermis (Czuchra et al., 2006). *In vitro*, keratinocytes with the YY/AA mutation have no β1 integrin activation, and decreased expression of other integrin subunits, including β4, α6 and α2 (Czuchra et al., 2006). Mice with keratinocyte-restricted expression of either Y783A or Y795A have much less severe epidermal defects (Meves et al., 2013). These individual mutations lead to patchy hair loss, but normal proliferation, epidermal

adhesion and hemidesmosome localization (Meves et al., 2013). *In vitro*, keratinocytes containing the Y783A mutation experience adhesion and spreading defects, and rapid terminal differentiation, implying that binding of Talin to β1 inhibits keratinocyte differentiation (Meves et al., 2013). Mice containing both Y783F and Y795F mutations (YY/FF mice) develop normally and have normal skin (Meves et al., 2011). However, these mice are less susceptible to DMBA-TPA induced skin tumorigenesis (Meves et al., 2011). Mutation of each residue alone does not have any effect on susceptibility to tumor formation (Meves et al., 2011). Although Talin1, Talin2, Kindlin1 and Kindlin2 preferentially bind to wild-type β1 over YY/FF β1 in vitro, binding to the mutants is only reduced by approximately 50% (Meves et al., 2011). This indicates that the YY/FF mouse may have hypomorphic β1 activity, which is sufficient to block tumor formation but not to affect normal skin homeostasis.

Integrin β1 binds to α1, α2, α3, α4, α5, α6, α7, α8, α9, α10, α11 and αv. Integrin β1 heterodimers bind to Laminin (α1β1, α2β1, α3β1, α6β1, α7β1, α10β1), Collagen (α1β1, α2β1, α10β1, α11β1), Thrombospondin (α2β1, α3β1, α4β1), Fibronectin (α4β1, α5β1, α8β1, αvβ1, αvβ3), Osteopontin (α4β1, α5β1, α8β1, α9β1, αvβ1), Tenascin (α8β1, α9β1), VCAM-1 (α4β1, α9β1), LAP-TGFβ (αvβ1) or Vitronectin (α8β1) (Humphries et al., 2006). As summarized in Table1.1, integrin α1, α2, α7, α10 and α11 knockout mice are viable and fertile, with no apparent epidermal defects and no skin-specific knockout mice exist (Bengtsson et al., 2005; Chen et al., 2002; Gardner et al., 1996; Mayer et al., 1997; Popova et al., 2007; Werner et al., 2000). Integrin α4, α5 and α8 knockout mice die in utero or immediately after birth, and no skin-specific knockout mice exist (Gurtner et al., 1995; Müller et al., 1997; Yang et al., 1993).

Integrin α3-null mice exhibit skin blistering and basement membrane disorganization, as well as kidney and lung defects that lead to lethality shortly after birth (Kreidberg et al., 1996). Mice with epidermis-specific ablation of integrin α3 exhibit the same skin blistering defect and additional hair follicle and wound healing abnormalities (Conti et al., 2003; DiPersio et al., 2000; Margadant et al., 2009). Previously, human skin disease had not been associated with mutations in integrin α3, or any other FA integrin. Recently, however, homozygous mutations in the integrin

α3 gene were described in three patients with skin blistering disease (Has et al., 2012). These three mutations are different, but are all predicted to lead to loss of integrin α3 function (Has et al., 2012). All three of these patients died within 2 years of birth due to infection or multi-organ failure associated with reduced kidney and lung barrier function, similar to the phenotype seen in integrin α3-null mice (Has et al., 2012; Kreidberg et al., 1996). It was also recently shown that mice with a skin-specific deletion of integrin α3 have significantly reduced susceptibility to tumor formation upon DMBA-TPA treatment (Sachs et al., 2012). The authors show that this reduced susceptibility to tumor development is the result of increased epidermal turnover seen in mouse epidermis lacking α3, leading to increased differentiation and shedding of the cells that accumulate mutations upon carcinogen treatment (Sachs et al., 2012). Despite this reduced tumor formation, the Squamous Cell Carcinomas that do form in mouse skin lacking α3 show reduced differentiation, an indication of increased malignancy, suggesting that integrin α3 plays dual roles in tumor formation and progression (Sachs et al., 2012).

Several other β1-binding integrins are utilized in specific epidermal contexts. For instance, integrin α9 plays a crucial role in enhancing keratinocyte migration and proliferation during wound healing (Singh et al., 2009). Integrin α2 was shown to play a key role in HPV-driven SCC tumorigenesis and metastasis (Tran et al., 2011). K14-HPV16/ITGA2$^{-/-}$ mice had reduced lymph node metastases in comparison to K14-HPV16/ITGA2$^{+/+}$ mice (Tran et al., 2011). In addition, SCC cell lines developed from tumors in the K14-HPV16/ITGA2$^{-/-}$ mice had reduced tumor growth and increased tumor latency compared to SCC lines derived from K14-HPV16/ITGA2$^{+/+}$ mice (Tran et al., 2011). While it remains to be seen whether this metastasis phenotype is microenvironment-dependent, this study indicates that targeting integrin α2 may be a viable therapeutic target for HPV-driven SCC.

αv integrins

αv integrin binds to β1, β3, β5, β6 and β8. None of these integrin heterodimers bind to Collagen and Laminin, but instead bind to ligands with RGD binding motifs, such as Fibronectin

(αvβ1, αvβ3, αvβ6), Vitronectin (αvβ3, αvβ5), Osteopontin (αvβ1, αvβ3, αvβ5, αvβ6), LAP-TGFβ (αvβ1, αvβ3, αvβ6, αvβ8), Thrombospondin (αvβ3) and von Willebrand Factor (αvβ3) (Humphries et al., 2006). Most αv knockout mice die in utero due to placental defects, but approximately 20% are born and die shortly after birth, likely due to hemorrhage (Bader et al., 1998). Notably, β3, β5 and β6 knockout mice are viable and fertile, and thus the embryonic lethality of the αv knockout mice is likely due to the action of either αvβ1 or αvβ8 (Huang et al., 1996; Huang et al., 2000a; Reynolds et al., 2005; Zhu et al., 2002).

It has long been recognized that αv integrins are up-regulated during wound healing in humans; however, wound healing has not been examined in the skin-conditional αv knockout mouse (Cavani et al., 1993; Clark et al., 1996; Savar et al., 2014). β3 knockout mice display accelerated wound healing; however, as shown in later chapters, β3 is not expressed in epidermal keratinocytes and thus this phenotype is likely due to altered signaling within stromal fibroblasts (Reynolds et al., 2005). Young integrin β6 null mice show no defects in wound healing; however, aged β6 null mice show delayed wound healing compared to age-matched controls (AlDahlawi et al., 2006; Huang et al., 1996). In contrast, constitutive expression of integrin β6 in the epidermis leads to formation of chronic wounds (Häkkinen et al., 2004). Integrin β5 null mice show no difference in the rate of cutaneous wound healing, though this was not tested in aged mice (Huang et al., 2000a). The epidermal contribution to these phenotypes is unclear since β5 and β6 have not been ablated specifically in mouse skin.

αv integrins have been suggested to play both tumor-promoting and tumor-suppressive roles in epithelial tissues. In mouse skin, αv deletion cooperates with p53 loss to transiently promote initial SCC formation, but ultimately results in decreased tumor growth (Savar et al., 2014). Integrin αv knockout in the mouse eyelids and conjunctiva also seems to promote SCC formation (McCarty et al., 2008). Integrin β6 has a growth-suppressive role in the mouse skin and hair follicles, since skin and hair follicles lacking β6 are thicker with more Ki67+ cells (Xie et al., 2012). However, in humans, αvβ6 overexpression correlates with decreased survival in human cervical SCC, αvβ6 is over-expressed in epidermal squamous cell carcinoma, and αvβ6 promotes

invasion in human oral SCC cell lines (Hazelbag et al., 2007; Nystrom et al., 2006; Reuter et al., 2009). These conflicting data could reflect inherent differences between mouse and human skin.

TGFβ signaling in wound healing and tumorigenesis

The transforming growth factor β (TGFβ) isoforms—TGFβ1, TGFβ2, and TGFβ3—are secreted cytokines that bind to a heterodimers of TGFβRI and TGFβRII, which form serine/threonine kinase receptors. Ligand binding leads to phosphorylation of both Smad2 and Smad3, which then bind to Smad4 to form transcription factor complexes that translocate to the nucleus to control gene expression. TGFβ signaling is known to promote the expression of cyclin dependent kinase inhibitors p21 and p15, and suppress the expression of pro-proliferation protein c-myc (Gordon and Blobe, 2008; Massagué, 2008). TGFβ also promotes the acquisition of motile, mesenchymal traits through up-regulation of Snail and Slug transcription factors (Gordon and Blobe, 2008; Massagué, 2008).

After synthesis, the TGFβ dimer interacts with a Latency Associated Peptide (LAP) and a Latent TGF-β binding protein (LTBP) in the extracellular matrix (Annes et al., 2003). TGFβ must be released from this complex in order to have biologic activity (Annes et al., 2003). TGFβ release can be mediated directly or indirectly by integrin heterodimers (Annes et al., 2003). Specifically, αv integrins have a well-established role in activating latent TGFβ through force-dependent or MMP-dependent mechanisms (Mamuya and Duncan, 2013). Furthermore, several integrin genes are direct transcriptional targets of TGFβ-Smad signaling. Thus, the integrin-TGFβ interaction serves as a feed-forward mechanism to potentiate the signaling pathway effects.

TGFβ's role in promoting granulation tissue formation during wound healing is well-appreciated (Desmoulière et al., 1993; Penn et al., 2012). TGFβ stimulates migration of fibroblasts and endothelial cells into the wound tissue and promotes deposition of ECM proteins. However, the role of TGFβ signaling in re-epithelialization of wound keratinocytes is controversial. Re-epithelialization is inhibited in mice that overexpress TGFβ1 in basal keratinocytes, and is accelerated in mice that lack TGFβRII in keratinocytes or lack Smad2 or Smad3 in the whole

mouse, suggesting that TGFβ signaling delays wound re-epithelialization (Amendt et al., 2002; Ashcroft et al., 1999; Chan et al., 2002; Falanga et al., 2004; Guasch et al., 2007; Werner and Grose, 2003). However, TGFβ signaling promotes expression of ECM proteins and integrins. Additionally, integrins that are known to activate latent TGFβ, such as the αv integrins, are over-expressed at the wound edge (Cavani et al., 1993; Clark et al., 1996). Furthermore, previous efforts have linked TGFβ signaling to Focal Adhesion Kinase (FAK) activity and/or FAK protein expression through a variety of different mechanisms (Cicchini et al., 2008; Kracklauer et al., 2003; Thannickal et al., 2003; Wang et al., 2004; Wendt and Schiemann, 2009). FAK is essential for keratinocyte survival, proliferation and migration (Essayem et al., 2006; Mitra et al., 2005; Sulzmaier et al., 2014). Thus, the effects of TGFβ on re-epithelialization may be dose-dependent and highly localized.

Due to its pleiotropic signaling effects, TGFβ has a dual role in cancer progression: it is thought to both inhibit cell proliferation, yet promote the epithelial-mesenchymal transition and tumor metastasis. The anti-proliferative effects of TGFβ signaling are evident in the skin, where disruption of TGFβ signaling elements results in higher susceptibility to malignant skin cancer (Bornstein et al., 2009; Cui et al., 1996; Glick, 2012; Glick et al., 1994; Go et al., 2000; Guasch et al., 2007; Mordasky Markell et al., 2010; Wang et al., 1997). However, this may be highly dependent on the dose of TGFβ signaling, since reduction in TGFβ1 expression leads to reduced papilloma formation in mouse skin (Glick, 2012; Pérez-Lorenzo et al., 2010). Despite this, loss-of-function mutations in TGFβ signaling pathway elements, such as Smad2/3/4, or TGFβRII, are commonly found over the course of tumor progression (Bellam and Pasche, 2010; Glick, 2012; Logullo et al., 2003; Markowitz et al., 1995; Xie et al., 2003). In the absence of Smads, TGFβ can initiate non-canonical signaling pathways, including ERK1/2 activation, JNK/p38 activation, PI3K/Akt activation and Rho GTPase activation, which can all contribute to tumor progression (Zhang, 2009). The contribution of non-canonical TGFβ signaling to tumor progression remains unclear.

Focal Adhesion Kinase in skin

Focal Adhesion Kinase (FAK) in normal skin

Focal Adhesion Kinase (FAK) has been shown to be both a signaling kinase and an adaptor protein that helps link integrin adhesion complexes to the Actin cytoskeleton (Mitra et al., 2005; Parsons, 2003). While FAK is only indirectly associated with β integrin cytoplasmic domains through binding to Paxillin and Talin, it is rapidly recruited to focal adhesions and auto-phosphorylated upon cellular adhesion to ECM proteins (Figure 1.3). This auto-phosphorylation can lead to recruitment and activation of a variety of downstream signaling proteins (Mitra et al., 2005; Parsons, 2003).

FAK is required for mouse development, since FAK-null mice die during embryogenesis at about E8.5, with mesodermal defects (Furuta et al., 1995a; Furuta et al., 1995b). This phenotype is highly similar to the phenotype of the Fibronectin knockout mouse, which also shows specific defects in mesoderm development (George et al., 1993). This suggests that FAK is essential for focal adhesions involving the Fibronectin-binding integrins, including: α4β1, α5β1, αIIbβ3, αvβ3, αvβ6, and αvβ8. Autophosphorylation is required for FAK function in vitro; however, mice lacking the autophosphorylation site of FAK have a slightly different phenotype than FAK knockout mice (Corsi et al., 2009). Mice lacking exon 15 of FAK, which contains the Y397 autophosphorylation site, proceed through embryonic development until E12.5, 5 days longer than FAK-null mice (Corsi et al., 2009). These mutant mice display hemorrhage, edema, and vascular remodeling defects at E12.5 (Corsi et al., 2009). While it remains clear that this autophosphorylation plays an essential role in development, this study highlights the fact that FAK likely plays an important scaffolding role as well.

Skin-specific deletion of FAK leads to: hair cycle irregularities, sebaceous gland hypoplasia, and slight epidermal thinning (Essayem et al., 2006). Isolated keratinocytes from these mice undergo apoptosis in culture, potentially due to inability to adhere to tissue culture plastic (Essayem et al., 2006). The phenotypes of FAK loss are not nearly as striking as the

phenotype of β1 loss in the epidermis, indicating that FAK is only responsible for mediating a fraction of β1 integrin function in skin (Brakebusch et al., 2000; Raghavan et al., 2000).

Despite the epidermal defects, FAK deletion in the epidermis does not lead to defects in cutaneous wound healing (Essayem et al., 2006). However, FAK deletion in the intestinal epithelium leads to reduced epithelial proliferation in response to dextran-sulfate-sodium induced injury (Owen et al., 2011). Surprisingly, a FAK homologue, Pyk2 (Proline-rich protein tyrosine kinase 2), is expressed in the epidermis and contributes to wound healing *in vivo* (Koppel et al., 2014; Schindler et al., 2007). However, Pyk2 appears to be primarily localized to the nucleus in epidermal keratinocytes and controls re-epithelialization through activation of PKCδ and MMPs (Koppel et al., 2014; Schindler et al., 2007). Thus, the relationship of Pyk2 to focal adhesion signaling is unclear.

Focal Adhesion Kinase (FAK) in Squamous Cell Carcinoma

FAK expression and activity is elevated in multiple epithelial cancers, including Squamous Cell Carcinoma. In a mouse model of SCC driven by loss of TGFβRII in the mouse epidermis, enhanced integrin-FAK-Src signaling and keratinocyte migration was observed (Guasch et al., 2007). Further, loss of only one FAK allele significantly reduces papilloma formation upon DMBA-TPA treatment (McLean et al., 2001). Loss of both alleles prevents papilloma progression to SCC (McLean et al., 2004). FAK was shown to be necessary for phosphorylation of ERK downstream of Ras in cultured cells, and loss of FAK reduced migration of keratinocytes *in vitro* (McLean et al., 2001; McLean et al., 2004). Use of a FAK kinase inhibitor, PF-562,271, also blocks tumor cell migration, anchorage independent growth, and SCC xenograft growth (Figure 1.3B) (Serrels et al., 2012). This inhibition of FAK activity correlates with a decrease in phosphorylation of Src at tyrosine 416 (Serrels et al., 2012). Skin-specific loss of FAK also prevents phorbol ester induced skin carcinogenesis, potentially due to prevention of β-catenin-induced stem cell mobilization in the bulge of the hair follicle (Ridgway et al., 2012).

Inhibition of Src, a kinase that intricately associates with FAK at FA complexes also shows the same effect on preventing stem cell mobilization (Ridgway et al., 2012).

While FAK clearly plays a pro-tumorigenic role, loss of FAK in SCC also results in increased resistance to radiation therapy (Graham et al., 2011). This resistance appears dependent on p53-mediated induction of p21(Graham et al., 2011). In many contexts, FAK has been shown to both bind p53 and mediate its degradation (Golubovskaya and Cance, 2010; Golubovskaya et al., 2005; Lim et al., 2008). While further studies are required to verify this phenomenon in an orthotopic *in vivo* context, this result suggests that the viability of FAK as a therapeutic target may depend on p53 status.

C-myc in wound healing and tumorigenesis

C-myc is a basic Helix-Loop-Helix (bHLH) transcription factor that is involved in regulating expression of genes involved in cell cycle progression and apoptosis. Myc regulates gene expression by dimerizing to Max and binding to Enhancer Box sequences (E-boxes) and recruiting histone acetyltransferases (HATs) to modify the chromatin and induce gene expression. It can also repress gene expression through binding to Miz-1 and removing the p300 co-activator. Myc regulates up to 15% of the human genome, and its major targets serve to promote cell cycle progression (through induction of Cyclin D2 and CDK4 and repression of p21, p15 and GADD45), promote anchorage-independent growth (through repression of integrins and N-cadherin), promote metabolism and protein synthesis (through induction of lactate dehydrogenase, ornithine decarboxylase, glutaminase, and the ribosomal proteins EIF4E and EIF2A), promote angiogenesis (through induction of IL1β and miR17-92 and repression of thrombospondin) and promote chromosomal instability and production of reactive oxygen species (ROS) (Dang, 1999; Dang, 2012; Eilers and Eisenman, 2008; Meyer and Penn, 2008). Myc can also trigger apoptosis in a p53-dependent manner by inducing expression of the p14ARF gene, or in a p53-independent manner through induction of pro-apoptotic protein Bax (Hoffman and Liebermann, 2008).

C-myc knockout in the epidermis during development leads to severe skin defects, including fragility, hypoproliferation and impaired wound healing (Zanet et al., 2005). However, inducible c-myc deletion in adult mouse epidermis is well tolerated, with no obvious skin abnormalities (Oskarsson et al., 2006). These phenotypes are consistent with the intestinal epithelium, where c-myc is necessary for crypt formation but dispensable for crypt homeostasis (Bettess et al., 2005). C-myc is thus able to function differently based on various environmental stresses and physiological states.

It is clear that c-myc promotes tumorigenesis in nearly every human cancer, including skin cancer. In fact, c-myc amplification was shown in 50% of SCCs from patients undergoing immune suppression therapy (Boukamp, 2005). The effects of c-myc over-expression in the skin depend on the promoter used. Interestingly, over-expression of c-myc in the epidermis using the K14 promoter leads to hyperproliferative sebaceous glands and sebaceous adenomas upon treatment with carcinogens, indicating that c-myc can influence keratinocyte fate (Honeycutt et al., 2010). Expression of c-myc in suprabasal layers of the epidermis using an involucrin promoter reverses keratinocyte differentiation and induces papilloma formation (resembling pre-cancerous actinic keratosis) without carcinogen treatment (Pelengaris et al., 1999). Inducible deletion of c-myc in the epidermis (using the K5 promoter) protects the skin from DMBA-TPA induced tumors, through a p21-dependent mechanism (Oskarsson et al., 2006). While the individual skin phenotypes differ slightly between models, it is clear that c-myc promotes proliferation and neoplastic transformation in the epidermis.

Signaling pathways controlling protein translation

The first step in cap-dependent eukaryotic translation initiation is binding of initiation factors (eukaryotic Initiation Factors—eIFs) to the 5’ cap and the 5’UTR of the mRNA to hold the mRNA in place for binding to the small ribosomal subunit, the 40S (Merrick, 2004; Silvera et al., 2010). Translation is intiated with an initiator methionine-tRNA complex. Once this complex has entered the small ribosomal subunit, it signals for association of the large subunits (60S) to form a

complete ribosome (80S), which carries out translation elongation (Merrick, 2004). While most mRNAs are translated in a cap-dependent manner, some mRNAs contain an Internal Ribosome Entry Site (IRES), which allows translation initiation without scanning for the start codon, termed cap independent translation (Komar and Hatzoglou, 2011; López-Lastra et al., 2005; Merrick, 2004). mRNAs that are able to undergo cap-independent translation include Cyclin D1, c-Jun and c-myc, which may use this translation mechanism in response to certain types of cellular stress (Komar and Hatzoglou, 2011; López-Lastra et al., 2005).

Much of the regulation of protein synthesis centers on formation of the eIF4F initiation complex (Silvera et al., 2010). This complex consists of the initiation factors eIF4A, eIF4G and eIF4E, and is essential for initiation of protein translation. 4E-BP family members are crucial for regulating the pool of available eIF4E in the initiation complex. 4E-BPs bind to eIF4E and prevent eIF4E from incorporating into the initiation complex. Phosphorylation of 4E-BP prevents it from binding and inhibiting eIF4E. mTOR, a serine/threonine kinase that is activated by Akt, directly phosphorylates 4E-BP to prevent its association with eIF4E to promote cap-dependent translation (Laplante and Sabatini, 2009; Wang and Proud, 2006).

Another layer of regulation lies in the stimulation of eIF4A activity by eIF4B (which is not a member of eIF4F) (Andreou and Klostermeier, 2014; Silvera et al., 2010). eIF4B can be phosphorylated by two different kinases: p70S6K (S6 Kinase) or p90RSK (ribosomal S6 kinase) (Silvera et al., 2010). P70S6K is activated by mTOR, while p90RSK is activated by MAPK signaling. Phosphorylation of eIF4B stimulates the ATPase and RNA helicase activities of eIF4A (Andreou and Klostermeier, 2014). p70S6K and p90RSK are also known to directly phosphorylate ribosomal protein S6 (RPS6), which is a component of the 40S ribosomal subunit and directly stimulates translation (Silvera et al., 2010). These kinases phosphorylate RPS6 on different sites: p70S6K phosphorylates RPS6 at Serines 240/244 while p90RSK phosphorylates RPS6 at Serine235.

As described earlier, integrins clearly play a role in promoting translation through their activation of the PI3K-Akt signaling pathway. Interestingly, it has been shown that localized

translation occurs at focal adhesion complexes, likely providing a mechanism for rapid synthesis of proteins at the leading edge of cells (Chicurel et al., 1998; Katz et al., 2012).

Therapeutic targeting of integrins and focal adhesion proteins

Inhibitors targeting integrin activation and the kinases FAK and ILK are in various stages of development, with clinical trials currently ongoing for integrin inhibitors, integrin blocking antibodies, and FAK inhibitors. Although *in vitro* data support the use of ILK kinase inhibitors for therapy, no clinical trials have been started for those compounds.

Cilengitide (EMD 121974) is an RGD-based peptide targeted against αvβ3 and αvβ5 integrins, which are up-regulated on blood vessels during tumor angiogenesis (Brooks et al., 1994). In preclinical studies, this drug showed induction of apoptosis of angiogenic endothelial cells, and additional direct anti-tumor activity (Scaringi et al., 2012). While preclinical models showed promise, only a fraction of glioblastoma patients respond to therapy, and there is variability in response of patients with other types of tumors to the drug (Scaringi et al., 2012). Treatment of patients with squamous cell carcinomas of the head and neck with cilengitide resulted in partial response or stable disease for all patients tested, and randomized phase II clinical trials are currently in progress (Vermorken et al., 2011). More recently, it was shown that low concentrations of this inhibitor actually stimulate tumor growth by promoting VEGFR-2 trafficking to the endothelial cell surface (Reynolds et al., 2009). It is therefore possible that dose of the drug is highly important in tumor response, which could account for some of the variability seen thus far.

CNTO-95 (intetumumab) is a fully humanized anti-αv-integrin monoclonal antibody which was also developed to target angiogenic blood vessels and some primary tumors, but broadly binds to all αv heterodimers (Trikha et al., 2004). The expression of αv integrins has been shown to be essential for survival of melanoma cells in three-dimensional cultures, and thus most of the clinical trials for this antibody have been for stage IV melanoma patients (Bao and Strömblad, 2004). This therapy was well tolerated in Phase I trials, and has shown variable success in phase

II trials (Mullamitha et al., 2007; O'Day et al., 2011; Robinson et al., 2012). There is a trend toward improved survival, but it is not yet significant and studies with larger patient cohorts may be necessary.

In preclinical studies, inhibition of FAK kinase activity shows promising anti-tumor activity for a variety of different types of malignancies. A specific inhibitor, PF-00562271, has shown safety and some efficacy in phase I trials for advanced solid tumors (including head and neck tumors) (Infante et al., 2012). Phase I trials are currently ongoing for a second FAK kinase inhibitor, GSK2256098.

Another potential strategy for targeting integrin activation in cancer is to target specific extracellular matrix ligands. Secretion of proteases during tumorigenesis can lead to cleavage of ECM components to generate new ligands with distinct structure and binding affinity for specific integrin heterodimers. Cleavage of type IV Collagen into two epitopes, HU177 and HUIV26, occurs in the extracellular matrix surrounding melanoma tumors. This Collagen cleavage exposes additional integrin-binding motifs within these epitopes that enhance signaling of αvβ3 within angiogenic blood vessels (Xu et al., 2001). Blocking antibodies against these epitopes have shown anti-angiogenic, anti-tumor and anti-metastasis efficacy (Roth et al., 2006). Additionally, increased shedding of HU177 is observed in melanoma patient sera, and has been shown to correlate with poor prognosis and disease progression (Hamilton et al., 2010; Ng et al., 2008). More work is required to determine if additional epitopes are released, and if this differs between tumor types.

Thesis objectives

While several integrins have well-understood roles in skin homeostasis and tumorigenesis, the roles for many specific subunits—in particular the αv class of heterodimers—remains poorly understood. Given the up-regulation of αv integrins in human wounds and human Squamous Cell Carcinomas, we hypothesize that αv integrins play crucial roles in these physiological processes. In Chapter 3, we utilize a multiplexed shRNA screen to identify αv

integrins as crucial mediators of organotypic skin formation. We further define a fundamental role for αv (and its binding partners β5 and β6, but not β1 and β8) in organotypic tissue proliferation, but not maintenance, and hyperproliferation during wound healing *in vivo*. In Chapter 4, we define the specific signaling mechanism through which integrin αv controls cell cycle progression. We determine an integrin αv→TGFβ→FAK→p38→p90RSK mechanism that controls c-myc translation to promote cellular proliferation. This is the first time that c-myc has been shown to be controlled by αv integrins. In Chapter 5, we demonstrate that αv and its binding partners β5 and β6 are necessary for squamous cell carcinoma invasion in organotypic culture. We also show that blockade of αv integrins blocks SCC tumor formation *in vivo*.

TABLES

Integrin α1	-viable, fertile and no apparent abnormalities (Gardner et al., 1996)	N/A	N/A
Integrin α2	-Healthy, viable, fertile (Chen et al., 2002) -No change in re-epithelialization or BM deposition, but increase in neoangiogenesis during wound healing (Grenache et al., 2007; Zweers et al., 2007)	N/A	-K14-HPV mice crossed with α2-null mice shows decreased lymph node metastases and tumor formation (Tran et al., 2011)
Integrin α3	-survive until birth, but die shortly after due to kidney and lung defects -minor blistering of the epidermis, but normal stratification (Kreidberg et al., 1996)	-disorganized BM -blistering at epidermal-dermal junction -spatial and temporal differentiation is intact (DiPersio et al., 1997; DiPersio et al., 2000) -hair loss and impaired hair follicle growth (Conti et al., 2003) -enhanced re-epithelialization during wound healing (Margadant et al., 2009) -enhanced epidermal turnover (Sachs et al., 2012)	-significantly reduced papilloma formation upon DMBA-TPA treatment of mice lacking α3 in the epidermis -SCCs that form are more poorly differentiated (Sachs et al., 2012)
Integrin α4 (VCAM-1)	-required for formation of umbilical cord and placenta during development -mostly embryonic lethal E8.5, but a small number of viable, fertile mice (Gurtner et al., 1995)	N/A	N/A
Integrin α5	-mesodermal defects and embryonic death at E10-11 (Yang et al., 1993)	N/A	N/A
Integrin α6	-embryonic lethal at E14.5-E18.5 -skin blistering similar to epidermolysis bullosa (Georges-Labouesse et al., 1996) -normal differentiation and stratification of the epidermis (DiPersio et al., 2000; Georges-Labouesse et al., 1996)	-mild hyperproliferation, blistering and inflammation upon tamoxifen-induced deletion in epidermis (Niculescu et al., 2011)	See integrin β4

Integrin α7	-viable, fertile mice (Mayer et al., 1997) -muscular dystrophy -defective axonal elongation (Werner et al., 2000)	N/A	N/A
Integrin α8	-death immediately after birth likely due to renal deficiencies (Müller et al., 1997)	N/A	N/A
Integrin α9	-normal at birth, but die at day 6-12 due to respiratory failure -edema and lymphocyte infiltration into chest wall (Huang et al., 2000b)	-Poor re-epithelization during wound healing (Singh et al., 2009)	N/A
Integrin α10	-viable, fertile -stunted growth of long bones (Bengtsson et al., 2005)	N/A	N/A
Integrin α11	-viable, fertile -dwarfism and defective tooth movement (Popova et al., 2007)	N/A	N/A
Integrin αv	-mostly embryonic lethal at E9.5, but 20% of mice born alive -defects in placental function -intracerebral and intestinal hemorrhage -cleft palates (Bader et al., 1998)	N/A	-Induction of SCC formation upon dual-ablation of p53 and αv -Slower SCC growth upon αv deletion (Savar et al., 2014)
Integrin β1	-embryonic lethal -die immediately after attaching to uterine epithelia and invading the stroma, around E5 (Fassler and Meyer, 1995; Stephens et al., 1995)	-Severe hair loss -reduced numbers of hemidesmosomes -disruption in BM and blistering -K14-Cre model shows normal spatial and temporal differentiation, but K5-Cre model shows enhanced differentiation -K14-Cre model shows epidermal thinning, but K5-Cre model shows epidermal thickening (Brakebusch et al., 2000; Raghavan et al., 2000) -poor re-epithelialization during wound healing (Grose et al., 2002) -K14-CreER 4-OHT excision in adult epidermis	-Activating mutation T1881β1 stimulated conversion of papillomas to SCCs upon DMBA-TPA (Ferreira et al., 2009) -Blocking antibodies against integrin β1 block tumor formation and progression in a human tissue graft model of SCC (Reuter et al., 2009)

		has no apparent phenotype (López-Rovira et al., 2005)	
Integrin β3	-enhanced re-epithelialization during wound healing (Reynolds et al., 2005)	N/A	N/A
Integrin β4	-die shortly after birth due to respiratory and intestinal failure and skin fragility -skin blistering defects similar to epidermolysis bullosa -normal stratification of the epidermis (Dowling et al., 1996)	-loss of hemidesmosomes, skin blistering, but normal differentiation and proliferation (DiPersio et al., 2000; Raymond et al., 2005)	-β4 knockout or blocking antibodies prevented Ras-driven tumorigenesis in human tissue graft model of SCC (Dajee et al., 2003)
Integrin β5	-Viable, fertile and no apparent abnormalities(Huang et al., 2000a)	N/A	N/A
Integrin β6	-Hair loss -Inflammation of skin and lungs (Huang et al., 1996)	-retarded hair follicle regression after depilation -enhanced keratinocyte proliferation(Xie et al., 2012)	N/A
Integrin β8	-65% die at midgestation due to insufficient vasculogenesis -35% die shortly after birth due to intracerebral hemorrhage -leaky brain capillaries and endothelial hyperplasia (Zhu et al., 2002)	N/A	N/A

Table 1: Functional roles for integrins in mouse development and mouse skin.

FIGURES

Figure 1.1

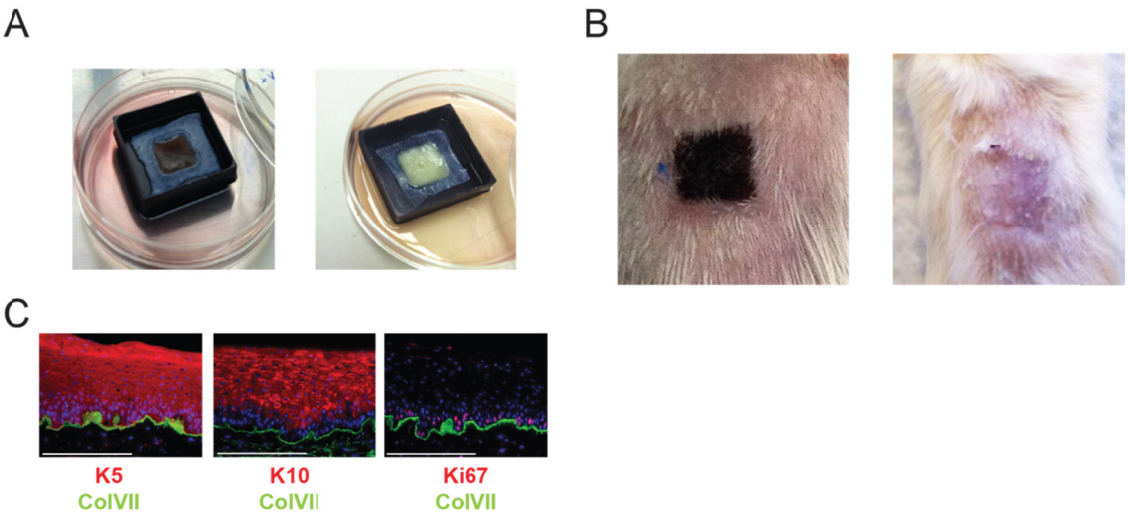

Figure 1.1: Organotypic and orthotopic human skin model used in this study. **A.** Images of organotypic human skin with or without melanocyte incorporation. Human skin is cultured at the air-liquid interface to induce stratification and differentiation. **B.** Human skin from (**A**) grafted onto immunocompromised mice. **C.** Immunofluorescence images of human skin from (**A**). Skin was stained with Keratin5 (K5), Collagen VII (ColVII, marks the basement membrane), Keratin10 (K10, suprabasal differentiation marker) and/or Ki67 (proliferation marker).

Figure 1.2

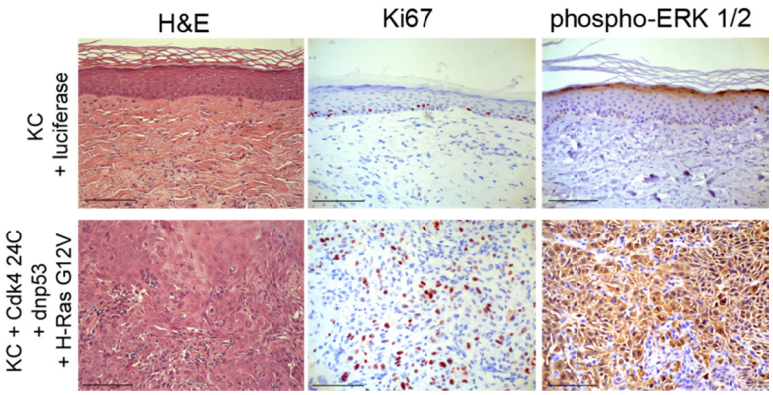

Figure 1.2: Human skin or human skin tumors from *in vivo* orthotopic xenografts. Hematoxylin & Eosin (H&E) stain, Ki67 immunohistochemistry or phospho-ERK1/2 immunohistochemistry was performed on 3-week old normal skin (top) or genetically engineered skin tumors (bottom) that were grafted onto immunocompromised mice.

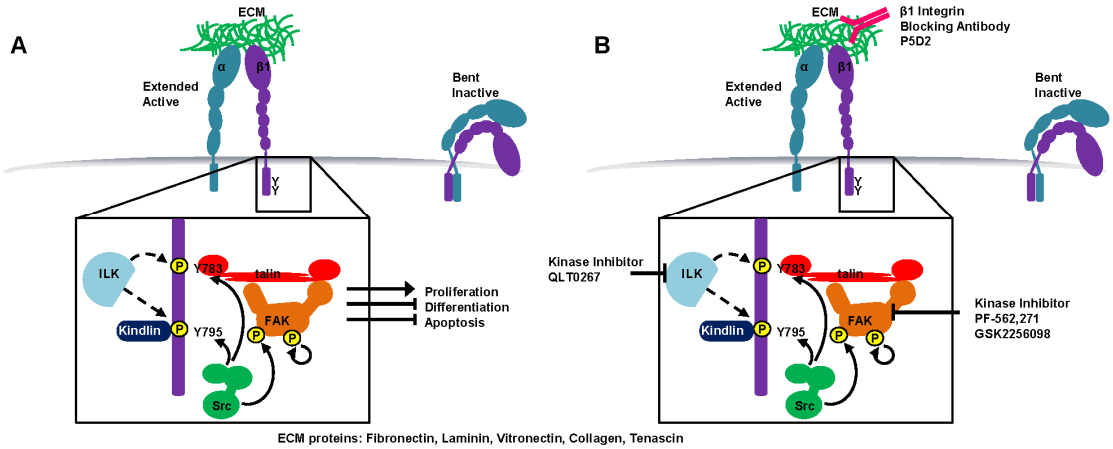

Figure 1.3: Depiction of focal adhesion structure, key phosphorylation events and therapeutics targeting individual focal adhesion proteins for treatment of cSCC. **A.** In normal basal keratinocytes, integrin binding to the ECM initiates Talin binding to the membrane proximal NPxY motif (Y783) and Kindlin binding to the membrane distal NPxY motif (Y795). FAK is recruited to the adhesion and undergoes auto-phosphorylation at Y397. Src kinase phosphorylates both NPxY tyrosines on the β1 integrin tail, and phosphorylates active FAK at Y925. It remains controversial whether ILK phosphorylates β1 integrin at these same sites. This adhesion assembly and phosphorylation sequence ultimately promote cell cycle progression, and inhibit differentiation and apoptosis programs. **B.** Three current strategies in development for treatment of cSCC are: blocking β1 integrin with a P5D2 blocking antibody, inhibiting ILK kinase activity using QLT0267, and inhibiting FAK kinase activity using PF-562,271 or GSK2256098.

CHAPTER 2

Materials and Methods

Parts of this chapter have been previously published in:

Duperret EK, Dahal A, Ridky TW. Focal adhesion-independent integrin αv regulation of FAK and c-myc is necessary for 3D skin formation and tumor invasion. *J Cell Sci.* 2015; 128(21):3997-4013.

Duperret EK, Oh SJ, McNeal A, Prouty SM, Ridky TW. Activating FGFR3 mutations cause mild hyperplasia in human skin, but are insufficient to drive benign or malignant skin tumors. *Cell Cycle.* 2014;13(10):1551-1559.

Materials and Methods

Cell culture and reagents

Primary human keratinocytes, melanocytes and fibroblasts were isolated from neonatal foreskins obtained from the Hospital of the University of Pennsylvania. Foreskins were incubated in 50:50 dispase (Fisher):DMEM (Dulbecco modified Eagle medium, high glucose 4.5g/L) + 5% FBS (fetal bovine serum, Invitrogen) mixture overnight at 4□C. The epidermis was carefully peeled from the underlying dermis and incubated in trypsin for 10 minutes at 37□C. The trypsin was neutralized with DMEM + 5% FBS and 1% antibiotic/antimycotic (Gibco) and spun at 300 g for 5 minutes. The supernatant was removed, and the pellet was plated in keratinocyte media containing 50% Gibco Keratinocyte-SFM + L-glutamine + EGF and BPE, 50% Gibco Cascade Biologics 154 medium for keratinocytes and 1% penicillin/streptomycin (100U/mL, Gibco) for keratinocyte culture, or Melanocyte Medium 254 (Gibco) with Human Melanocyte Growth Supplement and 1% penicillin/streptomycin (100U/mL, Gibco) for melanocyte culture. For

fibroblast isolation, the dermis was chopped into small pieces, and incubated in 1mL collagenase (10mg/mL, Roche) at 37ºC for 15 minutes. 1mL of 0.05% trypsin (Gibco) was added and incubated for another 10 minutes at 37ºC. 1mL of DMEM + 5% FBS was added to quench the trypsin, and the pieces of dermis were removed and discarded. The remaining solution was centrifuged at 300g for 5 minutes. The supernatant was removed and the pellet plated in DMEM + 5% FBS + 1% antibiotic/antimycotic. 293T cells, Phoenix cells, A375 cells, SK-MEL-2 cells, SK-MEL-5 cells, WM2664 cells and SK-MEL-28 cells were purchased from ATCC and also cultured in DMEM + 5% FBS + 1% antibiotic/antimycotic. All small molecules and recombinant proteins used are listed in Table 2.2.

Hybridoma culture and antibody purification

The mouse L230 and 10D5 hybridoma cell lines were obtained from ATCC (HB-8448 and RB44-10D5.19-.21) and cultured according to ATCC guidelines. Supernatant was collected and filtered using a 0.22μm filter. Antibody was isolated from supernatant and concentrated using the Nab Protein G Spin Kit (Thermo). Antibody concentration was quantified by measuring absorbance at 280nm.

Lentiviral and retroviral constructs

A list of hairpins used in this study is included in Table 2.3. The following pRRL constructs were used in this study: pRRL-c-myc, pRRL-Cdk4 R24C, pRRL-Cyclin D1 WT, pRRL-Cyclin D1 T286A, pRRL-dnp53 (R248W), pRRL-FAK, pRRL-H-Ras G12V, pRRL-luciferase, pRRL-MKK6(glu), pRRL-Skp2, and pRRL-SuperFAK (K578E, K581E). These constructs were PCR amplified from cDNA or from addgene plasmids, and ligated into the pRRL lentiviral vector. The following LZRS retroviral constructs were used in this study: LZRS-ER-HRas G12V, LZRS-Cdk4 R24C, LZRS-luciferase, and LZRS-MKK7. The following TRIPZ lentiviral constructs were used in this study: TRIPZ-β3, TRIPZ-luci-puro, TRIPZ-5'UTR c-myc-luci-puro, and TRIPZ-luci-3'UTR c-myc-puro.

Lentivirus and retrovirus production and transduction

Phoenix cells and HEK293T cells were used for retrovirus and lentivirus production, respectively. HEK293T cells were seeded at 70% confluency on 6-well plates and transfected with 1.22μg lentiviral plasmid mixed with packaging plasmids pCMVΔR8.91 (0.915μg) and pUC-MDG (0.305μg) per well using Fugene6 transfection reagent (Promega). Phoenix cells were transfected using the same protocol without the packaging plasmids. 10mM sodium butyrate (Sigma) was added 16 hours after transfection, and cell culture media was replaced 24 hours after transfection and virus-producing cells were moved to 32ºC. Human keratinocytes, melanocytes and fibroblasts were transduced at 10-40% confluence with lentivirus harvested 48 and 72 hours post-transfection of packaging cells. Lentivirus was filtered through a 45-μm filter (Argos) and supplemented with 5μg/mL of polybrene (hexadimethrine bromide, Sigma). Subsequently, cells were spun at 300g for 1 hour at room temperature. Complete growth media was replaced after 15 minutes of incubation at 37□C.

Antibodies and immunoblot analysis

Adherent cells were washed with PBS and then lysed with RIPA Lite lysis buffer: 50mM Tris pH 7.5, 150mM NaCl, 1mM EDTA, 1% NP-40 containing protease inhibitors (Roche) and phosphatase inhibitors (Roche). Lysates were quantified using Bradford assay, and reduced in Laemmli sample buffer containing β-mercaptoethanol (BioRad). Cell lysates were subjected to SDS gel electrophoresis in 4-15% Tris-Glycine precast polyacrylamide gels (BioRad) in running buffer (25mM Tris, 192mM glycine, 0.1% SDS, pH 8.3). Protein was transferred to PVDF membrane (Millipore) using a Trans-blot Semi-Dry Transfer Cell (BioRad) in semi-dry transfer buffer. Membranes were blocked with 5% milk in TBST or 5% BSA in TBST and incubated in primary at 4ºC overnight. After incubation with HRP secondary antibody (cell signaling) for 30 minutes-1 hour at 4ºC, proteins were detected using ECL Western Blotting Detection Reagents (GE-Amersham Biosciences) or Luminata Crescendo Western HRP Substrate (Millipore). All antibodies used are listed in Table 2.2.

RNA Isolation and qPCR

RNA was isolated using an RNeasy Plus Mini Kit (Qiagen), and RNA was converted to cDNA using the Applied Biosystems High Capacity RNA to cDNA kit. qPCR was performed using Power SYBR Green Master Mix using a ViiA 7 Real-Time PCR System (Life Techologies). Relative expression levels were calculated using the $2^{-\Delta\Delta Ct}$ method. All qPCR primers used are listed in Table 2.1.

Immunofluorescence

Skin tissues were embedded in Tissue-Tek OCT compound and sectioned at 8μm thickness using a cryostat. Tissue sections were fixed in cold methanol for 2 minutes. Cultured cells were fixed and permeabilized using microtubule stabilization buffer (MTSB, 0.1M PIPES, pH 6.75, 1mM EGTA, 1mM MgSO4, 4% (w/v) poly(ethylene glycol), 1% Triton X-100, 2% Paraformaldehyde). Both tissue sections and cultured cells were blocked in 5% horse serum in PBS for 30 minutes and incubated 1% horse serum in PBS for primary and secondary antibody incubation (30 minutes each). For FAK staining, cells were fixed in cold methanol for 10 minutes instead of paraformaldehyde. Tissue sections were mounted using Prolong Gold Antifade plus DAPI reagent. Images of tissues were taken using an Olympus BX-61 inverted microscope and images of cultured cells were taken using a Zeiss LSM 710 Confocal Microscope. For BrdU staining, tissues were fixed in cold 70% EtOH for 5 minutes at room temperature. Tissue sections were rinsed with PBS, incubated in 1.5M HCl for 30 minutes, then rinsed in PBS again. Tissues were blocked in 5% horse serum + 0.3% Triton X-100 in PBS for 60 minutes, then incubated in primary antibody overnight in 1% BSA in PBS. Secondary antibody was incubated in 1% BSA for 1 hour at room temperature. For TUNEL staining, TUNEL enzyme and TUNEL label (Roche) were used according to the manufacturer's guidelines. All antibodies used are listed in Table 2.2.

Immunohistochemistry

Tissue was fixed using 10% neutral-buffered formalin. Immunostaining was performed on 5 μm formalin fixed paraffin embedded (FFPE) skin sections. Briefly, tissue sections were deparaffinized in xylene and rehydrated in alcohol. For antigen retrieval, tissues were immersed in 10 mM citrate buffer pH 6.0 and heated at 95°C for 10 min, cooled at RT, and washed 10 times for 3 min. Endogenous peroxidase was quenched with 3% H_2O_2 and subsequently washed 2–3 times with PBS. Tissue sections were incubated with blocking buffer (1% BSA and 10% normal goat serum in PBS) for 30 min and primary antibody at 4°C overnight. Following multiple washes, goat anti-rabbit HRP conjugated secondary antibodies were incubated for 20 min at RT. The signal was further amplified with DAB mix solution (Abcam). Slides were counterstained, dehydrated, and mounted with a coverslip. The following antibodies were used for IHC: Ki67 and phospho-ERK1/2 (Cell Signaling).

Immunoprecipitation

Keratinocytes were lysed in RIPA for membrane proteins (TBS pH 7.5 supplemented with 2mM $CaCl_2$, 1mM $MgCl_2$, 1% NP-40 and 1% Triton X-100 plus protease and phosphatase inhibitors). The Pierce Crosslink Immunoprecipitation Kit was used for immunoprecipitation according to manufacturer's protocol (Thermo). All antibodies used for immunoprecipitation are listed in Table 2.2.

Fluorescence Activated Cell Sorting

For all doxycycline-inducible experiments, keratinocytes were sorted to achieve maximum hairpin induction. pTRIPZ transduced human keratinocytes were induced with doxycycline for 24 hours prior to cell sorting. Cells were trypsinized and resuspended in 1X PBS containing 1% BSA in a polypropylene tube (Falcon) at a density of $10x10^6$ cells/mL. The top 20% of RFP+ cells were sorted onto 6-well plates containing keratinocyte growth medium using a BD FACSAria II cell sorter, at the UPenn Flow Cytometry & Cell Sorting Facility. Cells were allowed to recover from the sort in doxycycline-free media for 1-2 weeks prior to experimentation.

Propidium Iodide staining and flow cytometry

Keratinocyte nuclei were isolated and stained with propidium iodide using the CycleTEST PLUS DNA Reagent Kit (BD). Cells were analyzed using a BD FACSCalibur in the UPenn Flow Cytometry & Cell Sorting Facility. Data were analyzed and percentages calculated using ModFit software.

Luciferase Assay

Firefly luciferase activity was measured using Dual-Glo Luciferase Assay System (Promega) on a BD Monolight 3096 Microplate Luminometer.

Organotypic culture

Split-thickness human skin was obtained and washed in PBS containing penicillin/streptomycin, and incubated at 37^{o}C for 7-10 days. PBS was changed every 2 days. The epidermis was separated from the dermis and subsequently discarded. The dermis was washed and incubated in PBS at 4^{o}C for 6-12 weeks. PBS was changed every 2-3 days. For assembly of organotypic tissue, the dermis was cut into 1cm^2 square pieces and placed into 12 well culture plates with the basement membrane side facing down. 100,000 fibroblasts were seeded into each well and incubated at 37^{o}C with 5% humidified CO_2 for 3-4 days. The dermis with FB was elevated to a sterilized annular dermal support tissue culture insert device in a manner such that the basement membrane was oriented up. Several drops of BD matrigel were placed on the bottom of the dermis to create a seal. The growth media was changed to KGM (3:1 mixture of DMEM:Ham's F12 supplemented with 10% FBS, adenine (1.8x 10^{-4}M), hydrocrtisone (0.4µg/mL), insulin (5µg/mL), cholera toxin (1x 10^{-10}M), EGF (10ng/mL), transferrin (5µg/mL), and triido-L-thyronine (1.36ng/mL)). Epithelial cells were seeded onto the BM side at density of 1x10^6 per cm^2, in a total volume of 80µL. For incorporation of human melanocytes, KGM was replaced with Melanocyte Xenograft Seeding Media (MXSM). MXSM is a 1:1 mixture of KGM and Keratinocyte Media 50/50 (Gibco) containing 2% FBS, 1.2mM calcium chloride, 100nM ET-3

(endothelin-3), 10ng/mL rhSCF (recombinant human stem cell factor), and 4.5ng/mL r-basic FGF (recombinant basic fibroblast growth factor). $1.5x10^5$ melanocytes and $5.0x10^5$ keratinocytes were suspended in 80uL MXSM. For organotypic skin, the upper chamber was kept dry and exposed only to air while the media on the lower chamber was changed every other day. Organotypic skin tissue was harvested at 10-14 days, and organotypic transformed tissue was harvested at 10 days. For BrdU labeling, organotypic tissue was incubated with BrdU labeling reagent (Invitrogen) at 1:100 dilution in KGM for 1 hour.

Invasion assay

For invasion measurements, we established organotypic tissues (described in detail above) containing keratinocytes transduced with mutant Cdk4 (R24C) and oncogenic H-Ras (G12V) in the epidermal compartment and primary, non-transduced human fibroblasts in the dermal compartment. These epidermal transformed keratinocytes spontaneously invade through the basement membrane of these organotypic tissues, into the dermis. We quantified invasion area (in mm^2) per field by imaging these tissues across the length of the entire $1cm^2$ tissue. We measured the area of K5+ labeled epidermal keratinocytes that invaded past the basement membrane (labeled with CollagenVII) into the dermis using ImageJ. We then averaged the invasive area across the entire tissue, and then across biological replicates.

Organotypic re-epithelialization assay

Re-epithelialization assay runways were 3D printed through the UPenn biomedical library. Runways were sterilized in 70% ethanol in H_2O prior to use. Human keratinocytes and melanocytes were seeded onto half of the 3D runway platform, and the cover was placed on top to prevent keratinocyte migration to the other half. After 5 days, the cover was removed and the tissue was treated with antibodies and proteins. Tissue was harvested at day 10 after seeding.

Human skin xenografts

Organotypic human skin was assembled (as described previously) without fibroblasts, and incubated at 37°C for 3-4 days before being grafted onto SCID mice. For skin grafting, SCID mice were anesthetized in an isoflurane chamber, and 1 cm^2 of epidermis was removed on the dorsal region of the mouse, down to fascia. Reconstituted human skin was sown onto the mouse dorsal region with individual interrupted stitches using 6–0 nylon sutures. Mice were dressed with Bactroban ointment, Adaptic, Telfa pad, and Coban wrap. Mice were unwrapped 2 weeks after grafting.

Blocking antibody treatment

In organotypic culture, the following antibodies were used at a concentration of 7μg/mL (with media changes every other day): L230 (ATCC hybridoma), 10D5 (ATCC hybridoma), Mouse IgG (Thermo), P1F6 (Iowa hybridoma bank), and P5H9 (Iowa hybridoma bank). For *in vivo* wound healing experiments, mouse IgG, mouse IgG1 (BioXCell) or L230 were delivered subcutaneously underneath the xenograft in PBS. 100μg of antibody/mouse was delivered every day, beginning the day prior to wounding. For *in vivo* tumor experiments, mouse IgG or L230 were delivered subcutaneously underneath the xenograft in PBS. 100μg of antibody/mouse was delivered every other day, beginning the day prior to doxycycline administration, until the end of the experiment.

In vivo wound healing

Human skin xenografts were wounded approximately 6 weeks after grafting. Wounding was performed using a 2mm punch biopsy. Human skin and dermis was removed, while the fascia and muscle layer remained intact. Wounds were dressed with Bactroban ointment, Adaptic, Telfa pad, and Coban wrap, and monitored every day.

Quantification and statistical analysis

Tissue thickness, tumor invasion and tumor cross-section area were quantified using ImageJ software. Focal adhesion size and number were also quantified using ImageJ software. For experiments with 2 groups, statistical significance was measured using a student's t-test, unless otherwise indicated in figure legend. For experiments with >2 groups, one-way ANOVA was used to measure statistical significance. For experiments in which ANOVA showed significance, Tukey's HSD (honest significance difference) test was performed. *=$p<0.05$, **=$p<0.005$, ***=$p<0.0005$, and NS= not statistically significant. TCGA data was generated by the TCGA Research Network: http://cancergenome.nih.gov/. TCGA data was downloaded using the cbioportal R package. Kaplan-Meier analysis was done using R, and statistical significance was calculated using the log-rank test. Heat maps were generated using MATLAB.

TABLES

Target	Sequence (5'→ 3')
Integrin β1 F	GCGCGTGCAGGTGCAATGAA
Integrin β1 R	ACACACTGTCCGCAGACGCA
Integrin β3 F	GAGGCGGACGAGATGCGAGC
Integrin β3 R	CCCAGAGGCAGGGCCTCATCA
Integrin β4 F	CAACCCCACAGAGCTGGTGCC
Integrin β4 R	TGCTTTTTCCCGGCATTGGGA
Integrin β5 F	CGGCCCGGTGACAAGACCAC
Integrin β5 R	TCTGGTACCTCGGTGCCGTGT
Integrin β6 F	TGGGGCCTCGCTGTGAGTGT
Integrin β6 R	CAGTCGCCGTTACCTCCGCA
Integrin β7 F	TGCGGAGGCTTTGGTCGCTG
Integrin β7 R	CAGCCTGGGCATTGGTCGCA
Integrin β8 F	GTGCCAGGTGCCTTGCGCT
Integrin β8 R	CTTCGGCTCCTGGACGCAGC
Integrin α1 F	CGCTGGAAGATGATCACGGGG
Integrin α1 R	TCTCGGGACCAGAAGAGGGCA
Integrin α2 F	TCACCGAGGTGACCAGATTGGCT
Integrin α2 R	TGCCCTCGGGGCCTTCAAGA
Integrin α3 F	GGTGGGCGCCCCCTACTACT
Integrin α3 R	GGAGCTCCCACAGCAATATCCTGA
Integrin α4 F	CGAGAGCGCATGGCTTGGGA
Integrin α4 R	CGCACCCACTAGGAGCCATCG
Integrin α5 F	CCCCGGGCTCCTTCTTCGGA
Integrin α5 R	CCAGGAGCCGAGAGCCTTTGC
Integrin α6 F	ATGTGGCGGTGGTGGACCTCA
Integrin α6 R	GGAGCTCCAACTGCAATATCTGGGT
Integrin α7 F	GGCACGGCCAACTGTGTGGT
Integrin α7 R	TCACTGGGATCACTGTGGAGGCA
Integrin α9 F	GTGGGCGCACCAAAGGCAGA
Integrin α9 R	AGCACAGGCCAACACACGGC
Integrin α10 F	TGCCCAACGCTGCCCAACAT
Integrin α10 R	CCCTCCCGCCGACTGAGCTT
Integrin α11 F	ATAAGTGGCTGGTCGTGGGCG
Integrin α11 R	GGCCGAGGCGCATGTTGTCT
Integrin αD F	TCCCCTCAACGCGCTGCTCA
Integrin αD R	TCCCACCACGAGTCGAGATCCA
Integrin αE F	TGGACACTGGGACGGCCTCT
Integrin αE R	CCGGGAGCGGAACACAACCG
Integrin αv F	TGGGTTGTGGAGTTGCTCAGTGC
Integrin αv R	AGTGGTAACCAATGTGGAGTTGGTG
Actin F	CTGGAACGGTGAAGGTGACA
Actin R	TCTGGACTTGGGAGAGGACT
Blue Barcode (BBC) F	TGGACAAGGGCGGCAACAGC
Blue Barcode1 (BBC1) R	GTTGATTGTCGACCTGTGAA
Blue Barcode2 (BBC2) R	GTTGATTGTCGACAGACCTA
Blue Barcode3 (BBC3) R	GTTGATTGTCGACTCTGAGA
Blue Barcode4 (BBC4) R	GTTGATTGTCGACGACATCA
Blue Barcode5 (BBC5) R	GTTGATTGTCGACGCAATAT
Blue Barcode6 (BBC6) R	GTTGATTGTCGACTAGGATT

Blue Barcode7 (BBC7) R	GTTGATTGTCGACCGCCGGT
Blue Barcode8 (BBC8) R	GTTGATTGTCGACATTTCCT
Cyan Fluorescent protein (CFP) F	ACAGATGCCAGTTCCACACC
Cyan Fluorescent protein (CFP) R	CCTTGTCCAGGTCGGTTCTG
c-myc F	AGGGAGATCCGGAGCGAATA
c-myc R	GTCCTTGCTCGGGTGTTGTA
FAK F	GGGTCCGATTGGAAACCAAC
FAK R	CTGAAGCTTGACACCCTCGT
MAPK11 F	GGAGATGACCGGCTATGTGG
MAPK11 R	ATATGTCCGGGCGTGTTCTG
MAPK14 F	TCTGTGTGTGCTGCTTTTGAC
MAPK14 R	TTGTTCAGATCTGCCCCCAT
RPS6KA1 F	GGAGGGCCACATCAAACTCA
RPS6KA1 R	AGCTTCGCCTTCAGAATCAGT
RPS6KA2 F	CCAAAGAGGTCATGTTCACGGA
RPS6KA2 R	AGTACGCTCTCTTGTCGTGG
RPS6KA3 F	AGACCATCTACATAGCCTGGGA
RPS6KA3 R	AGCATTTCAAACATTAACACACCA

Table 2.1: List of qPCR primers used in this study.

Target	Antibody/Company	Application	Concentration
β-actin	Cell Signaling 8H10D10	Immunoblot	1:5000
Phospho-Akt S473	Cell Signaling D9E	Immunoblot	1:2000
Akt	Cell Signaling 11E7	Immunoblot	1:1000
Phospho-c-Jun Ser73	Cell Signaling D47G9	Immunoblot	1:1000
c-Jun	Cell Signaling 60A8	Immunoblot	1:1000
c-myc	Cell Signaling D84C12	Immunoblot	1:1000
Cdk4	Santa Crus H-303	Immunoblot	1:500
Cyclin D1	Millipore Ab-3	Immunoblot	1:500
phospho-eIF4B Ser422	Cell Signaling #3591	Immunoblot	1:1000
eIF4B	Cell Signaling #3592	Immunoblot	1:1000
Phospho-ERK1/2 T202/Y204, T185/Y187	Millipore AW39R	Immunoblot	1:1000
ERK1/2	Millipore 06-182	Immunoblot	1:1000
Phospho-FAK Y397	Cell Signaling D20B1	Immunoblot	1:1000
Phospho-FAK Y925	Cell Signaling #3284	Immunoblot	1:1000
FAK	Cell Signaling #3285	Immunoblot	1:1000
Integrin α4	Cell Signaling #4600	Immunoblot	1:1000
Integrin α10	Millipore AB6030	Immunoblot	1:1000
Integrin αv	BD 21/CD51	Immunoblot	1:1000
Integrin β1	Abcam 12G10	Immunoblot	1:200
Integrin β3	Santa Cruz D11	Immunoblot	1:100
Integrin β5	Cell Signaling #4708	Immunoblot	1:1000
Integrin β6	Santa Cruz C-19	Immunoblot	1:200
Integrin β8	Santa Cruz G-17	Immunoblot	1:200
P21	Cell Signaling 12D1	Immunoblot	1:500
P27	Cell Signaling D69C12	Immunoblot	1:1000
phospho-p38 T180/Y182	Cell Signaling #9211	Immunoblot	1:1000
P38	Cell Signaling #9212	Immunoblot	1:1000
Phospho-p70 T389	Cell Signaling #9205	Immunoblot	1:1000
P70 S6 kinase	Cell Signaling 49D7	Immunoblot	1:1000
Phospho-Rb S795	Cell Signaling #9301	Immunoblot	1:1000
Rb	Cell Signaling 4H1	Immunoblot	1:1000
phospho-RPS6 Ser235/236	Cell Signaling 91B2	Immunoblot	1:1000
Phospho-RPS6 Ser240/244	Cell Signaling D68F8	Immunoblot	1:1000
RPS6	Cell Signaling 54D2	Immunoblot	1:1000
Phospho-p90RSK Thr 573	Cell Signaling #9346	Immunoblot	1:1000
RSK1/RSK2/RSK3	Cell Signaling 32D7	Immunoblot	1:1000
Skp2	Cell Signaling #2652	Immunoblot	1:1000
phospho-Smad3 Ser423/425	Cell Signaling C25A9	Immunoblot	1:1000
Smad3	Cell Signaling #9523	Immunoblot	1:1000
Phospho-Src family Y416	Cell Signaling #2101	Immunoblot	1:1000
Src	Cell Signaling 32G6	Immunoblot	1:1000
Talin 1	Cell Signaling #4021	Immunoblot	1:1000

Vinculin	Millipore MAB3574	Immunoblot	1:2000
Alexa Fluor 488 Phalloidin	Life Technologies	Immunofluorescence	1:40
BrdU	Cell Signaling Bu20a	Immunofluorescence	1:1600
Collagen VII	Millipore MAB2500	Immunofluorescence	1:200
Collagen VII	Calbiochem 234192	Immunofluorescence	1:200
Cytokeratin 10	Covance DE-K10	Immunofluorescence	1:100
FAK	Santa Cruz sc-932	Immunofluorescence	1:50
Integrin αv	L230, hybridoma ATCC	Immunofluorescence	7μg/mL
Integrin β1	Abcam 12G10	Immunofluorescence	1:200
Integrin β3	Santa Cruz D-11	Immunofluorescence	1:200
Keratin5	Covance PRB-160P	Immunofluorescence	1:5000
Ki67	Thermo 9106	Immunofluorescence	1:200
Paxillin	Abcam Y113	Immunofluorescence	1:200
PCNA	Cell Signaling D3H8P	Immunofluorescence	1:1000
Vinculin	Millipore MAB3574	Immunofluorescence	1:200
Integrin αv	Millipore AB1930	Immunoprecipitation	1:50
Normal Rabbit IgG	Cell Signaling 2729	Immunoprecipitation	1:50
PF-573228	Sigma-Aldrich	Small molecule	1μM in DMSO
BI-D1870	Santa Cruz	Small molecule	1μM in DMSO
SB 202190	Sigma-Aldrich	Small molecule	1μM in DMSO
Cytochalasin D	Sigma-Aldrich	Small molecule	1μM in DMSO
MMP-2/MMP-9 inhibitor I	Calbiochem CAS 193807	Small molecule	10nM in DMSO
Doxycycline hyclate hydrochloride	Sigma-Aldrich	Small molecule	2μg/mL in H_2O
4-hydroxytamoxifen	Sigma-Aldrich	Small molecule	100nM in 100% EtOH
Cycloheximide	Cell Signaling	Small molecule	10μg/mL in DMSO
TGFβ1	R&D	Recombinant protein	0.1pM-1nM
Rat tail Collagen		Recombinant protein	25μg/mL in 0.02M acetic acid
Fibronectin	Fisher	Recombinant protein	10μg/mL in PBS
Vitronectin	Sigma	Recombinant protein	0.1μ/mL in H_2O

Table 2.2: List of antibodies, small molecules and recombinant proteins used in this study.

Target	ID #	Hairpin sequence (5'→3')
ITGB1	TRCN0000029646	TACATTCTCCACATGATTTGG
ITGB3	TRCN0000003234	ATAGTACTGGAATCTGACGAC
ITGB4	TRCN0000057768	AAGGATGGAGTAGCTGAGGAG
ITGB5	TRCN0000057743	TTGAAGCCATTTCATAGCGGG
ITGB6	TRCN0000057707	AATACTACTGCAAGGGTTGGC
ITGB7	TRCN0000057721	TTAGGAATCAGTTTACTCAGC
ITGB8	TRCN0000057763	ATTCTATTGAATCAACTGAGC
ITGA1	TRCN0000057750	TTAAAGGTTGTGTTTCGAGGG
ITGA2	TRCN0000057731	TATATAGCACTATCTGGCCGG
ITGA3	TRCN0000057715	TTTACCATGCTAAGCGAGGTC
ITGA4	TRCN0000029654	GCTCCGTGTTATCAAGATTAT
ITGA4	TRCN0000029655	CCAAACTGATAAGCTGTTCAA
ITGA4	TRCN0000029656	TTGCATTCATTACTGCTCCCG
ITGA5	TRCN0000029652	AATTCTGACTCGTTCCTGAGG
ITGA6	TRCN0000057775	ATCGTTATCAAACTCGATCCG
ITGA7	TRCN0000057709	ATCTAACACATAGTCCAGGGC
ITGA9	TRCN0000057740	ATAGTAGATGTTCTTCCAGCG
ITGA10	TRCN0000057726	CGGCTAAAGGATGGGATTCTT
ITGAV	TRCN0000010768	TTTATCCTGTTTCGACCTCAC
ITGAV	TRCN0000003239	ATTCTCAAGATTAGCTCAGTC
ITGAV	V3THS_365149	TGTCGTCTGGAAGTCTCCT
MAPK11	TRCN0000196579	GAGAATCTACACGCATGTATG
RPS6KA1	TRCN0000001385	GCTCTATCTCATTCTGGACTT
RPS6KA1	TRCN0000001386	GAAGGAGACCATGACACTGAT
PTK2	TRCN0000001620	CCGGTCGAATGATAAGGTGTA
PTK2	TRCN0000001621	CGACAGCAACAGGAAATGGAA

Table 2.3: List of short hairpin RNAs (shRNAs) used in this study.

CHAPTER 3

The role of αv integrins in human skin tissue generation, maintenance and wound healing

Parts of this chapter have been previously published in:

Duperret EK, Dahal A, Ridky TW. Focal adhesion-independent integrin αv regulation of FAK and c-myc is necessary for 3D skin formation and tumor invasion. *J Cell Sci.* 2015; 128(21):3997-4013.

RESULTS

RNAi screen to identify integrins necessary for organotypic skin

In order to define functional roles for all integrins expressed in human epidermis, we designed an shRNA screen in human organotypic skin. We first determined which integrins are expressed in primary keratinocytes and found robust expression of 16 of the 26 integrin subunits (Figure 3.1A,B). The well-studied β3 integrin subunit was not expressed in human keratinocytes, though it was robustly expressed in human melanocytes (Figure 3.1A,B). We then screened shRNA libraries to identify individual hairpins with the ability to reduce transcript levels by more than 75% (Figure 3.1C).

Individual keratinocyte populations were transduced with each shRNA hairpin, and a second virus driving expression of a unique barcoded fluorescent reporter to allow for quantification of the relative representation of each cell population in a mixed group (Figure 3.2A). Pooled integrin knockdown cells and scrambled hairpin control cells were mixed at equal ratios and used to regenerate epidermis. The relative representation of each cell population in the starting mixture was compared to that in established day 14 tissue (Figure 3.2A). Several subunits appeared necessary for keratinocyte proliferation and survival, including α4, α5 and αv (Figure 3.2B). Keratinocytes lacking these subunits displayed a greater than 100-fold fitness disadvantage compared to controls (Figure 3.2B). We chose to focus functional studies on αv,

because 1) it was strongly selected against in the screen, 2) it dimerizes with nearly all β subunits, 3) it's role in human skin was poorly understood, and 4) it has been shown to promote cancer in other tissues (Ricono et al., 2009; Weis and Cheresh, 2011). In contrast to the keratinocyte results, we found that αv loss in melanocytes conferred no survival advantage or disadvantage in tissue (Figure 3.2B). This helps confirm that the fitness disadvantage in the αv knock down keratinocytes did not result from non-specific off target toxicity.

Integrin αv is necessary for organotypic skin tissue generation

Integrin αv is expressed in healing skin wounds (Cavani et al., 1993; Clark et al., 1996). We determined that αv is also robustly expressed in neonatal skin, with highest expression in the plasma membrane of proliferative basal layer cells (Figure 3.3A). To verify the critical role of αv in normal skin in a non-competitive context, we knocked down αv in human keratinocytes using two independent hairpins and seeded these cells in organotypic culture (Figure 3.3B). Loss of αv resulted in severely compromised tissue that was approximately 1/3 the thickness of controls, and lacked proliferative, BrdU+ basal cells (Figure 3.3B,C). This proliferation arrest was not caused by premature differentiation, as skin tissue lacking αv still lacks K10 expression in the basal layer (Figure 3.3B). This organotypic skin lacking integrin αv did not form viable tissue when grafted onto SCID mice, and only resulted in inflammation and scarring with no epidermis present (Figure 3.3D). These results indicate a crucial role for integrin αv in establishing human epidermis.

Integrin αv's major binding partners in skin are β5 and β6

Integrin αv has several potential binding partners including β1, β3, β5, β6 and β8, all of which except β3 are expressed in keratinocytes (Figure 3.4A,B). In immunoprecipitation and western blotting experiments, we found that αv bound to β5, β6 and β8, but not β1 (Figure 3.4B). To determine which β subunits are most critical in mediating the αv loss phenotype, we knocked down each β subunit individually (Figure 3.4C). β5, β6 and β8 are all obligate binding partners with αv and cannot bind to any other α subunit. Thus, knock down of each β subunit alone leads

to depletion of only one αv heterodimer. Immunoprecipitation experiments showed that knock down of one β subunit did not lead to increased αv heterodimerization with other β subunits (Figure 3.4D). In contrast, β5 knock down led to a slight reduction in αv immunoprecipitation with β6 and vice versa (Figure 3.4E).

To determine the specific effects of αvβ5, αvβ6 and αvβ8 on skin tissue generation, we knocked down each β subunit individually in keratinocytes and then seeded them onto our organotypic skin model (Figure 3.5A). We found that loss of αvβ5 or αvβ6 individually were able to phenocopy the loss of skin tissue proliferation seen upon loss of all αv heterodimers (Figure 3.5A-C). αvβ5 was slightly more essential than αvβ6, according to tissue thickness and BrdU quantification (Figure 3.5B,C). Knock down of β8 alone had no appreciable effect on skin tissue thickness and BrdU uptake, indicating that αvβ8 is dispensable for skin tissue generation (Figure 3.5B,C). These results correlate well with our shRNA screening results and also with the relative expression levels of each of these β subunits.

Knock down of integrin β1 in skin tissue leads to distinct morphological changes in comparison to αv loss (Figure 3.6A,B). Loss of β1 led to blistering at the epidermal-dermal junction, and no change in BrdU uptake (Figure 3.6A). In conclusion, the impairment in tissue formation in response to αv loss is due to the action of αvβ5 and αvβ6.

Integrin αv is required for organotypic skin tissue generation, but not tissue maintenance

These initial analyses focused on the roles of integrins in tissue generation, and in cultured, “activated” keratinocytes. To determine the effects of integrin αv loss on tissue maintenance, we developed a doxycycline-inducible integrin αv knock down system. We use a TRIPZ vector, where expression of an integrin αv hairpin and RFP are driven off of a doxycycline-inducible promoter. In order to get effective knock down in primary cells with this vector, we induced expression of the vector, and then flow sorted the cells for high RFP expression (top 20%). We then allowed the cells to recover in doxycycline-free media. We used this system to knock down αv at successive time points during organotypic tissue regeneration (Figure 3.7A).

Integrin αv loss occurred 3-4 days post doxycycline-induction, and persisted throughout the course of the experiment (Figure 3.7C). The phenotypic tissue effects of αv loss were seen only at the earliest time points with thin tissue and corresponding lack of BrdU incorporation (Figure 3.7B). Tissue treated with doxycycline 2 days prior to seeding (day -2) was slightly thicker than the tissue treated with dox 4 days prior to seeding (day -4). The day -2 tissue was able to proliferate for 1-2 days before αv knock down occurred, while the day -4 tissue displayed loss of αv prior to seeding. All other time points showed normal tissue thickness and normal basal epidermal proliferation (Figure 3.7D,E) despite robust loss of αv. These observations indicated that integrin αv is only necessary for the earliest stages of tissue generation, and is not required for maintenance of normal epidermis.

We next examined the effects of αv blockade with a blocking antibody targeting integrin αv, L230. This antibody is reported to target all αv heterodimers (Goswami et al., 2011; Weinacker et al., 1994). We found that treatment with 7μg/mL of blocking antibody led to efficient labeling of organotypic skin primarily in the basal epidermal cells (Figure 3.8C). We performed a similar organotypic tissue generation timecourse utilizing this antibody. We found that treatment of organotypic tissue with L230 blocking antibody at day 0 led to a reduction in tissue thickness, similar to that seen upon αv knock down (Figure 3.8A,B). However, treatment with L230 at a later time point, day 5, did not alter tissue thickness in this organotypic model (Figure 3.8A,B).

We wondered whether these data indicate that αv is required for wound re-epithelialization, but not normal epidermal tissue maintenance. We therefore developed an organotypic re-epithelialization assay utilizing a 3D-printed runway platform (Figure 3.9A). In this system, keratinocytes and melanocytes were seeded onto the left half of the runway, and were blocked from migrating to the right half using a 3D-printed cover (Figure 3.9A). Upon removal of the cover, keratinocytes were induced to migrate and cover the right half of the runway; however, we observed that human melanocytes do not migrate in this system (Figure 3.9A). Utilizing these runway stands, we began antibody treatment 5 days after seeding keratinocytes and melanocytes, at the same time the covers were removed and the keratinocytes were induced to

migrate (Figure 3.9B). Within this re-epithelialization system, it can be visually observed that the L230 blocking antibody prevents re-epithelialization compared to control antibody treatment (Figure 3.9C). Histological examination of this tissue shows that, while control tissue is able to re-epithelialize onto the right side of the tissue, L230 treated epidermis is not (Figure 3.9D). Additionally, the L230 treated tissue on the left side of the runway appeared histologically distinct from the control tissue, despite their similarity in tissue thickness (Figure 3.9E). The L230-treated tissue appeared fragile, with detachment of many epidermal cells from each other and from the basement membrane, after only 5 days of antibody treatment (Figure 3.9E).

Integrin αv is required for proliferation during human wound healing *in vivo*

We next utilized this αv blocking antibody to examine the effects on epidermal processes *in vivo*. We found that the L230 blocking antibody targets human αv, but not mouse αv. Staining of a human foreskin grafted onto a SCID mouse at the human-mouse junction revealed an absence of staining in the mouse epidermal compartment (Figure 3.10A). We next grafted human skin onto SCID mice and examined the effects of L230 treatment on this human skin *in vivo*. While treatment with this antibody led to efficient labeling of the human skin, it did not alter the thickness or overall histological appearance of the skin, compared to control antibody treatment over the course of one week (Figure 3.10B,C). This is in contrast to the L230 treatment in organotypic culture, which led to skin fragility (Figure 3.9E).

We next wondered whether L230 treatment would alter the course of wound healing in our *in vivo* model. As mentioned in the introduction, it has been shown that human skin grafted onto mice resists contraction upon wounding (Escámez et al., 2004). We tested this in our human skin xenograft model. We wounded human skin xenografts on SCID mice using a 2mm punch biopsy, which removed the epidermis and dermis, without altering the fascia and panniculosus carnosus layers (Figure 3.11). We monitored these wounds over time and found that these wounds re-epithelialized without contracting the size of the original xenograft (Figure 3.11). We next examined wound healing at day 2 or day 4 in xenografted mice treated with a mouse IgG (or

IgG1 isotype) control antibody or an L230, αv-blocking, antibody (Figure 3.12, 3.13). At day 2, none of the wounds had healed completely. In control tissue, the wound edge displayed much higher levels of epidermal proliferation compared to wound-adjacent tissue. At the wound edge, it was evident that the L230-treated epidermis was thinner and less proliferative than the control IgG-treated epidermis (Figure 3.12A,B). However, human epidermis that was far from the wound edge did not show any difference in proliferation or epidermal tissue thickness (Figure 3.12B,C). There was no significant difference in the distance that the epidermal tissue had migrated into the wound at this time point (Figure 3.12C). At day 4, all wounds had almost completely re-epithelialized, though the L230-treated wounds showed the same trend with reduced epidermal proliferation and epidermal thickness compared to mouse IgG1-treated epidermis (Figure 3.13A,B). These data indicate that αv integrins are necessary for rapid hyperproliferation in the wound environment, but are dispensable for normal tissue homeostasis.

FIGURES

Figure 3.1

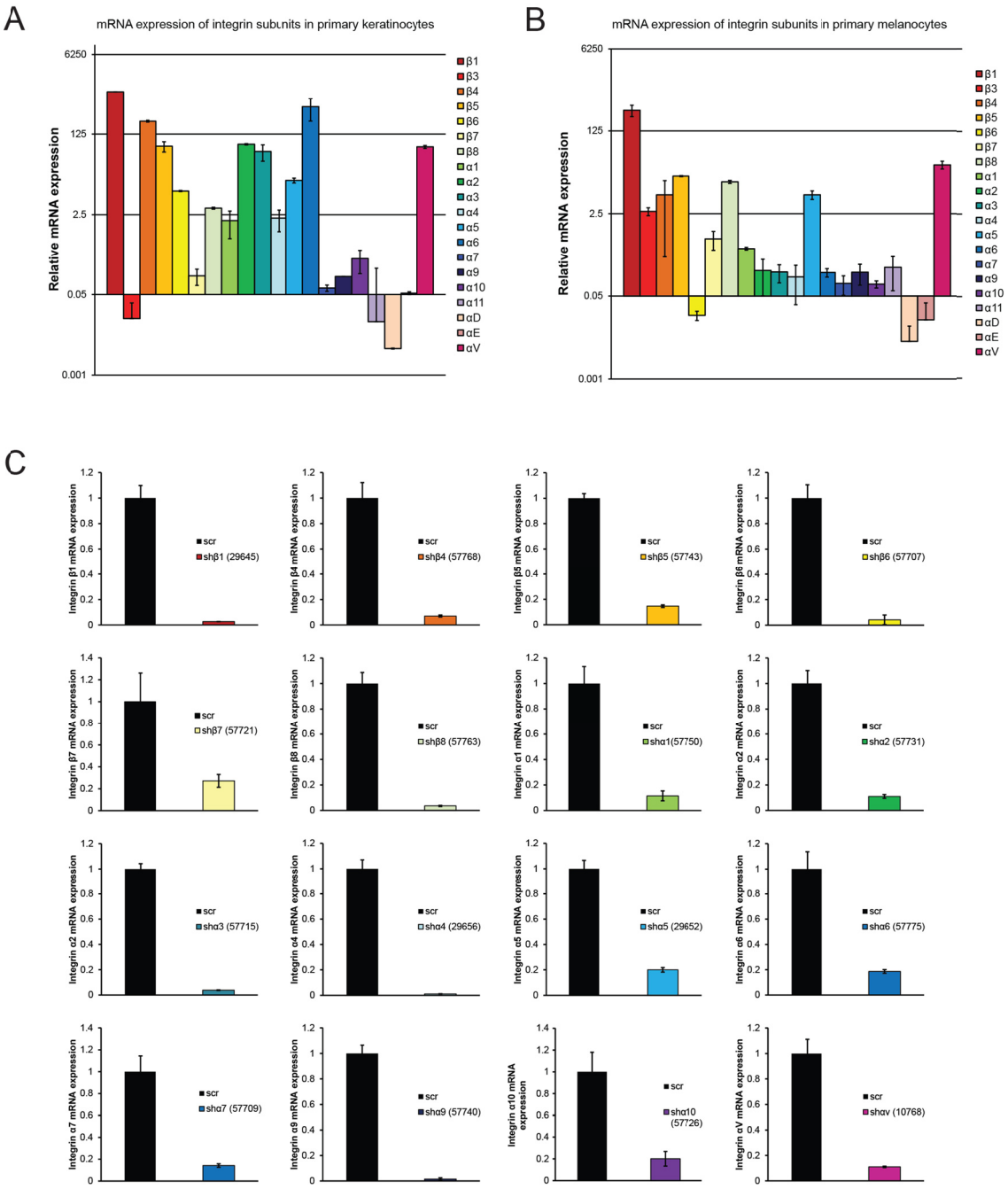

Figure 3.1: Integrin expression and knock down efficiency in keratinocytes and melanocytes. **A,B.** qPCR data showing relative expression levels of the different integrin subunits in cultured human keratinocytes (**A**) or melanocytes (**B**). **C.** Knock down efficiency of integrin hairpins in

cultured human keratinocytes (only the subunits that are expressed within 2000-fold of integrin β1 are shown). Data shown represents the mean of 2 biological replicates ± SD.

Figure 3.2

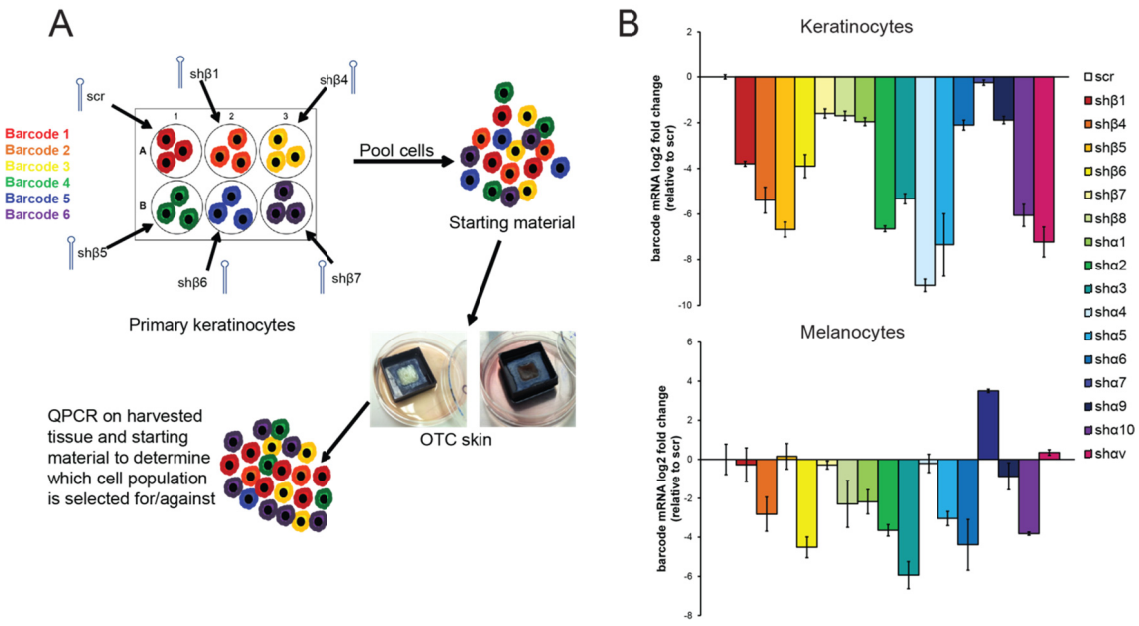

Figure 3.2: RNAi screen to identify integrins necessary for skin tissue generation. **A.** Schematic for competition integrin screen. In brief, individual populations of keratinocytes or melanocytes were each transduced with an integrin hairpin and a unique barcode. Cells were pooled at equal ratios and seeded onto human dermis. Extra cells from starting material were saved for qPCR analysis. Tissue was harvested 14 days after seeding for RNA extraction. **B.** Quantification of integrin knock down competition screen. Values represent fold change in barcode mRNA in harvested tissue compared to starting material. Values are normalized to cells infected with a scramble (scr) hairpin. (n=3 independent organotypic culture tissues per experiment, mean ± SD).

Figure 3.3

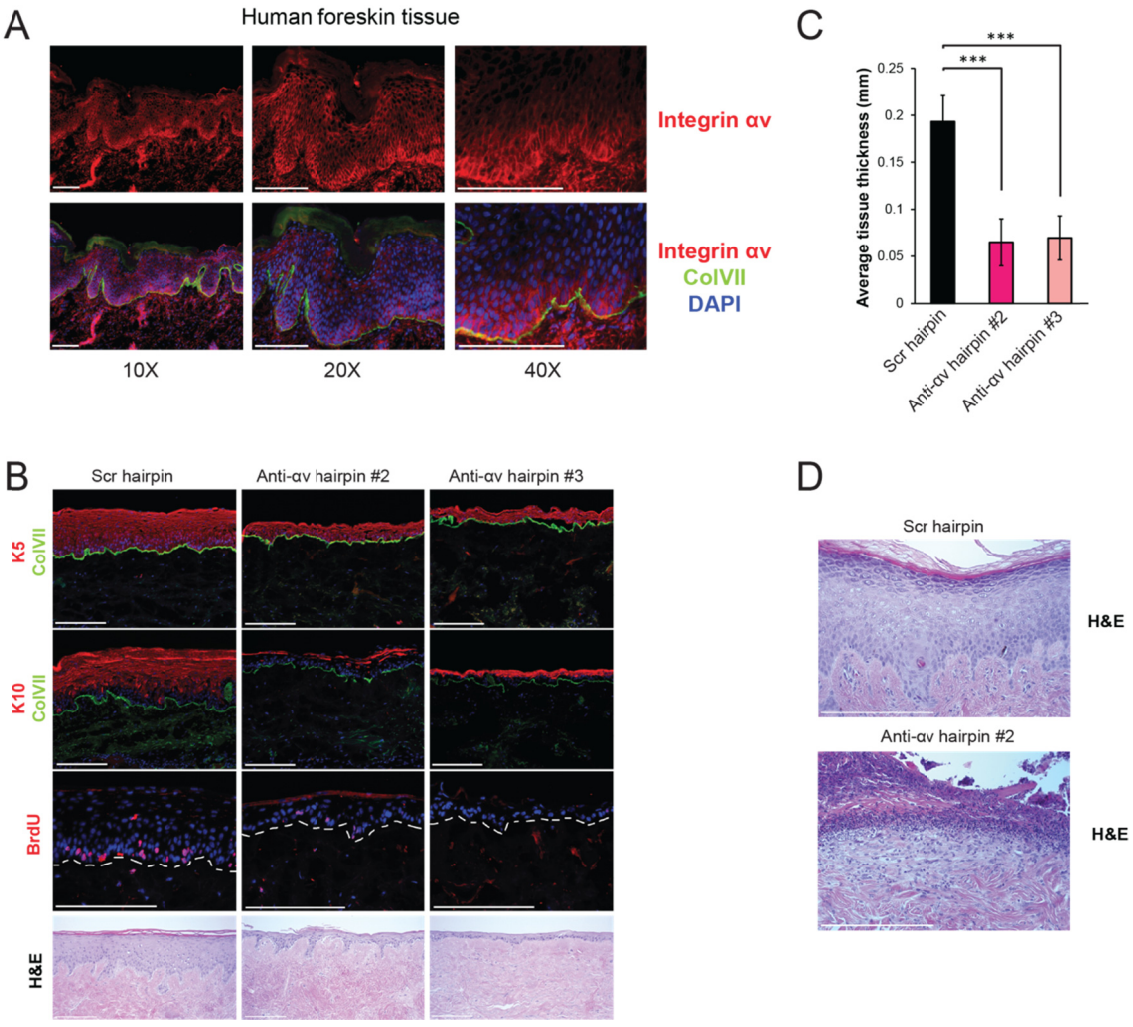

Figure 3.3: Integrin αv knock down prevents organotypic tissue formation and proliferation and prevents skin tissue grafting *in vivo*. **A.** Images of human neonatal foreskin tissue stained using αv antibody. **B.** Morphological analysis of organotypic tissue made with keratinocytes infected with indicated shRNA showing BrdU, K5, K10 and ColVII staining. Bottom panel shows Hematoxylin & Eosin (H&E) stain. **C.** Quantification of tissue thickness from (**B**), measured in mm (mean ± SD). Measurements taken from 2 experiments, each performed with n=3 organotypic culture tissues. P= 3.55×10^{-6} using one-way ANOVA. **D.** Organotypic skin made with keratinocytes infected with the indicated hairpins was grafted onto SCID mice. Hematoxylin &

Eosin (H&E) stain shows tissue graft failure (inflammation and scarring) upon αv knock down.

***=p<0.0005, using Tukey's post hoc HSD.

Figure 3.4

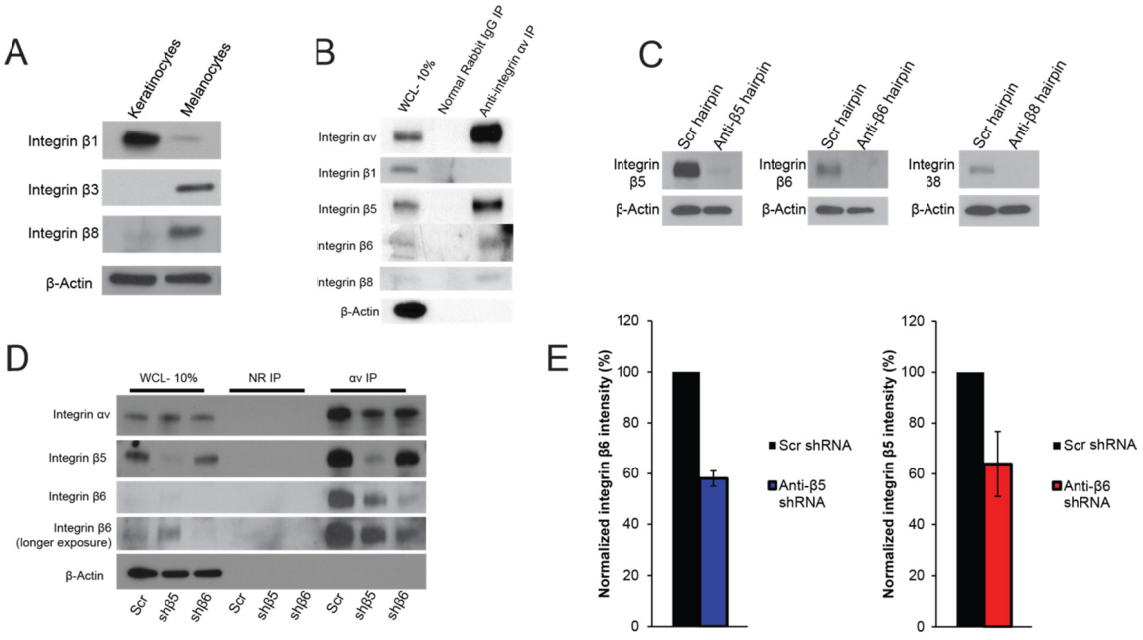

Figure 3.4: Integrin αv binding partners in skin. **A.** Western blot showing integrin expression in keratinocytes compared to melanocytes. **B.** Immunoprecipitation of αv in keratinocytes and subsequent western blot for β subunits. **C.** Western blots showing knock down efficiency of β5, β6 and β8 hairpins in keratinocytes. **D.** Immunoprecipitation of αv in keratinocytes transduced with a control hairpin, β5 hairpin or β6 hairpin and subsequent western blot for various integrin subunits. **E.** Quantification of western blots from (**D**). Shown are averages from 3 replicates (mean ± SD).

Figure 3.5

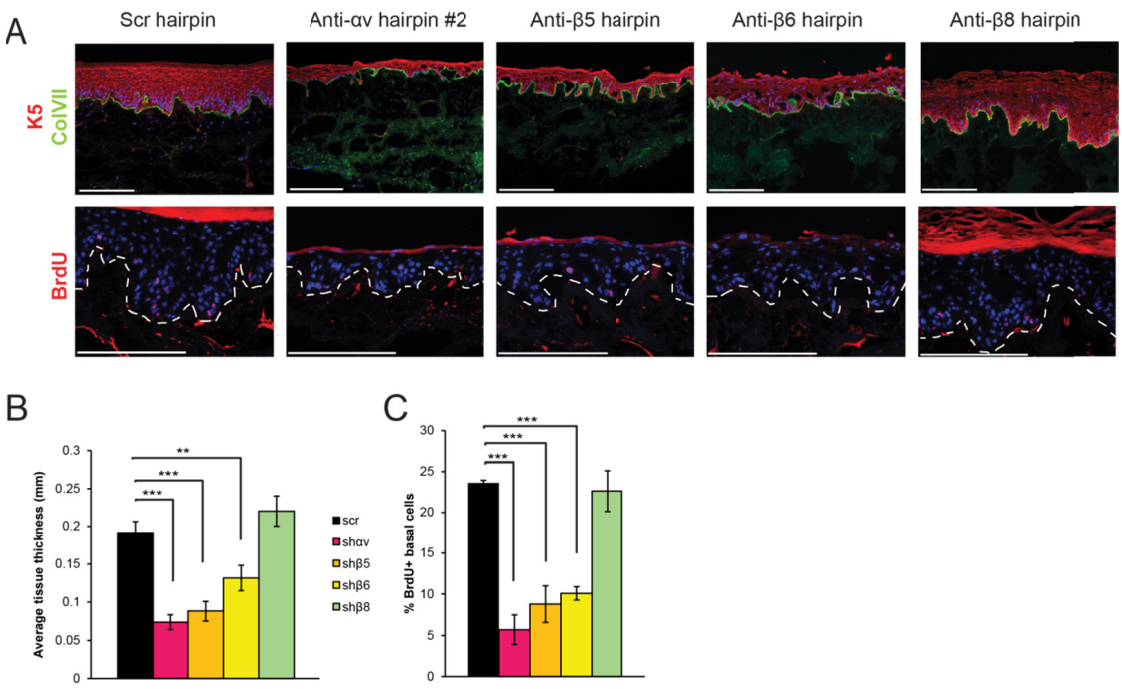

Figure 3.5: Integrin αv controls skin tissue generation through binding partners β5 and β6. **A.** Morphologic analysis of organotypic tissue made with keratinocytes infected with a control hairpin, or hairpins targeting αv, β5, β6 or β8. Tissue is stained for K5/ColVII or BrdU. **B.** Quantification of tissue thickness from (**A**), measured in mm (mean ± SD). N=3 independent organotypic tissues. $P=1.07x10^{-6}$ using one-way ANOVA. **C.** Quantitation of BrdU uptake from (**A**), measured as the percentage of BrdU+ basal epidermal cells (mean ± SD). N=3 independent organotypic tissues. $P=3.01x10^{-7}$ using one-way ANOVA. **=p<0.005, ***=p<0.0005, using Tukey's post hoc HSD. Scale bar= 200μm.

Figure 3.6

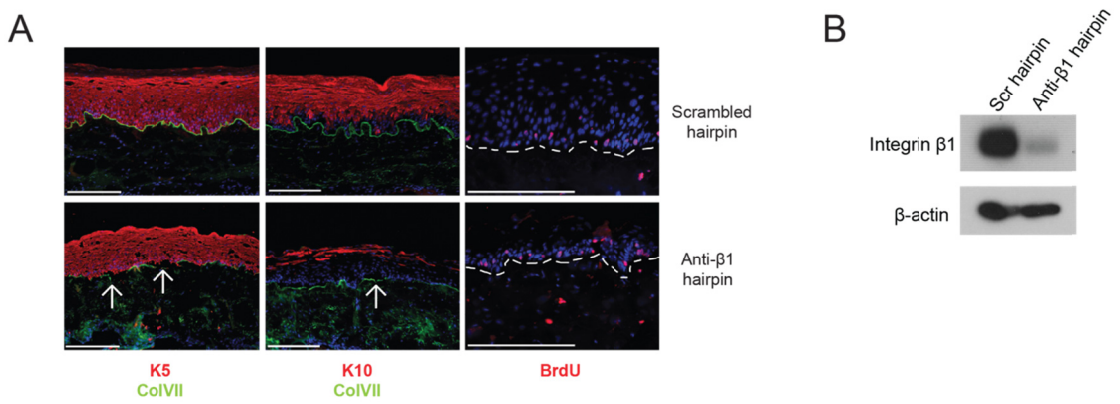

Figure 3.6: Integrin β1 knock down alters epidermal adhesion but not proliferation. **A.** Morphologic analysis of organotypic tissue made with keratinocytes infected with a control hairpin or a hairpin targeting integrin β1. Tissue is stained for K5/ColVII, K10/ColVII or BrdU. Arrows indicate areas of basement membrane disruption. **B.** Western blot showing efficiency of β1 knock down in cultured keratinocytes. Scale bar= 200μm.

Figure 3.7

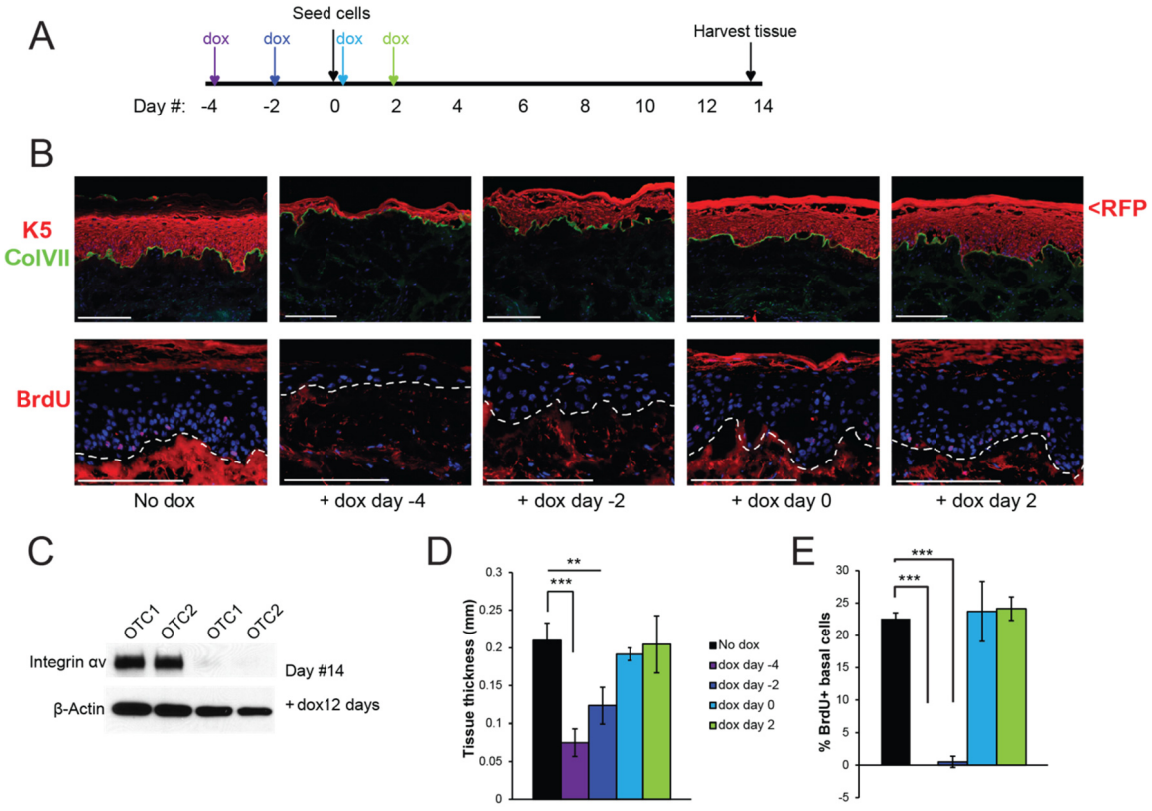

Figure 3.7: αv integrins are required for skin tissue generation but not tissue maintenance in organotypic culture. **A.** Experimental setup. Human keratinocytes infected with TRIPZ-shαv and sorted with flow cytometry were induced with doxycycline at various time points in organotypic culture (indicated with arrows): 4 days prior to seeding, 2 days prior to seeding, day of seeding, 2 days post seeding. **B.** Morphological analysis of organotypic tissue in doxycycline-inducible timecourse experiment described in (**A**). Representative images were taken from 2 independent experiments each performed in triplicate. **C.** Western blot from tissue lysates that were not treated with dox, or treated with dox for 12 days. **D.** Quantification of tissue thickness from (**B**), measured in mm (mean ± SD). Representative analysis from 2 independent experiments. Each experiment contained 3 independent organotypic tissues. P=0.00015 using one-way ANOVA. **E.** Quantification of BrdU+ basal epidermal cells from (**B**) (mean ± SD). Representative analysis from 2 independent experiments. Each experiment contained 3 independent organotypic tissues.

$P=7.52x10^{-8}$ using one-way ANOVA. Scale bar=200μm. **=p<0.005, ***=p<0.0005, using Tukey's post hoc HSD.

Figure 3.8

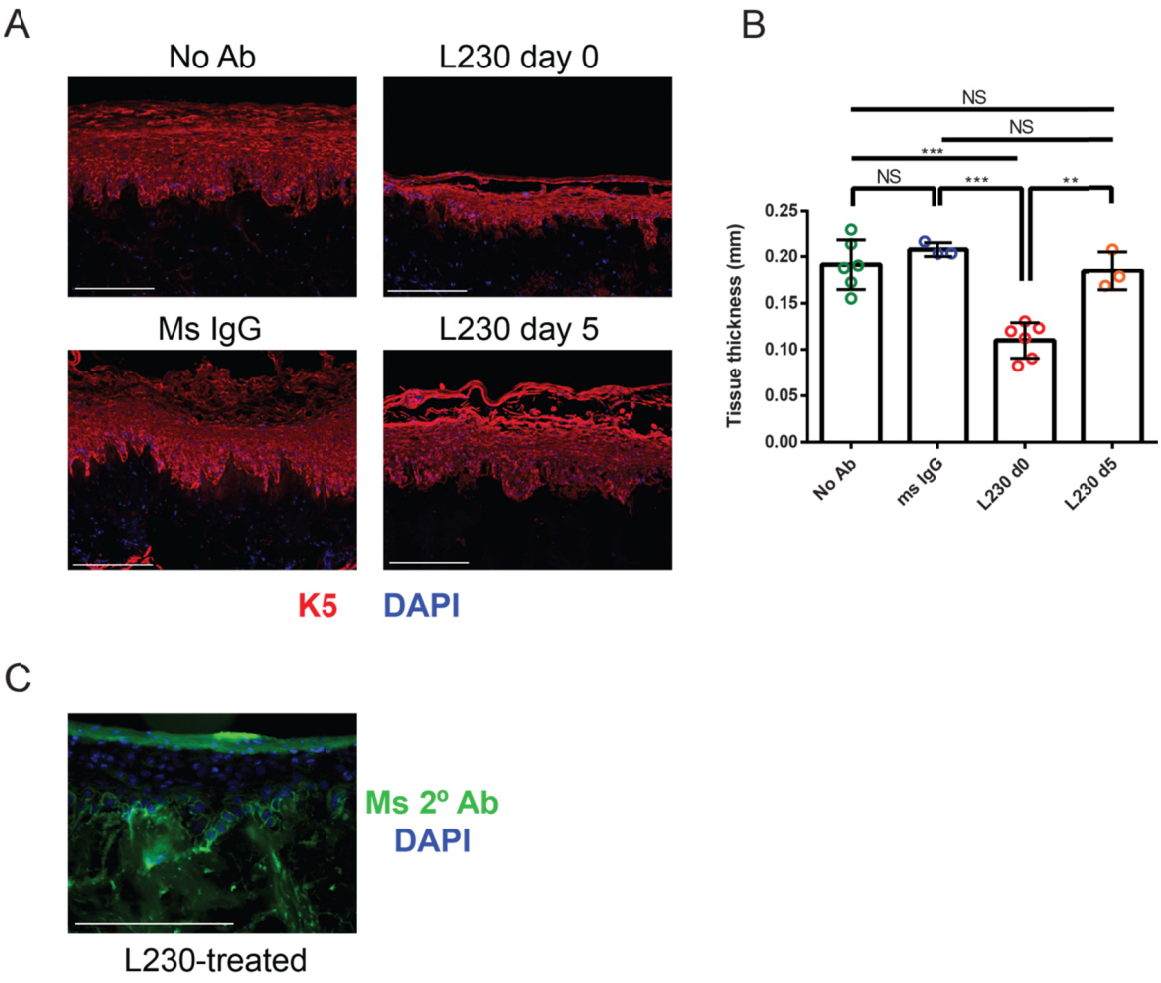

Figure 3.8: Blocking antibody targeting integrin αv recapitulates the effects of integrin αv shRNA knock down in organotypic culture. **A.** Morphologic analysis of organotypic epidermis treated with the indicated antibodies (mouse IgG, control, or L230, αv blocking antibody) and stained with Keratin 5. **B.** Quantification of the tissue thickness from A, in mm. Represented are the mean ± SD. P<0.0001 using one-way ANOVA. n=3-6 organotypic tissues per group. **C.** Immunofluorescence staining of L230-treated tissue with secondary antibody only to show L230 binding to keratinocytes near the basal layer. Scale bar=200μm. NS= not statistically significant. **=p<0.005, ***=p<0.0005, using Tukey's post hoc HSD.

Figure 3.9

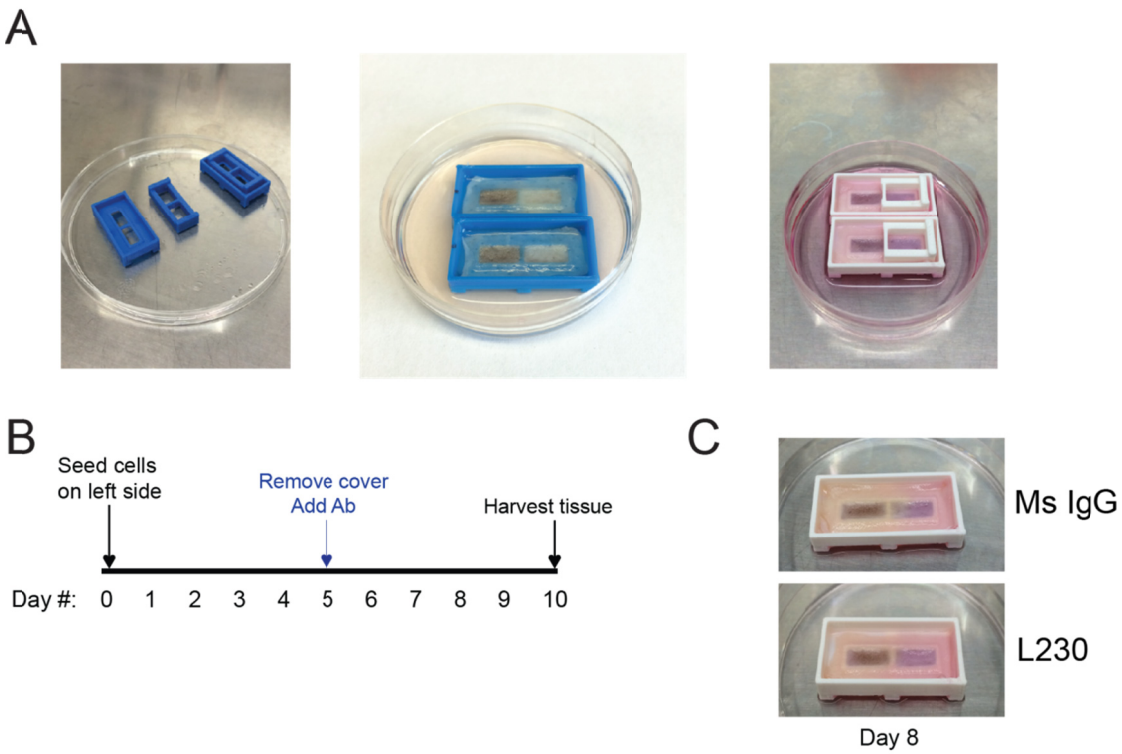
A
B
Seed cells
on left side
Remove cover
Add Ab
Harvest tissue
Day #: 0 1 2 3 4 5 6 7 8 9 10
C
Ms IgG
L230
Day 8
D
Ms IgG
L230
E
Ms IgG
L230

Figure 3.9: Blocking antibody targeting integrin αv blocks re-epithelialization in an organotypic wound healing model. **A.** Images of 3D printed runway for organotypic re-epithelialization assay. **B.** Timecourse for organotypic re-epithelialization assay. Keratinocytes and melanocytes are seeded onto the left side of the runway on day 0, and the right side of the runway is blocked using cover until day 5. On day 5, blocking antibodies are added, and keratinocytes migrate over to the right side over the course of 5 days, until the tissue is harvested on day 10. **C.** Visualization of re-epithelialization assay upon treatment with control (Ms IgG) antibody or L230 antibody. L230 clearly blocks re-epithelialization at day 8 of the assay. **D.** Representative Hematoxylin & Eosin (H&E) stain for tissue shown in (**C**), harvested at day 10. Arrow indicates the start of re-epithelialization. Scale bar=1mm. **E.** Representative H&E images of left portion of tissue shown in (**C**), that is not induced to re-epithelialize. Scale bar=100μm.

Figure 3.10

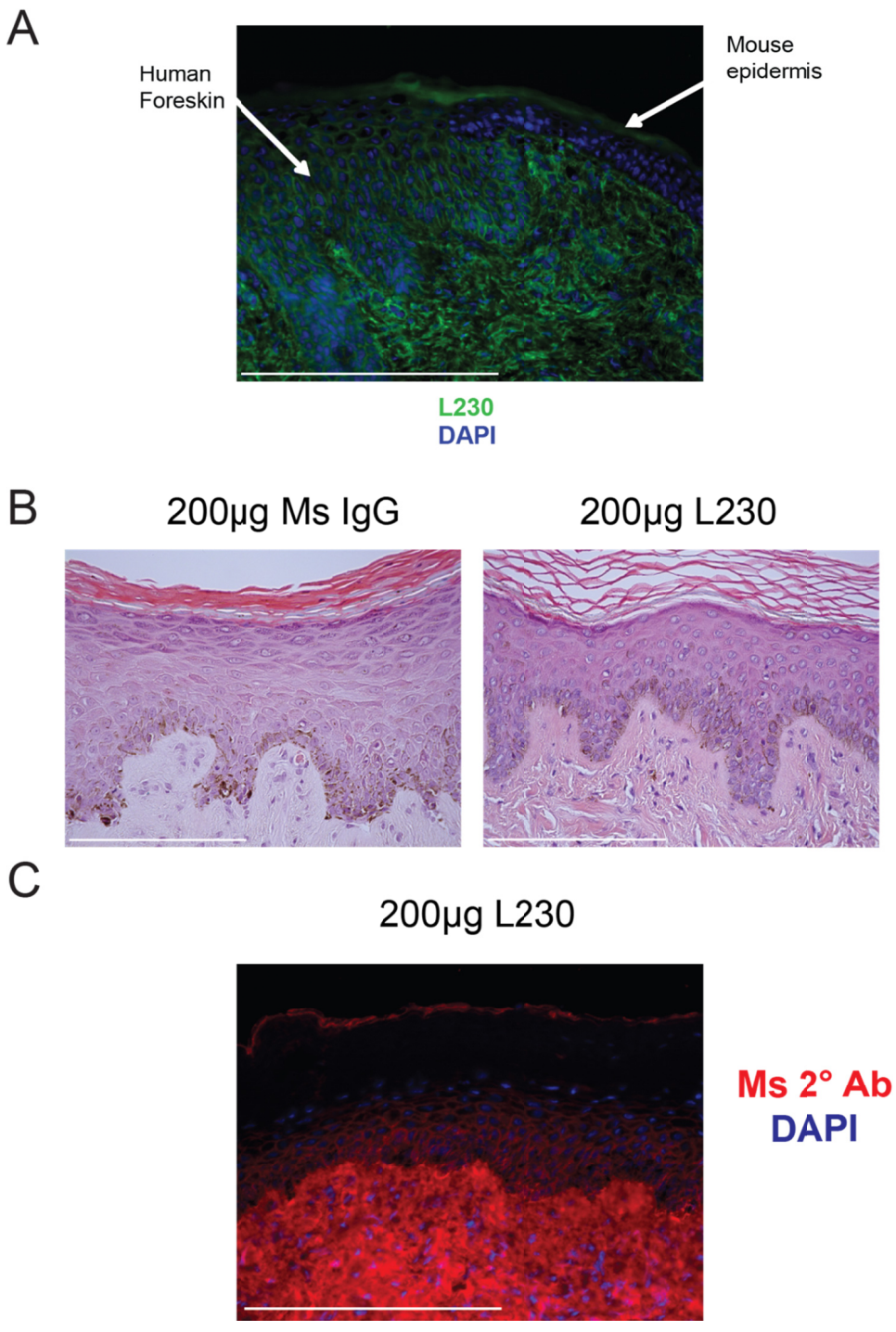

Figure 3.10: Blocking antibody targeting integrin αv (L230) is human-specific and does not alter normal human skin homeostasis *in vivo*. **A.** Immunofluorescence staining of a human foreskin

grafted onto a SCID mouse at the human-mouse junction. Tissue was stained with L230 to show that L230 is a human-specific antibody. **B.** Representative images of normal human skin grafted onto SCID mice, treated with a mouse IgG control antibody or L230 blocking antibody over the course of one week (200μg of antibody, administered subcutaneously every other day). **C.** L230-treated human tissue *in vivo*, stained with secondary antibody only to show efficient labeling of human keratinocytes with antibody. Scale bar= 200μm.

Figure 3.11

Figure 3.11: Human skin xenograft wounds heal via re-epithelialization without contraction. Images of human skin xenograft wound healing over time. Pigmented human organotypic skin was grafted onto a SCID mouse and wounded with a 2mm punch biopsy. The wound was monitored every day over the course of 5 days. The human skin wound heals without contraction.

Figure 3.12

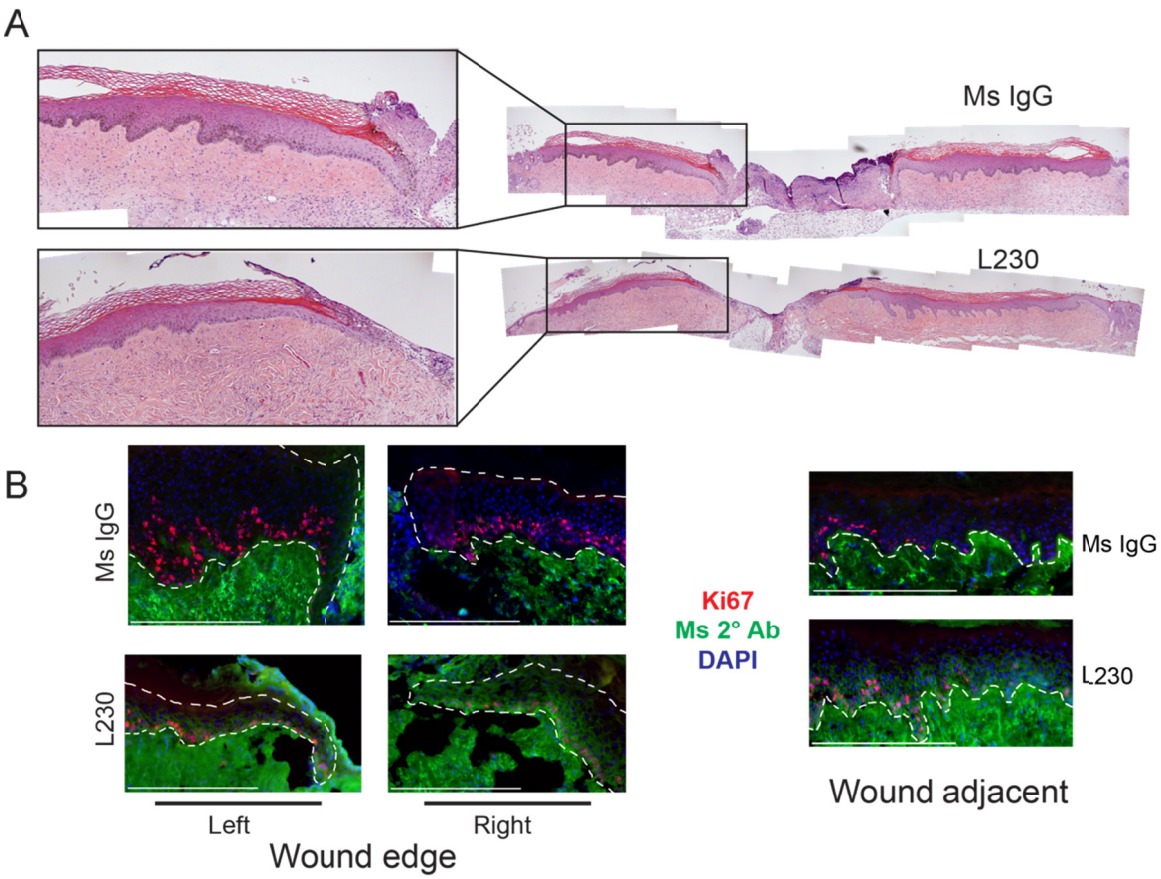

Figure 3.12: Integrin αv is necessary for proliferation during wound healing of human skin *in vivo* at day 2. **A.** Representative Hematoxylin and Eosin (H&E) stains for wounds from mice treated

with a control mouse IgG antibody or an L230 antibody. Mice were treated with 100μg of antibody per day, beginning the day prior to wounding. Wounds were harvested 2 days after wounding. **B.** Representative images of Ki67 and mouse secondary antibody labeling of wound edge and wound adjacent tissue. Dotted lines outline epidermal part of wound. **C.** Quantification of %Ki67+ epidermal cells and epidermal thickness at wound edge and in wound adjacent tissue, and epidermal migration into wound (mm). Wound edge was considered within 0.25mm of wound. NS= not statistically significant. P values were calculated using a student's t-test. Scale bar= 200μm.

Figure 3.13

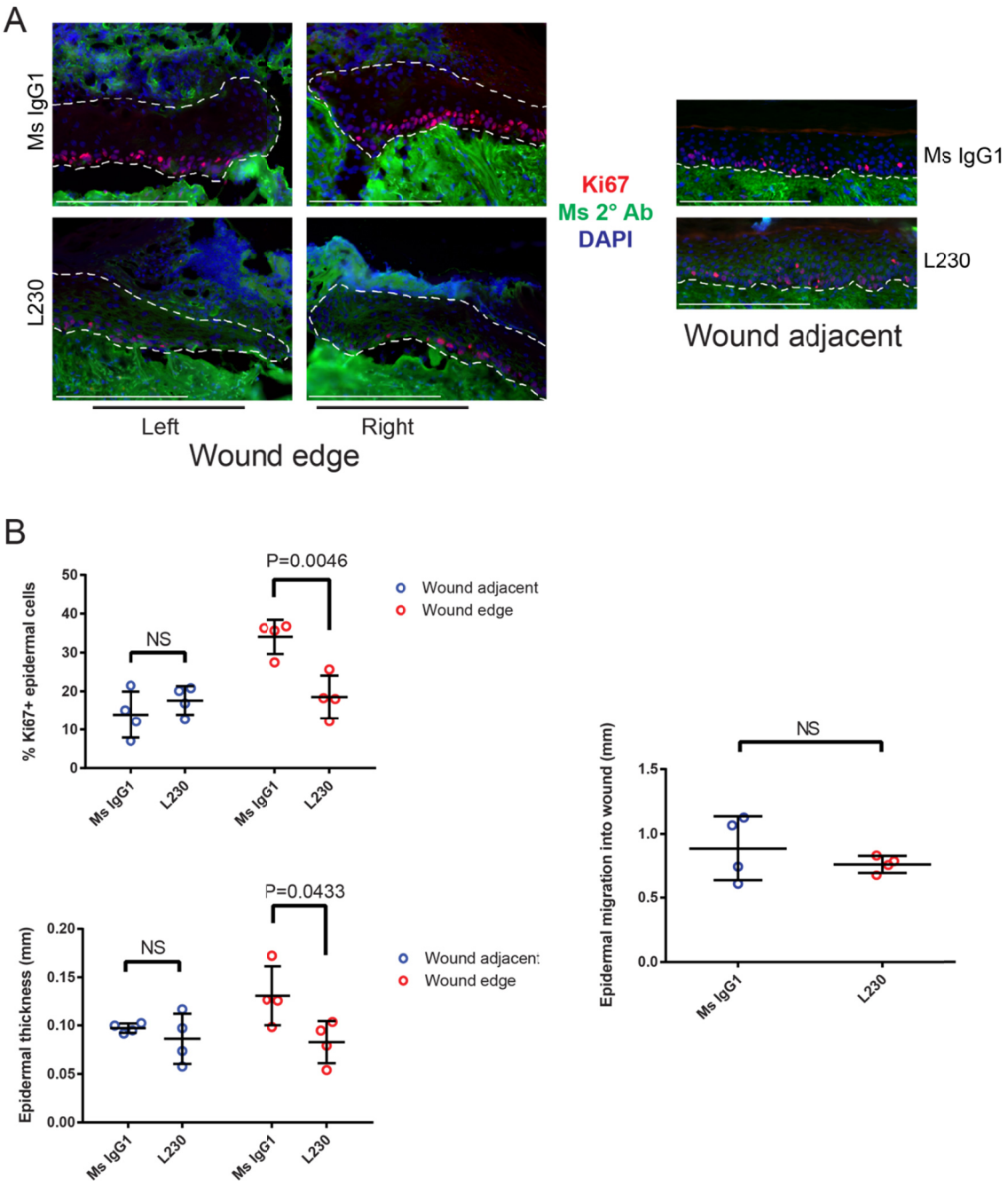

Figure 3.13: Integrin αv is necessary for proliferation during wound healing of human skin *in vivo* at day 4. **A.** Representative images of Ki67 and mouse secondary antibody labeling of wound edge and wound adjacent tissue. Dotted lines outline epidermal part of wound. Mice were treated with 100μg of antibody per day, beginning the day prior to wounding. Wounds were harvested 4

days after wounding. **B.** Quantification of %Ki67+ epidermal cells and epidermal thickness at wound edge and in wound adjacent tissue, and epidermal migration into wound (mm). Wound edge was considered within 0.25mm of wound. NS= not statistically significant. P values were calculated using a student's t-test. Scale bar= 200μm.

DISCUSSION

αv integrins and several of their ligands, including TGFβ, Thrombospondin and Vitronectin, are up-regulated in the wound environment (Longmate and Dipersio, 2014). It was previously unclear what the role for αv integrins were in this setting, since previous reports described no effect for β5 in wound healing, and only an effect of β6 in wound healing in aged mice (AlDahlawi et al., 2006; Huang et al., 1996; Huang et al., 2000a). Here, we have shown for the first time that αv integrins—primarily αvβ5 and αvβ6 are necessary for rapid proliferation during organotypic tissue generation and during epidermal wound re-epithelialization.

The remodeling of the extracellular matrix is a crucial event during the course of wound healing. It is essential to understand how keratinocytes respond to changes in the extracellular matrix to stimulate re-epithelialization of the wound. Dysregulation in the process of wound healing—at the level of inflammation, ECM deposition, ECM degradation or keratinocyte proliferation and migration—can result in chronic wound formation (Reinke and Sorg, 2012). Chronic wounds comprise a significant health burden in the United States, with over 6.5 million patients affected (Sen et al., 2009). Chronic wounds rarely occur in healthy populations, but rather are frequent in elderly populations and patients suffering from diabetes and obesity (Sen et al., 2009). Chronic wound types include venous stasis ulcerations, pressure sores and diabetic foot ulcers. Inflammation in non-healing skin wounds can promote secondary Squamous Cell Carcinoma formation within the wound itself (Trent and Kirsner, 2003). Currently, there are limited treatment options for chronic wounds, with only 2 FDA-approved therapies: platelet derived growth factor (PDGF) and a human skin equivalent (Mustoe, 2004). These treatments have limited clinical success, and there are no approved treatments that promote keratinocyte re-epithelialization.

Current strategies in development for treatment of chronic wounds target the processes of re-epithelialization, angiogenesis and/or tissue granulation (Mustoe, 2004). Current treatments in development include plasminogen administration, MMP-9 inhibition, keratinocyte growth factor (KGF) administration and granulocyte-macrophage colony stimulating factor (GM-CSF)

administration (Gooyit et al., 2014; Koria et al., 2011; Marques da Costa et al., 1997; Shen et al., 2012). However, activation of integrins to promote wound re-epithelialization has not been examined. Based on our results, activation of integrin αv using RGD-based peptides or agonistic antibodies may be a potential therapeutic strategy for treatment of chronic wounds. However, caution must be taken because β6 over-expression in the mouse results in chronic wound formation (Häkkinen et al., 2004).

This newly discovered role for αv integrins in epidermal proliferation may extend to other epithelial tissues. Thus far, the majority of research on αv integrins has focused on mesenchymal tissues and the hematopoietic system. Deletion of αv integrins in myeloid lineages causes depletion of Tregs (specifically, Th17 T helper cells), enhanced T cell activation and failure of macrophages and dendritic cells to properly remove apoptotic cells (Acharya et al., 2010; Lacy-Hulbert et al., 2007). These phenotypes are largely attributed to dysregulation of TGFβ signaling in response to αv loss. Depletion of αv in myofibroblasts results in reduced susceptibility to hepatic, pulmonary and renal fibrosis, also due to reduced TGFβ activation (Henderson et al., 2013). In the brain, αv loss in neural cells results in defective association between vessels and brain parenchyma, resulting in hemorrhage (McCarty et al., 2002; McCarty et al., 2005). The roles that αv plays in various tissues may be entirely dependent on the roles of TGFβ signaling in that particular tissue. The roles for αv in other epithelial tissues with proliferative basal cells, such as breast, colon, intestine, ovary, cervix, esophagus, and many others, are still unknown. Given the role for αv in re-epithelialization during cutaneous wound healing, this integrin may also contribute to mucosal wound healing in inflammatory bowel diseases like Crohn's disease or ulcerative colitis, thus opening up new therapeutic opportunities (Neurath, 2014).

Despite our evidence for a pro-proliferative role for integrin αv during wound healing, there are several reports for an anti-proliferative role of αv integrins in epithelial tissues. The role of integrin αv has been examined in epithelial cells of the eyelid and conjunctiva, and in a skin tumor model (McCarty et al., 2008; Savar et al., 2014). Deletion of αv in the eyelid and conjunctiva results in spontaneous squamous cell carcinoma formation, potentially due to

dysregulation of TGFβ signaling (McCarty et al., 2008). Deletion of αv in the mouse epidermis in the absence of p53 leads to accelerated tumor formation (potentially due to Akt activation), but then slowed tumor growth, potentially due to decreased immune cell infiltration and vascularization of the tumors (Savar et al., 2014). This was found to be a TGFβ-independent phenotype. Integrin β6 deficient mice show enhanced proliferation in hair follicles after depilation, also in a TGFβ-dependent manner (Xie et al., 2012). Some of these differences in phenotypes may be the result of the dose-dependent effects of TGFβ signaling. Partial blockade of αv integrins may have different effects compared to complete genetic ablation of this gene. Furthermore, TGFβ signaling may have slightly different effects in mouse and human skin. We will address the dependence of our αv phenotypes on TGFβ signaling more in Chapter 4.

CHAPTER 4

Focal adhesion-independent integrin αv control of cell cycle progression through TGFβ, FAK and c-myc signaling pathways

Parts of this chapter have been previously published in:

Duperret EK, Dahal A, Ridky TW. Focal adhesion-independent integrin αv regulation of FAK and c-myc is necessary for 3D skin formation and tumor invasion. *J Cell Sci.* 2015; 128(21):3997-4013.

RESULTS

Integrin αv does not localize to focal adhesions in keratinocytes

To identify critical αv-activated signaling pathways, we first examined its spatial localization relative to focal adhesions (FAs) in keratinocytes compared to dermal fibroblasts. Consistent with previous reports indicating a role for αv integrins in fibroblast adhesion maturation (Schiller et al., 2013), αv localized to large Paxillin-containing FAs in fibroblasts, while β1 localized to smaller, less mature, FAs (Figure 4.1A). In striking contrast, we found that αv did not associate with keratinocyte FAs, while β1 was tightly co-localized with all keratinocyte FAs (Figure 4.1B). We confirmed this result on a variety of different substrates, including Collagen, Fibronectin and Vitronectin (Figure 4.1C). Keratinocytes on these substrates still secrete β1 ligands and thus still form Paxillin-containing adhesions (Alitalo et al., 1982; Chung et al., 2011). However, Vitronectin, an αv-specific ligand, did not induce αv FAs (Figure 4.1C).

Integrin αv knock down did not alter the number or size distribution of FAs within keratinocytes grown on Collagen, Fibronectin or Vitronectin (Figure 4.2A,C). In contrast, β1 knock down in human keratinocytes abolished nearly all FA formation (Figure 4.2A). Loss of β1, but not αv, also significantly decreased cell spreading area and mechanical adhesion to the growth surface (Figure 4.2B).

Further, while β1 localized to the tips of actin filaments in keratinocytes, αv did not, indicating that αv likely does not connect the ECM to the actin cytoskeleton in keratinocytes (Figure 4.3C). Consistent with this idea, αv expression was not restricted to the cell-substrate basal adhesive surface in keratinocytes, and instead localized throughout the cell membrane (Figure 4.3A,B). We confirmed αv expression at the cell surface by immunofluorescence without permeabilization (Figure 4.3D).

The mechanistic basis for the differential αv localization between keratinocytes and fibroblasts is unclear. We considered the possibility that β3, which is absent in human keratinocytes yet present in fibroblasts, directs αv to FAs. To test this possibility, we expressed β3 in human keratinocytes and examined the localization of the αvβ3 heterodimer (Figure 4.4A,B). While we achieved high levels of β3 expression which localized to the plasma membrane, it was insufficient to direct αv to Paxillin-containing FAs (Figure 4.4B). Consistent with this, β3 depletion in human fibroblasts decreased the number of αv-containing FAs, but did not abolish them completely (Figure 4.4C).

Integrin αv controls cell cycle progression in keratinocytes

The differing roles of αv and β1 in keratinocyte adhesion are consistent with the tissue phenotypes observed upon knock down of each of these subunits in Chapter 3. Integrin αv knock down led to decreased tissue thickness and BrdU incorporation, while β1 knock down led to minor blistering at the dermal-epidermal junction, with no effects on tissue thickness or BrdU incorporation. Cultured keratinocytes on plastic lacking αv undergo the same cell cycle arrest, and exhibit a 4-5 fold increase in the G1/S ratio, measured using PI staining and flow cytometry (Figure 4.5A,C). Cultured keratinocytes lacking αv also lack Rb phosphorylation, consistent with activation of a G1-S cell cycle checkpoint (Figure 4.5B). αv knock down also led to decreased levels of total Rb, potentially due to the fact that Rb is an E2F transcriptional target (Shan and Chang, 1994).

To determine which signaling pathways are involved in cell cycle progression downstream of integrin αv, we examined several candidate pathways known to be involved in integrin signaling or cell cycle progression. We did not observe a change in Src signaling or Cdk4 levels; however, we observed a decrease in both total and phospho-c-Jun protein, and an increase in p27 protein (Figure 4.6A). Since c-Jun and other integrin-regulated pathways are known to control Cyclin D levels, we re-introduced wild-type or degradation resistant (T286A) Cyclin D1 to control or αv knock down cells (Figure 4.6B). However, over-expression of these proteins was insufficient to restore Rb phosphorylation in keratinocytes lacking αv (Figure 4.6B). We rescued c-Jun phosphorylation through expression of MKK7, an upstream activator of c-Jun (Figure 4.6C). Despite efficient rescue of c-Jun phosphorylation, this was insufficient to restore Rb phosphorylation to αv knock down cells (Figure 4.6C). We also observed a decrease in Skp2, an E3 ubiquitin ligase for p27, upon integrin αv knock down (Figure 4.6D). We hypothesized that the decrease in Skp2 might be responsible for the dramatic increase in p27 protein levels. However, re-expression of Skp2 in αv knock down cells was insufficient to rescue either p27 protein levels or Rb phosphorylation (Figure 4.6D). Even co-expression of a cyclin-dependent kinase inhibitor-resistant Cdk4 (R24C) and a dominant-negative p53 (dnp53) was insufficient to rescue the G1-S checkpoint blockade in αv knock down cells (Figure 4.6E).

Integrin αv controls cell cycle progression through a FAK→ c-myc signaling axis

Despite the lack of αv localization within keratinocyte FAs, we observed a near-complete loss of both phosphorylated and total Focal Adhesion Kinase (FAK), a key regulator of FA signaling, upon αv knock down (Figure 4.7A). We also observed a striking loss of c-myc protein levels with either αv knock down or specific FAK inhibition (Figure 4.7A,C). To gain further insight into mechanisms driving cell cycle arrest after αv loss, we used doxycycline-inducible αv shRNA to define the sequence and timing of the loss of downstream signaling pathways (Figure 4.7B). Integrin αv loss was nearly complete at 3 days post dox induction (dpi); FAK depletion followed at 4-5 dpi (consistent with FAK's long half-life), and ultimately c-myc loss at 6 dpi, immediately prior

to cell cycle arrest (Figure 4.7B). Unlike the other signaling pathways that we examined, re-expression of c-myc was sufficient to rescue the growth arrest without affecting upstream FAK levels (Figure 4.7D). This 2D cell culture phenotype was re-capitulated in organotypic culture, where re-expression of c-myc in αv-null skin was sufficient to rescue tissue thickness and basal cell proliferation, while preserving normal stratification and differentiation (Figure 4.7E-G). These data suggest that αv controls cell cycle progression through a FAK→c-myc signaling pathway.

While FAK loss in murine keratinocytes leads to anoikis in *in vitro* culture (McLean et al., 2004), we did not observe anoikis in our human αv-depleted keratinocytes lacking FAK (Figure 4.8A). In contrast, β1 depletion in keratinocytes led to significant anoikis (Figure 4.8A). To determine whether this discrepancy might be due to differences between mouse and human keratinocytes, we examined anoikis upon FAK inhibition in both human and murine primary keratinocytes (Figure 4.8A,B). While FAK inhibition did not induce anoikis in human keratinocytes, FAK inhibition in murine keratinocytes led to a modest increase in TUNEL staining (Figure 4.8A,B). These differences might be the result of *in vitro* culture conditions, since mouse keratinocytes lacking FAK can proliferate under certain optimized conditions (Schober et al., 2007).

Integrin αv controls FAK expression and activation through TGFβ signaling

We next questioned how αv controls FAK expression and activation. αv regulates FAK at the post-transcriptional level since αv loss does not alter FAK mRNA (Figure 4.9A). Previous efforts have linked TGFβ signaling to FAK activity and/or FAK expression through a variety of different mechanisms (Brooks et al., 1996; Cicchini et al., 2008; Kracklauer et al., 2003; Rolli et al., 2003; Thannickal et al., 2003; Wang et al., 2004; Wendt and Schiemann, 2009). Because of αv's role in activating latent TGFβ through force-dependent or MMP-dependent mechanisms, we questioned if this could explain the FAK loss observed upon αv depletion (Mamuya and Duncan, 2013). Consistent with the hypothesis that αv loss inhibits TGFβ, we observed a loss of Smad3 phosphorylation upon αv knock down (Figure 4.9B). We treated control or αv knock down cells

with exogenous TGFβ1 and observed a dose-dependent increase in both phospho- and total FAK protein in αv null cells that peaks at 10pM and tapers off at higher concentrations (Figure 4.9C). The lack of dose-dependent increase in FAK phosphorylation in control cells is potentially due to saturation of FAK activation (Asthagiri et al., 1999). This suggests that αv control of TGFβ signaling is at least partially responsible for maintaining FAK expression and activity.

We next wondered whether αv's regulation of TGFβ signaling was responsible for αv's role in re-epithelialization. We thus performed re-epithelialization assays using a pan-αv blocking antibody, L230, and an αvβ6 specific blocking antibody, 10D5. We also treated these runways with 1pM or 100pM TGFβ1. We found that both L230 and 10D5 significantly reduced epidermal re-epithelialization, though the effect of L230 was stronger (Figure 4.10A-C). We also found that addition of TGFβ1 in the presence of either L230 or 10D5 at least partially rescued re-epithelialization in a dose-dependent manner (Figure 4.10B,C). 100pM of TGFβ1 was sufficient to almost completely rescue both epidermal migration and epidermal thickness for both L230 and 10D5 treatments (Figure 4.10B,C). Thus, αv's control of epidermal re-epithelialization depends on TGFβ signaling.

To determine whether TGFβ is regulated by MMP or force dependent mechanisms in keratinocytes, we treated keratinocytes with either a dual MMP2/9 inhibitor or the actin polymerization inhibitor Cytochalasin D (Figure 4.11A). We observed a decrease in p-Smad3 with MMP inhibition, but not with Cytochalasin D-mediated cytoskeleton disruption (Figure 4.11A,B). These results suggest that αv does not control TGFβ signaling through adhesion-mediated forces, but rather through MMPs. It is also possible that MMPs and αv are required in parallel for regulation of TGFβ signaling.

To further explore the mechanism by which αv controls FAK protein in keratinocytes, we expressed wild-type FAK or hyperactive SuperFAK and then induced αv knock down. Exogenously expressed FAK or SuperFAK was properly phosphorylated at its Y397 auto-phosphorylation site in control cells (Figure 4.12A,C). Expression of exogenous FAK or SuperFAK was sufficient to rescue total FAK protein, but not FAK activity in αv-null keratinocytes

(Figure 4.12A,C). Furthermore, FAK localization at FAs was lost upon αv knock down, even in the presence of supplemental exogenous FAK (Figure 4.12B). This indicates that αv contributes to both FAK expression and FA localization in human keratinocytes.

Integrin αv and FAK control c-myc protein translation through p38 and p90RSK

αv and FAK regulation of c-myc protein occurs post-transcriptionally as c-myc transcript levels are unaltered upon either αv knock down or FAK inhibition (Figure 4.13D,E). We next examined c-myc half-life in αv knockdown or FAK inhibited cells and found no enhancement of c-myc protein degradation in either setting (Figure 4.13F,G). This indicates that αv and FAK likely influence c-myc translation. To test the hypothesis that c-myc protein translation is regulated by αv and FAK through elements in the 5' or 3'UTR, we generated chimeric reporter constructs containing doxycycline-inducible luciferase with 1) no UTRs, 2) the 5'UTR of myc, or 3) the 3'UTR of myc (Figure 4.13A). We transduced keratinocytes with these constructs, antagonized αv or FAK, and then induced luciferase expression. αv loss or FAK inhibition led to decreased luciferase activity only when the luciferase transcript contained the myc 5'UTR (Figure 4.13B,C). These findings indicate that αv and FAK control 5'UTR-dependent c-myc translation.

Cap-dependent c-myc protein translation is partially regulated by Akt-mTOR signaling in some settings (Gera et al., 2004). However, we observed an increase in both Akt and p70 S6K phosphorylation upon αv loss, indicating that c-myc translation is likely controlled through alternative αv and FAK- regulated pathways (Figure 4.14A). In that regard, ERK and p38 MAPK are also known to control 5'UTR-dependent c-myc translation through cap-dependent and –independent mechanisms (Shi et al., 2005; Stoneley et al., 2000; Subkhankulova et al., 2001). αv depletion did not consistently alter ERK1/2 phosphorylation, but did decrease p38 MAPK phosphorylation, indicating that this pathway may be involved in c-myc translation (Figure 4.14B). Furthermore, we observed a decrease in the phosphorylation of p90RSK upon αv knock down (Figure 4.14B). While ERK1/2 has a well-established role in phosphorylating p90RSK, p38 MAPK has also been shown to promote activation of p90RSK indirectly in some cell types (Roux et al.,

2007; Zaru et al., 2015). Furthermore, we observed a decrease in phosphorylation of two RSK translation machinery targets, RPS6 at Ser235 (but not Ser240) and eIF4B, upon αv knock down (Figure 4.14C) (Degen et al., 2013; Roux et al., 2007). RPS6 phosphorylation at Serine240 is controlled by p70 S6K (Pende et al., 2004). FAK inhibition or FAK knock down led to similar decrease in phosphorylation of both p38 MAPK and p90RSK (Figure 4.14D, 4.15A). This indicates that FAK activity is necessary for activation of these signaling pathways downstream of αv. To test whether lack of p38 activation was directly responsible for these signaling events, we next inhibited p38 (Figure 4.14E). Inhibition of p38 MAPK led to an immediate decrease in RSK phosphorylation, eIF4B phosphorylation, RPS6 Ser235 phosphorylation, c-myc protein expression and Rb phosphorylation without altering ERK1/2 activity or upstream FAK protein levels (Figure 4.14E). We confirmed these results with small molecule inhibitors by using genetic approaches. The p38 inhibitor SB202190 targets both p38α (encoded by MAPK14) and p38β (encoded by MAPK11). At the RNA level, MAPK11 is expressed 10-fold higher than MAPK14, and we thus targeted this transcript with shRNA (Figure 4.15B), which recapitulated the effects of the small molecule p38 inhibitor (Figure 4.15D). Furthermore, restoration of p38 phosphorylation levels in αv-null keratinocytes through expression of a constitutively active MKK6 mutant (MKK6(glu)) was sufficient to rescue cell growth and c-myc protein levels (Figure 4.14G). To test whether RSK activity was directly responsible for these signaling pathway changes, we inhibited RSK (Figure 4.14F). Inhibition of RSK led to a decrease in eIF4B phosphorylation, RPS6 Ser235 phosphorylation, c-myc protein expression, and subsequent growth arrest, without altering FAK levels (Figure 4.14F). We also confirmed these signaling pathway changes using genetic approaches. P90RSK1 (encoded by RPS6KA1) is the predominant p90RSK isoform expressed in keratinocytes (Figure 4.15B). Further, only hairpins targeting p90RSK1 (but not the other two isoforms) reduced pan-RSK1/2/3 levels in keratinocytes (Figure 4.15C). Knock down of p90RSK1 recapitulated the effects of the small molecule p90RSK inhibitor (Figure 4.15E). These data taken together support a pathway in which αv controls c-myc protein translation through activation of FAK, p38 and RSK (Figure 4.14H).

FAK, p38 and p90RSK are necessary for skin tissue generation, but not tissue maintenance

Next, we sought to determine whether the FAK→p38→p90RSK pathway mediating the effects of αv loss in cultured cells was similarly required in 3-D tissue. We inhibited each of these pathway elements at two different time points during epidermal tissue generation: day 0 and day 4. Inhibition of each pathway component led to a decrease in epidermal tissue thickness and S-phase basal cells when inhibitors were added at day 0, but not at day 4 (Figure 4.16A,B). Furthermore, organotypic tissue formed from αv knock down cells showed decreased FAK, c-myc, and p38 and p90RSK phosphorylation, indicating that this pathway is also active in organotypic tissue (Figure 4.16C). Taken together, these data indicate that the αv→FAK→p38→p90RSK signaling pathway plays a crucial role in organotypic epidermal tissue formation, but is relatively dispensable for epidermal maintenance.

FIGURES

Figure 4.1

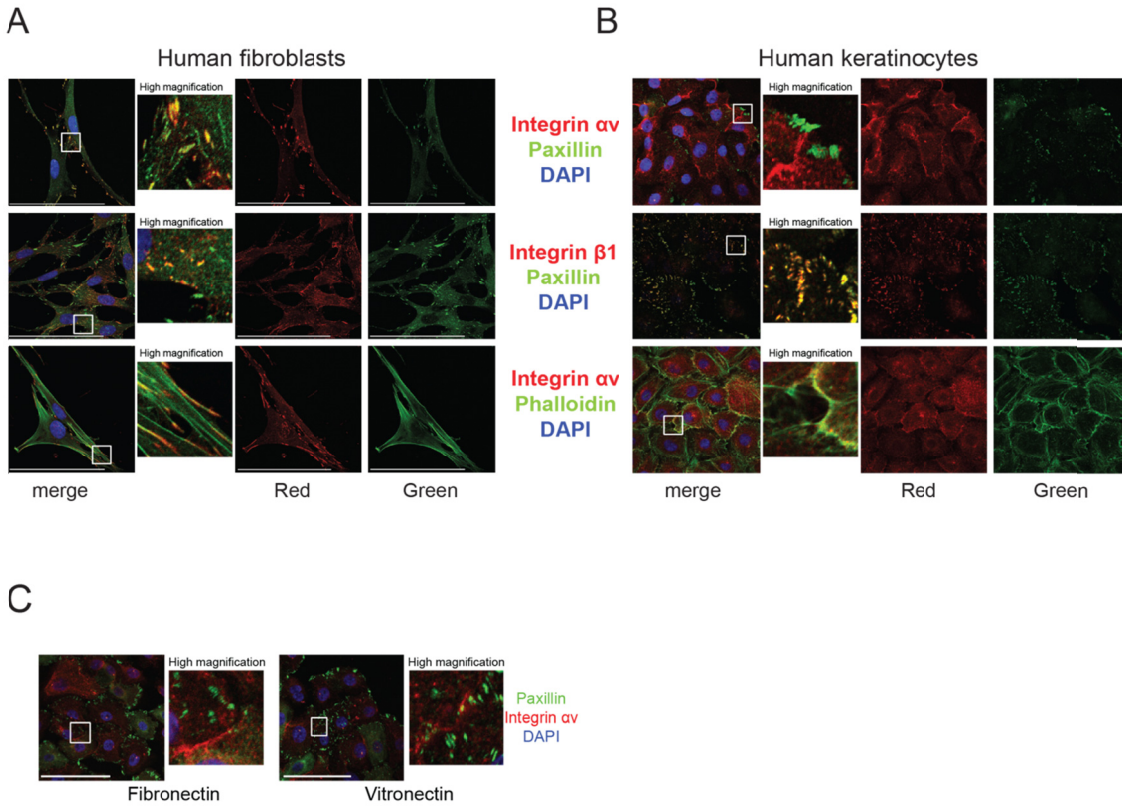

Figure 4.1: Integrin αv does not localize to focal adhesions in keratinocytes. **A,B.** Representative images of human fibroblasts (**A**) or human keratinocytes (**B**) cultured on Collagen stained for αv, β1 and Paxillin and/or incubated with Phalloidin, then imaged using confocal microscopy. **C.** Representative images of human keratinocytes cultured on Fibronectin or Vitronectin, then stained for αv and Paxillin and imaged using confocal microscopy. Scale bar= 100μm.

Figure 4.2

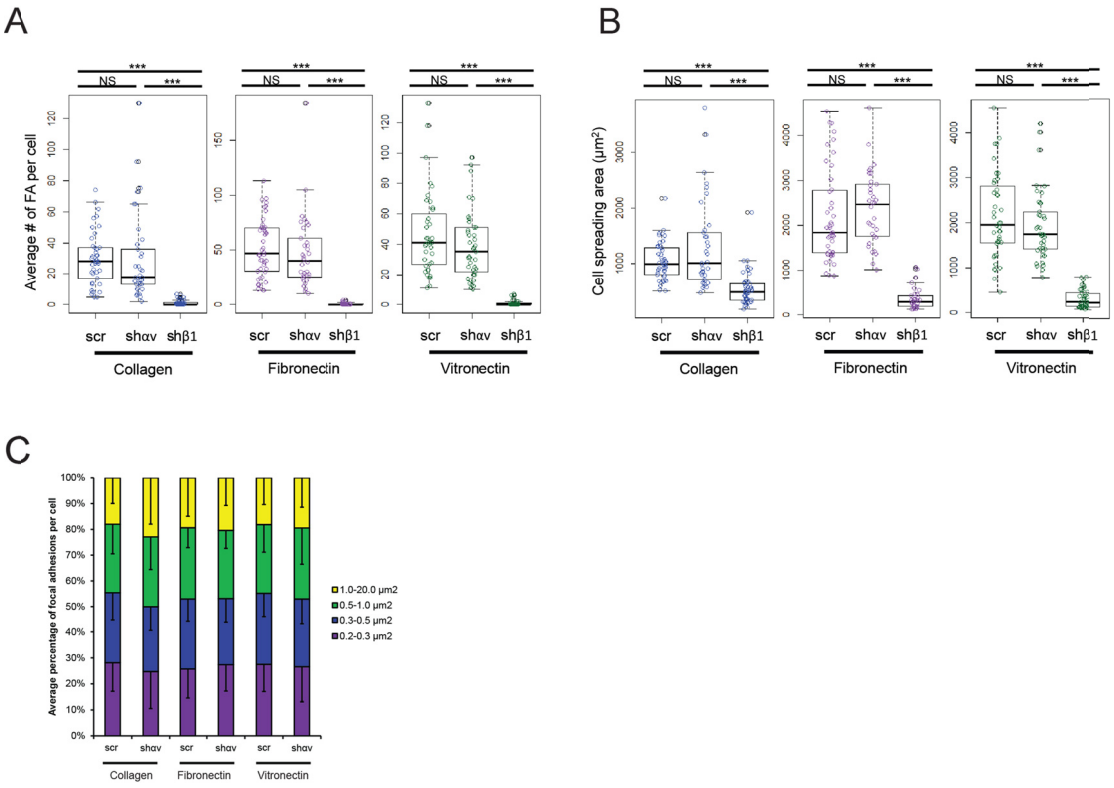

Figure 4.2: αv knock down does not alter the size, number or size distribution of focal adhesions. **A.** Boxplots showing quantification of the number of FAs per cell for keratinocytes infected with a scramble hairpin, an αv hairpin, or a β1 hairpin, and seeded onto coverslips coated with Collagen, fibronectin or Vitronectin (n=30-40 cells per condition**,** boxplot whisker ends are at 1.5 interquartile range). P=2.45x10^{-12} (Collagen), 8.15x10^{-15} (Fibronectin), 2x10^{-16} (Vitronectin) using one-way ANOVA. **B.** Boxplots showing quantification of cell spreading area for the same cells in (**A**). P=3.79x10^{-9} (Collagen), 2x10^{-16} (Fibronectin), 2x10^{-16} (Vitronectin) using one-way ANOVA. **C.** Quantification of the size distribution of focal adhesions upon αv or β1 knock down in human keratinocytes (n=30-40 cells, mean ± SD, none of the differences are statistically significant). ***=p<0.0005, using Tukey's post hoc HSD.

Figure 4.3

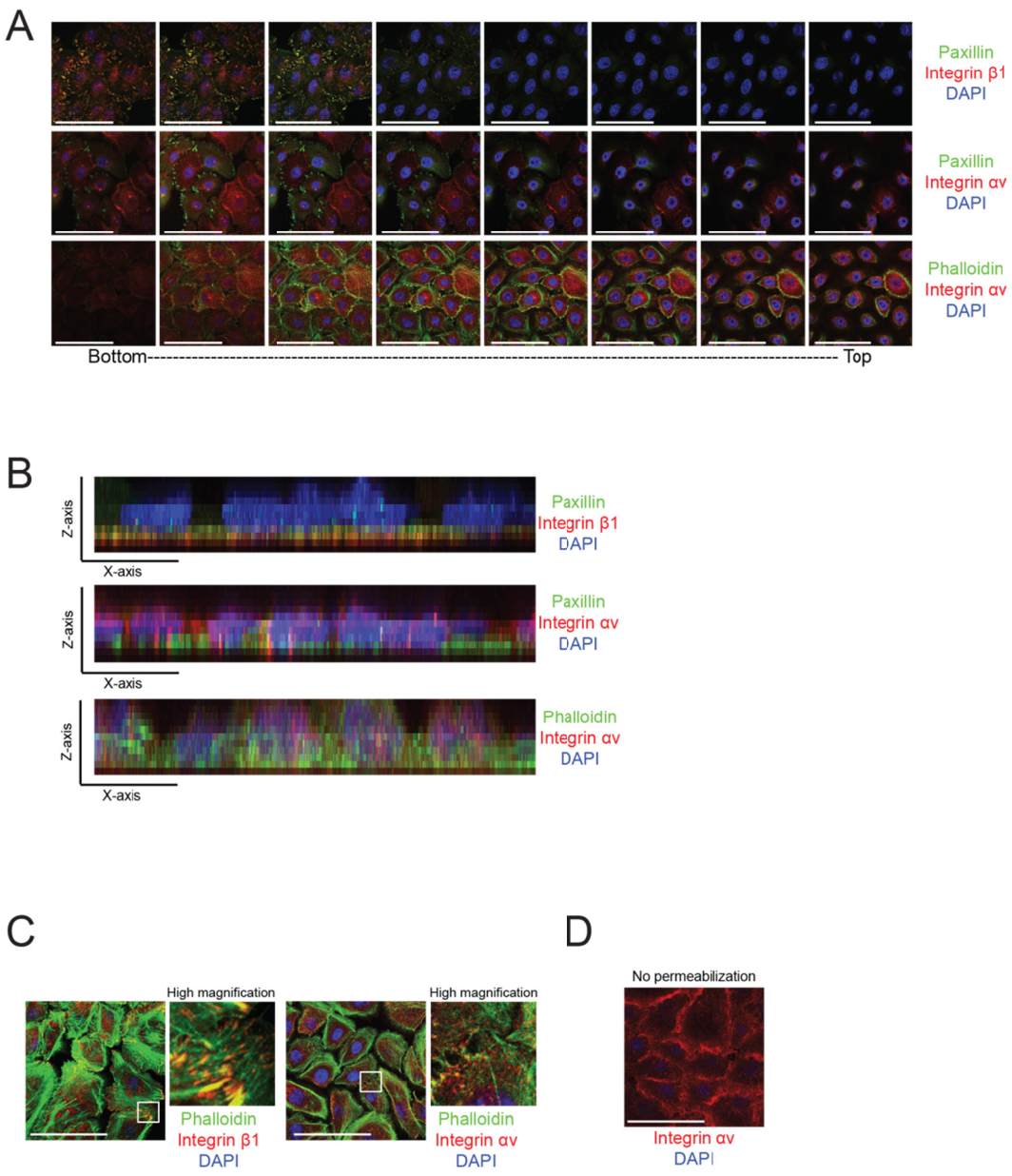

Figure 4.3: Integrin αv is not localized to the tips of actin filaments and is expressed throughout the cellular membrane. **A.** Confocal Z-stack of cultured human keratinocytes stained for integrin αv, Paxillin and Phalloidin, shown as individual panels. **B.** X-Z projections of the images shown in (**A**). The Z axis was stretched to 20X the original size to aid in visualization. **C.** Representative

images of keratinocytes stained with integrin β1, integrin αv and Phalloidin. Cells were plated on Collagen. **D.** Representative image of human keratinocytes stained with integrin αv (L230) without permeabilization. Scale bar= 100μm.

Figure 4.4

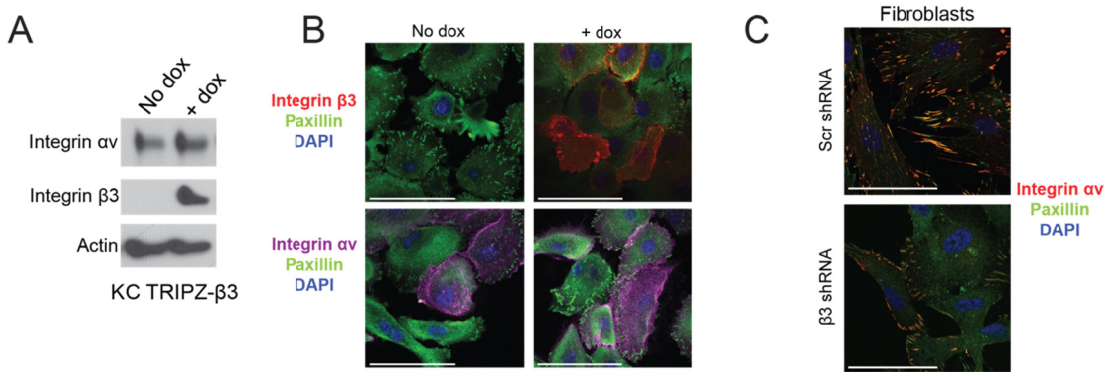

Figure 4.4: Expression of integrin β3 is insufficient to move αv to focal adhesions in keratinocytes. **A.** Western blot of human keratinocytes expressing pLenti-integrin αv and pTRIPZ-integrin β3, with and without doxycycline induction (2μg/mL for 24 hours). **B.** Representative images of human keratinocytes from (**A**), stained for integrin αv, integrin β3 and Paxillin and imaged using confocal microscopy. **C.** Representative images of human fibroblasts infected with a control hairpin or an integrin β3 hairpin, then stained for integrin αv (L230) and Paxillin. Scale bar= 100μm.

Figure 4.5

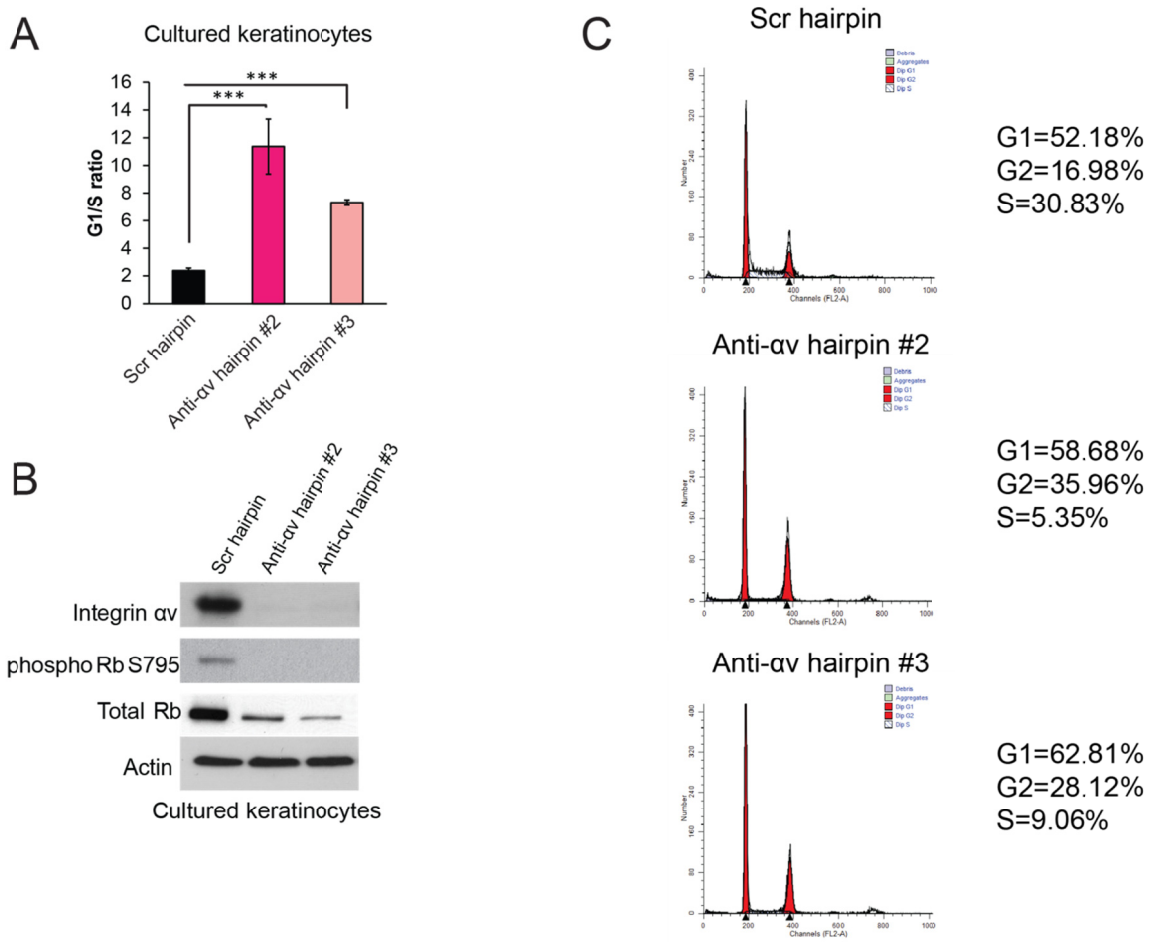

Figure 4.5: Integrin αv controls cell cycle progression in cultured keratinocytes. **A.** PI staining and flow cytometry was performed on cultured keratinocytes infected with indicated hairpins. The G1/S ratio was calculated from 3 biological replicates (mean ± SD). $P=2.0x10^{-4}$ using one-way ANOVA. **B.** Western blot showing changes in Rb signaling upon αv knock down with two independent hairpins. **C.** Representative flow cytometry plots used for quantification in (**A**). Cells were not gated, and percentages were calculated using ModFit. ***=p<0.0005 using Tukey's post hoc HSD.

Figure 4.6

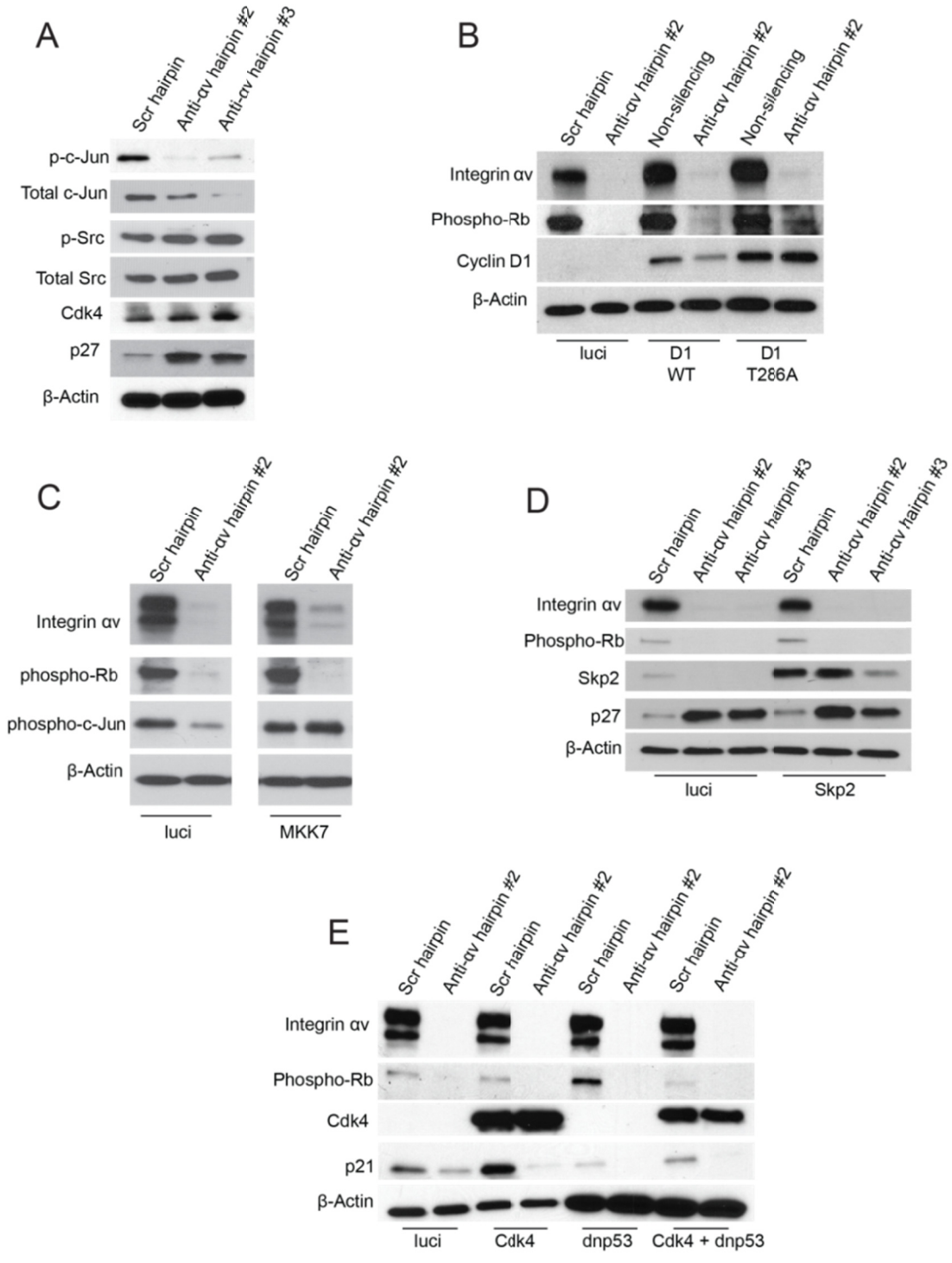
A
Scr hairpin
Anti-αv hairpin #2
Anti-αv hairpin #3
p-c-Jun
Total c-Jun
p-Src
Total Src
Cdk4
p27
β-Actin
B
Scr hairpin
Anti-αv hairpin #2
Non-silencing
Anti-αv hairpin #2
Non-silencing
Anti-αv hairpin #2
Integrin αv
Phospho-Rb
Cyclin D1
β-Actin
luci
D1 WT
D1 T286A
C
Scr hairpin
Anti-αv hairpin #2
Scr hairpin
Anti-αv hairpin #2
Integrin αv
phospho-Rb
phospho-c-Jun
β-Actin
luci
MKK7
D
Scr hairpin
Anti-αv hairpin #2
Anti-αv hairpin #3
Scr hairpin
Anti-αv hairpin #2
Anti-αv hairpin #3
Integrin αv
Phospho-Rb
Skp2
p27
β-Actin
luci
Skp2
E
Scr hairpin
Anti-αv hairpin #2
Scr hairpin
Anti-αv hairpin #2
Scr hairpin
Anti-αv hairpin #2
Scr hairpin
Anti-αv hairpin #2
Integrin αv
Phospho-Rb
Cdk4
p21
β-Actin
luci
Cdk4
dnp53
Cdk4 + dnp53

Figure 4.6: Evaluation of potential signaling pathways controlled by integrin αv in keratinocytes. **A.** Western blots of signaling pathway changes in cultured keratinocytes infected with a scrambled control hairpin, or two independent integrin αv hairpins. **B.** Western blots of signaling pathway changes in keratinocytes infected with a luciferase control, Cyclin D1 wild-type (D1 WT) or degradation-resistant Cyclin D1 T286A (D1 T286A), then infected with indicated shRNAs. **C.** Western blots of signaling pathway changes in cultured keratinocytes infected with a luciferase control or MKK7, then infected with indicated shRNAs. **D.** Western blots of signaling pathway changes in cultured keratinocytes infected with luciferase control or Skp2, then infected with the indicated shRNAs. **E.** Signaling pathway changes in cultured keratinocytes infected with luciferase control, Cdk4 R24C, dnp53, or both Cdk4 R24C and dnp53, then infected with the indicated shRNAs.

Figure 4.7

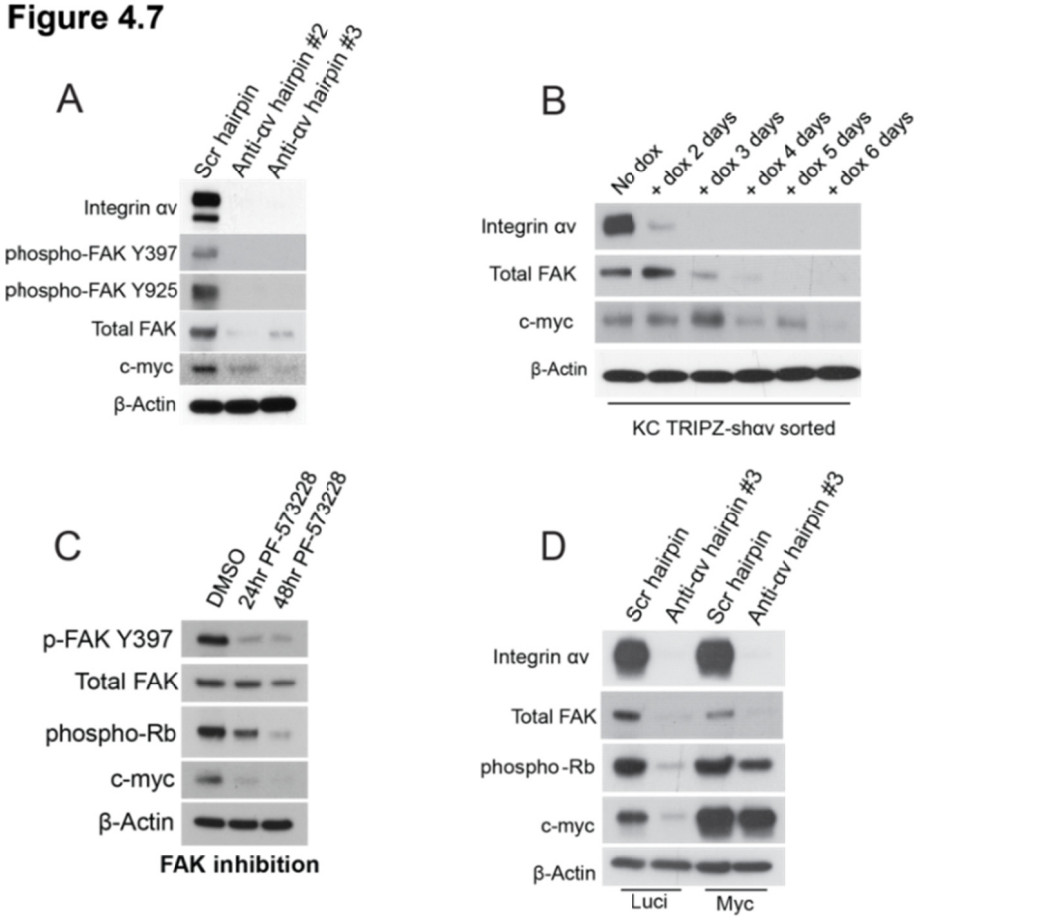
A
Scr hairpin
Anti-αv hairpin #2
Anti-αv hairpin #3
Integrin αv
phospho-FAK Y397
phospho-FAK Y925
Total FAK
c-myc
β-Actin
B
No dox
+ dox 2 days
+ dox 3 days
+ dox 4 days
+ dox 5 days
+ dox 6 days
Integrin αv
Total FAK
c-myc
β-Actin
KC TRIPZ-shαv sorted
C
DMSO
24hr PF-573228
48hr PF-573228
p-FAK Y397
Total FAK
phospho-Rb
c-myc
β-Actin
FAK inhibition
D
Scr hairpin
Anti-αv hairpin #3
Scr hairpin
Anti-αv hairpin #3
Integrin αv
Total FAK
phospho-Rb
c-myc
β-Actin
Luci
Myc

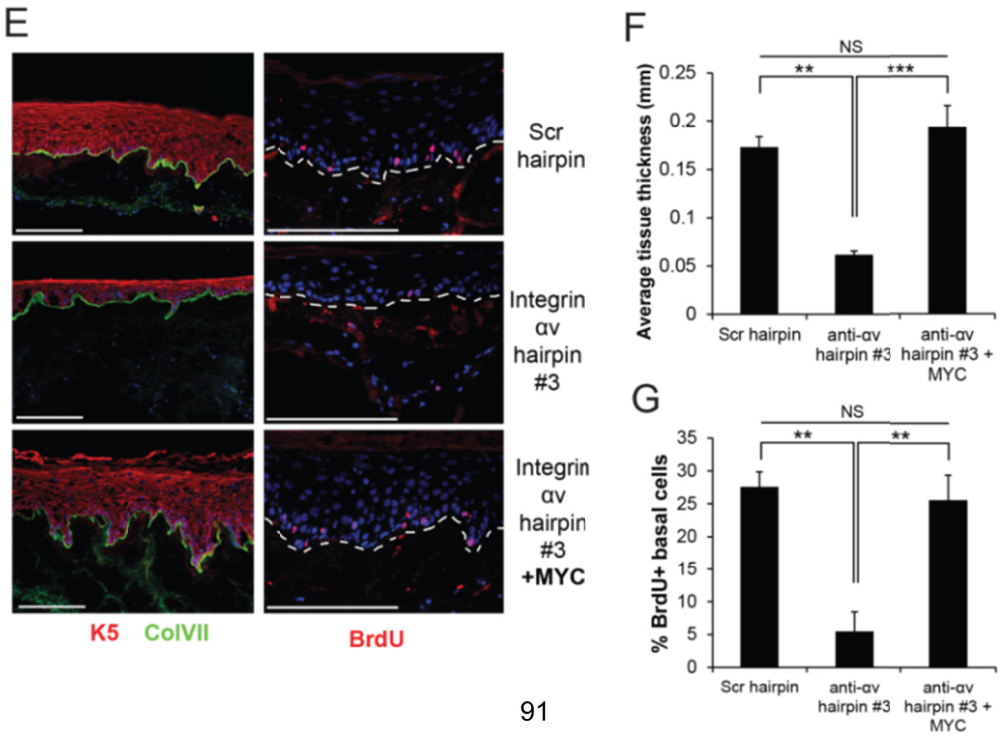
E
Scr hairpin
Integrin αv hairpin #3
Integrin αv hairpin #3 +MYC
K5
ColVII
BrdU
F
NS
**
***
Average tissue thickness (mm)
0.25
0.2
0.15
0.1
0.05
0
Scr hairpin
anti-αv hairpin #3
anti-αv hairpin #3 + MYC
G
NS
**
**
% BrdU+ basal cells
35
30
25
20
15
10
5
0
Scr hairpin
anti-αv hairpin #3
anti-αv hairpin #3 + MYC

Figure 4.7: Integrin αv controls cell cycle in keratinocytes through an αv→FAK→c-myc signaling axis. **A.** Western blot showing signaling pathway changes in keratinocytes infected with indicated shRNAs. **B.** Western blot showing temporal changes in signaling pathways upon αv loss using a doxycycline-inducible αv knock down. **C.** Western blot showing signaling pathway changes upon treatment of keratinocytes with DMSO or FAK inhibitor (1μM PF-573228) for 24 or 48 hours. **D.** Western blot showing signaling pathway changes upon expression of c-myc in keratinocytes infected with indicated hairpins. **E.** Morphological analysis of organotypic tissue made with keratinocytes infected with indicated hairpins and constructs. **F.** Quantification of tissue thickness from (**E**), measured in mm (mean ± SD). N=3 organotypic tissues. P=0.000253 using one-way ANOVA. **G.** Quantification of BrdU uptake from (**E**), measured as the percentage of BrdU+ basal epidermal cells (mean ± SD). N=3 organotypic tissues. P=0.000952 using one-way ANOVA. Scale bar= 200μm. *=p<0.05, **=p<0.005, ***=p<0.0005, using Tukey's post hoc HSD.

Figure 4.8

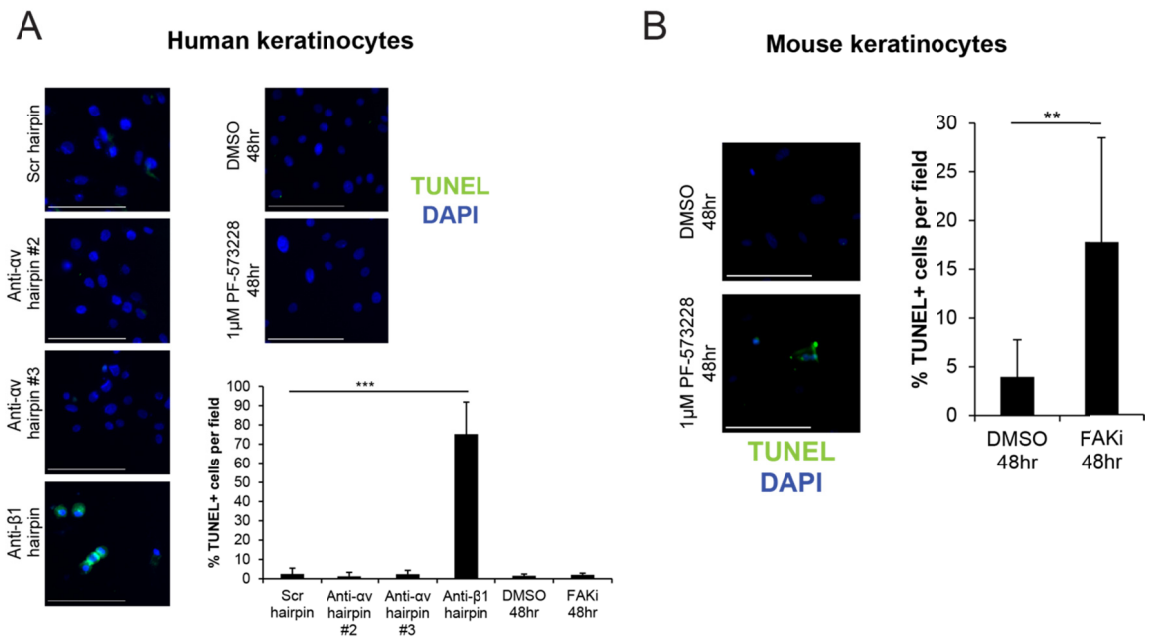

Figure 4.8: Integrin αv knock down or FAK inhibition do not induce anoikis in human keratinocytes. **A.** TUNEL staining in human keratinocytes infected with the indicated hairpins or treated with DMSO or 1μM FAK inhibitor (PF-573228) for 48 hours. The percentage of TUNEL+ cells per field was averaged across multiple images (mean ± SD). A total of 100-500 cells were analyzed per group. $P=5.42x10^{-12}$ using one-way ANOVA. ***=p<0.0005 using Tukey's HSD post-hoc test. **B.** TUNEL staining in mouse keratinocytes treated with DMSO or 1μM FAK inhibitor (PF-573228) for 48 hours. The percentage of TUNEL+ cells per field was averaged across multiple images (mean ± SD). A total of 400-500 cells were counted per group. **=p<0.005 using student's t-test. Scale bar= 100μm.

Figure 4.9

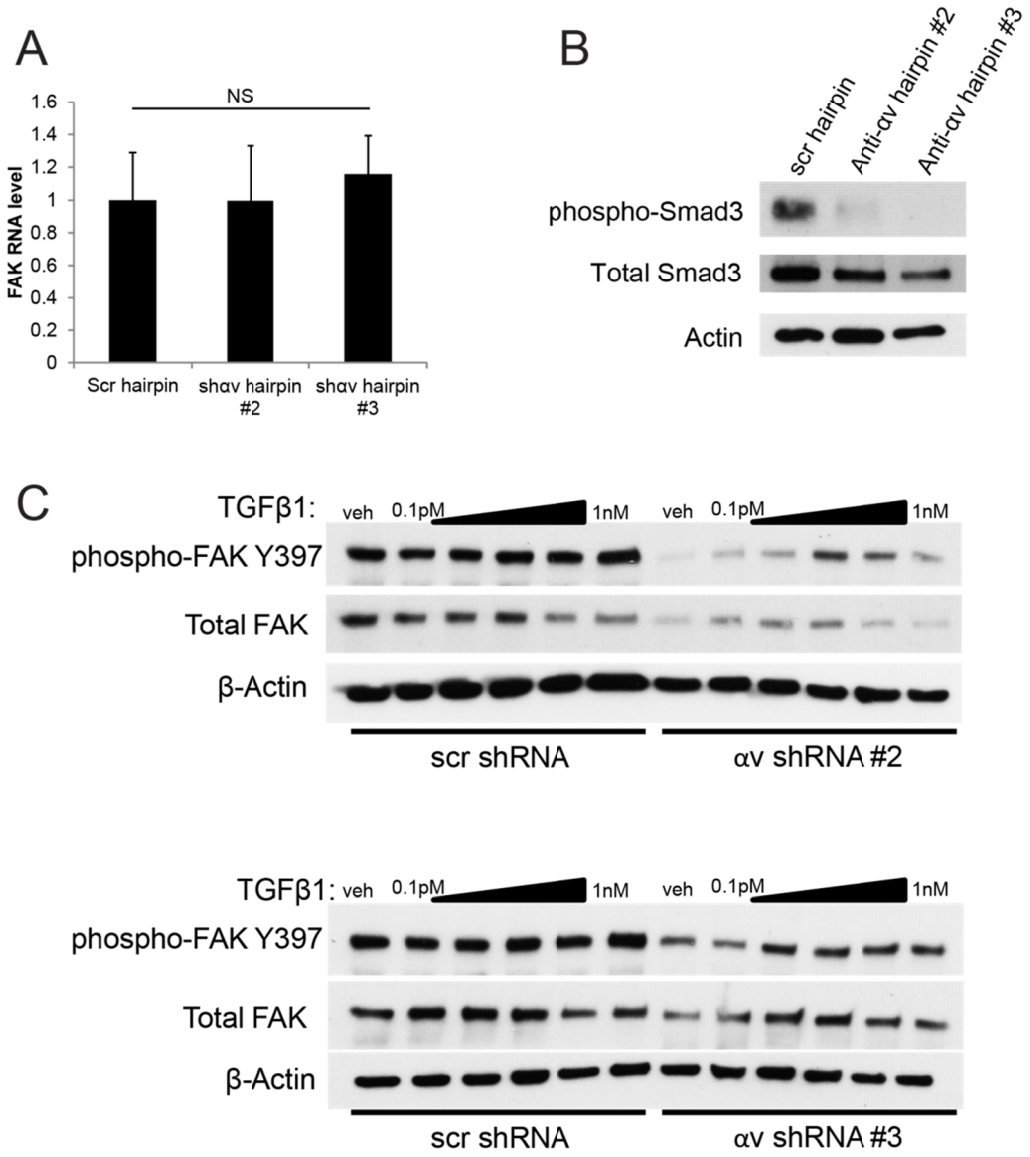

Figure 4.9: TGFβ signaling is partially responsible for αv's regulation of FAK signaling. **A.** qPCR for FAK transcript levels in keratinocytes infected with indicated shRNAs. NS= not statistically significant, measured with one-way ANOVA (P=0.906). **B.** Western blot showing signaling pathway changes in keratinocytes infected with indicated shRNAs. **C.** Western blot showing signaling pathway changes upon addition of varying doses of TGFβ1 in keratinocytes infected with indicated hairpins. TGFβ1 doses range from 0.1pM to 1nM, increasing by 10-fold.

Figure 4.10

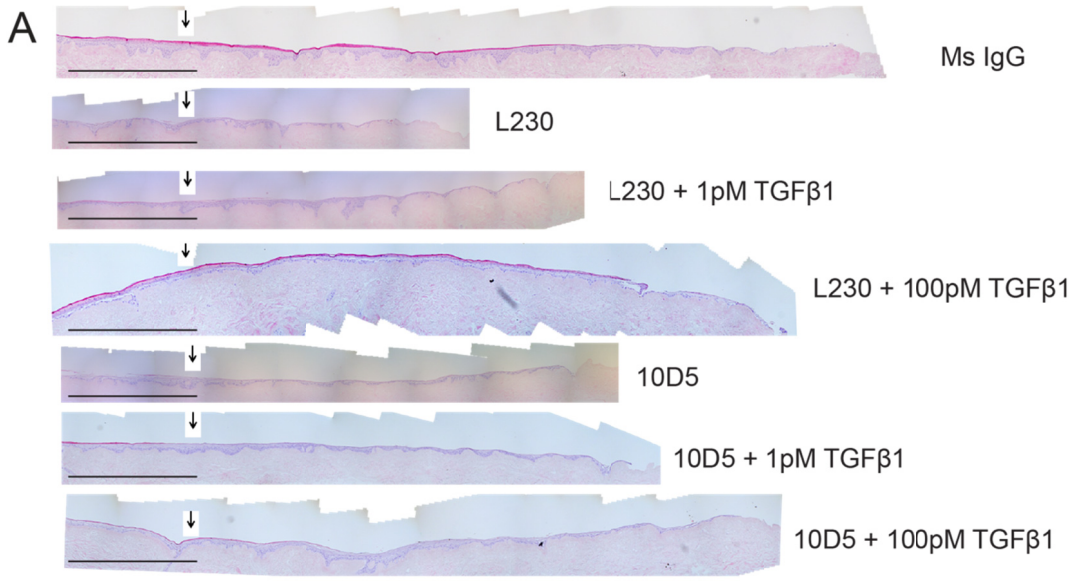
A
Ms IgG
L230
L230 + 1pM TGFβ1
L230 + 100pM TGFβ1
10D5
10D5 + 1pM TGFβ1
10D5 + 100pM TGFβ1

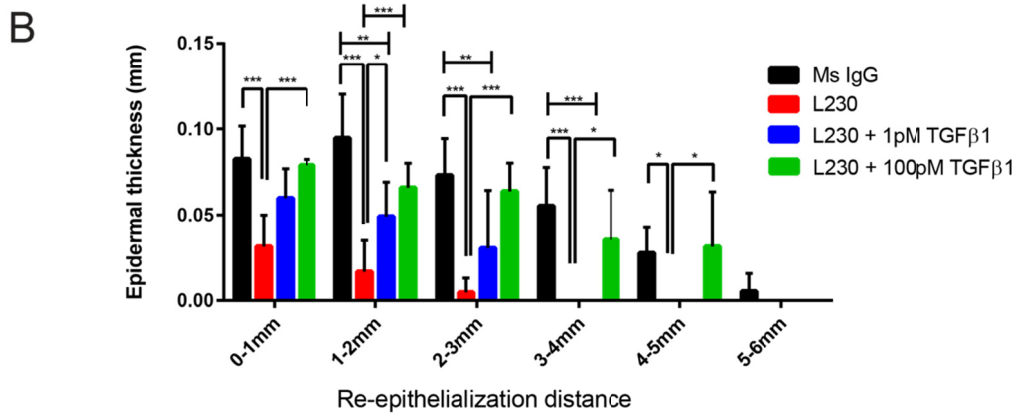
B
Epidermal thickness (mm)
0.15
0.10
0.05
0.00
0-1mm
1-2mm
2-3mm
3-4mm
4-5mm
5-6mm
Re-epithelialization distance
Ms IgG
L230
L230 + 1pM TGFβ1
L230 + 100pM TGFβ1

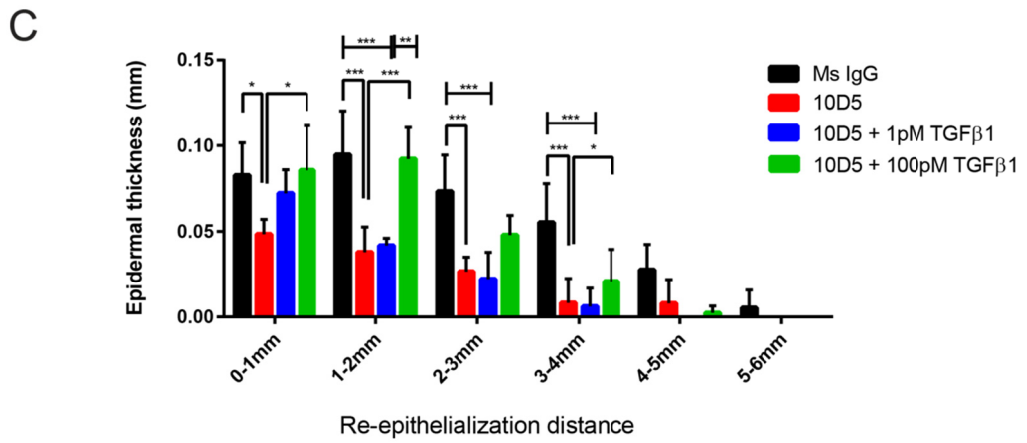
C
Epidermal thickness (mm)
0.15
0.10
0.05
0.00
0-1mm
1-2mm
2-3mm
3-4mm
4-5mm
5-6mm
Re-epithelialization distance
Ms IgG
10D5
10D5 + 1pM TGFβ1
10D5 + 100pM TGFβ1

Figure 4.10: αv's role in re-epithelialization is partially dependent on TGFβ signaling. **A.** Representative Hematoxylin & Eosin stain for runway re-epithelialization assay utilizing the indicated antibodies and TGFβ1 treatments. TGFβ1-containing media was replaced every day. Arrows indicate the starting edge for the re-epithelialization assay. **B,C.** Quantification of tissues from (**A**), in terms of epidermal thickness. Epidermal thickness was measured at various distances away from the starting edge of the re-epithelialization assay. The same mouse IgG control tissues are depicted in B and C for clarity. N=3-6 tissues per group. $p<0.005$ (**B**) and $p<0.05$ (**C**) by two-way ANOVA. *=$p<0.05$, **=$p<0.005$, ***=$p<0.0005$, calculated using Tukey's HSD post-hoc test. Scale bar= 1mm.

Figure 4.11

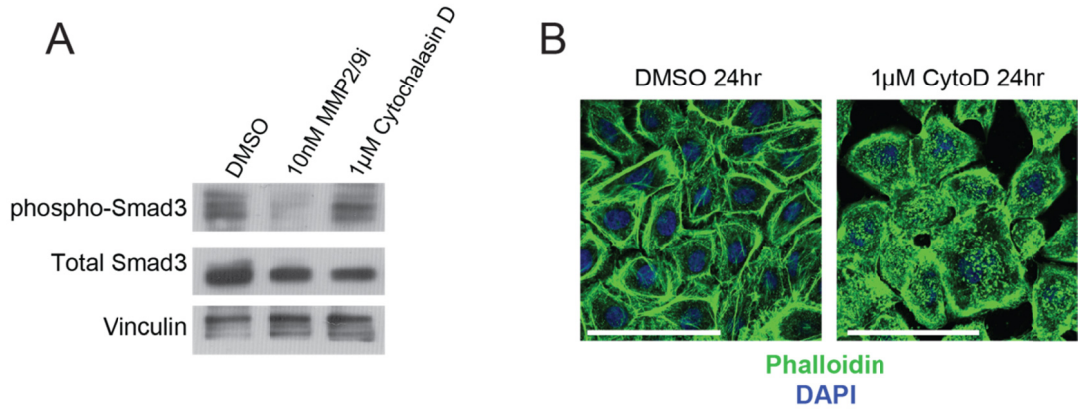

Figure 4.11: TGFβ signaling is controlled through MMPs, not actin-dependent forces, in keratinocytes. **A.** Western blot showing signaling pathway changes in keratinocytes upon treatment with 10nM MMP2/9 inhibitor or 1μM Cytochalasin D treatment for 24 hours. **B.** Phalloidin staining of keratinocytes treated with control (DMSO) or 1μM Cytochalasin D for 24 hours. Scale bar= 100μm.

Figure 4.12

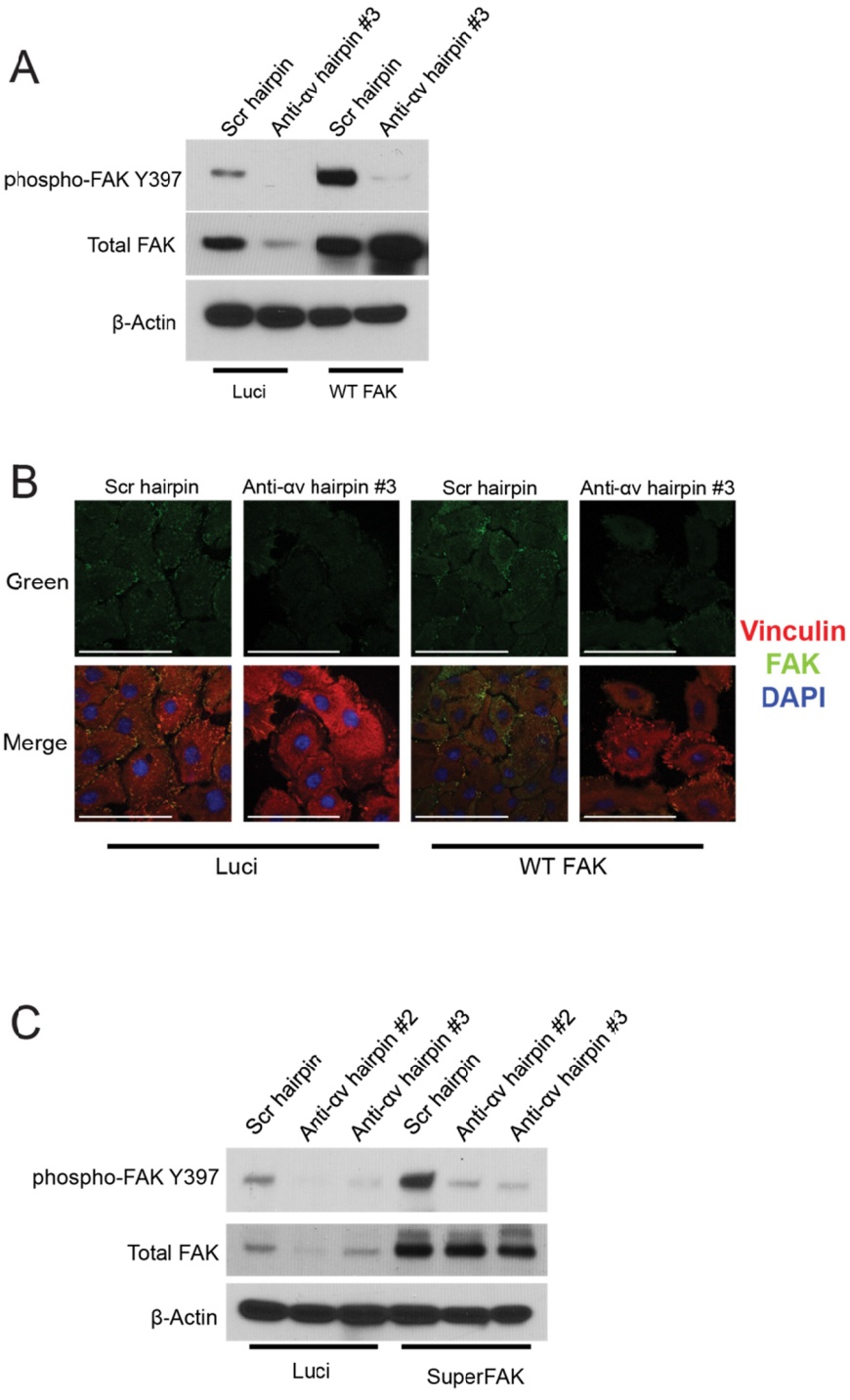

Figure 4.12: Re-expression of wild-type or SuperFAK is insufficient to restore FAK localization or activation in αv knock down keratinocytes. **A.** Western blots for keratinocytes expressing

luciferase or WT FAK and subsequently infected with a control hairpin or an integrin αv hairpin. **B.** Immunofluorescence images of the cells in (**A**), stained with FAK and Vinculin. **C.** Western blot for keratinocytes expressing luciferase or SuperFAK and subsequently infected with a control hairpin or two independent integrin αv hairpins. Scale bar=100μm.

Figure 4.13

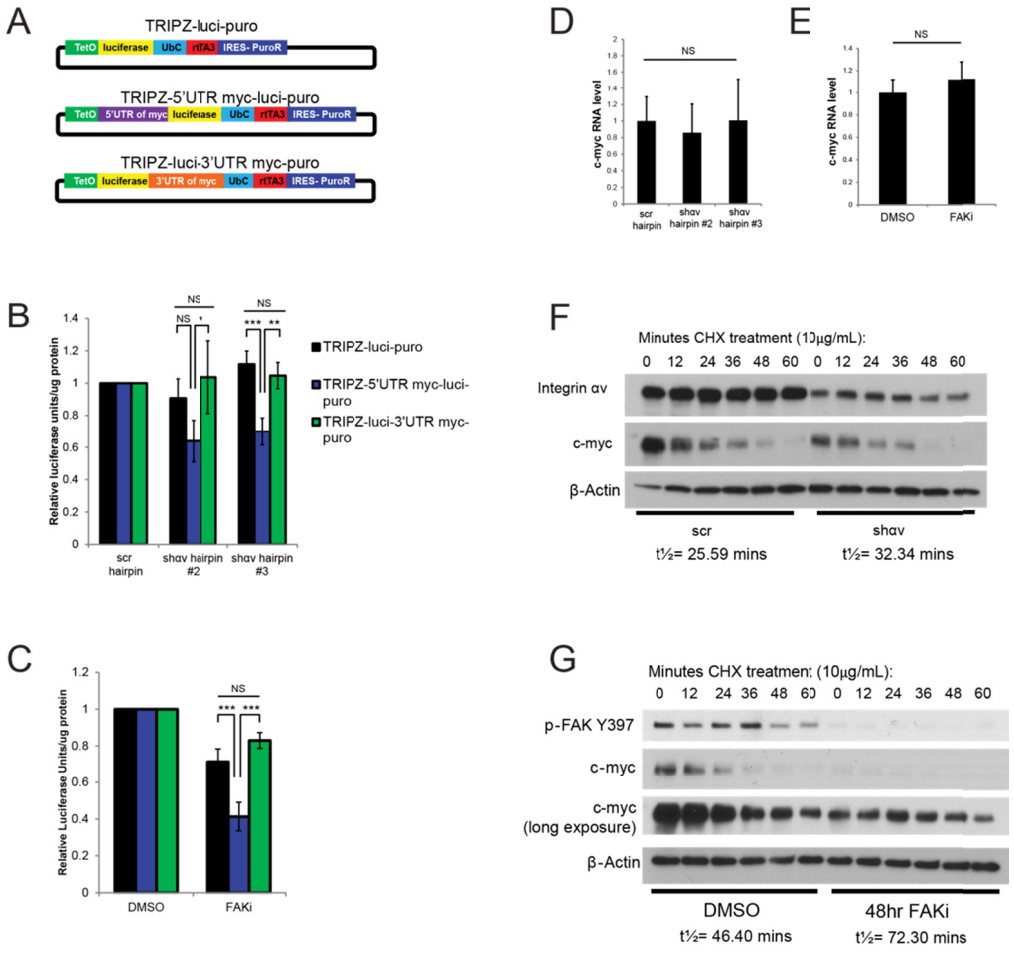

Figure 4.13: Integrin αv and FAK control 5'UTR-dependent c-myc translation in keratinocytes. **A.** Plasmid maps for chimeric luciferase constructs containing the 5'UTR or 3'UTR of c-myc. **B,C.** Luciferase activity measured after 6 hours of dox induction in keratinocytes infected with the chimeric constructs shown in (**A**) and subsequently infected with indicated hairpins (**B**) or treated with DMSO (vehicle) or 1μM PF-573228 (FAK inhibitor) for 24 hours (**C**). N=3 biological replicates. P=0.0217 (hairpin #2), 0.000111 (hairpin #3) (**B**) and 2.33×10^{-5} (**C**) using one-way ANOVA. **D.** qPCR for c-myc transcript levels in keratinocytes infected with indicated shRNAs. **E.** qPCR for c-myc transcript levels in cells treated with DMSO or 1μM PF-573228 (FAK inhibitor) for 48 hours. **F.** Cycloheximide (CHX, 10μg/mL) timecourse and subsequent western blot in keratinocytes infected with scramble hairpin or integrin αv hairpin. **G.** Cycloheximide (CHX,

10μg/mL) timecourse and subsequent western blot in keratinocytes treated with DMSO (vehicle) or 1μM PF-573228 (FAK inhibitor) for 48 hours. *=$p<0.05$, **=$p<0.005$, ***=$p<0.0005$ using Tukey's HSD post-hoc test.

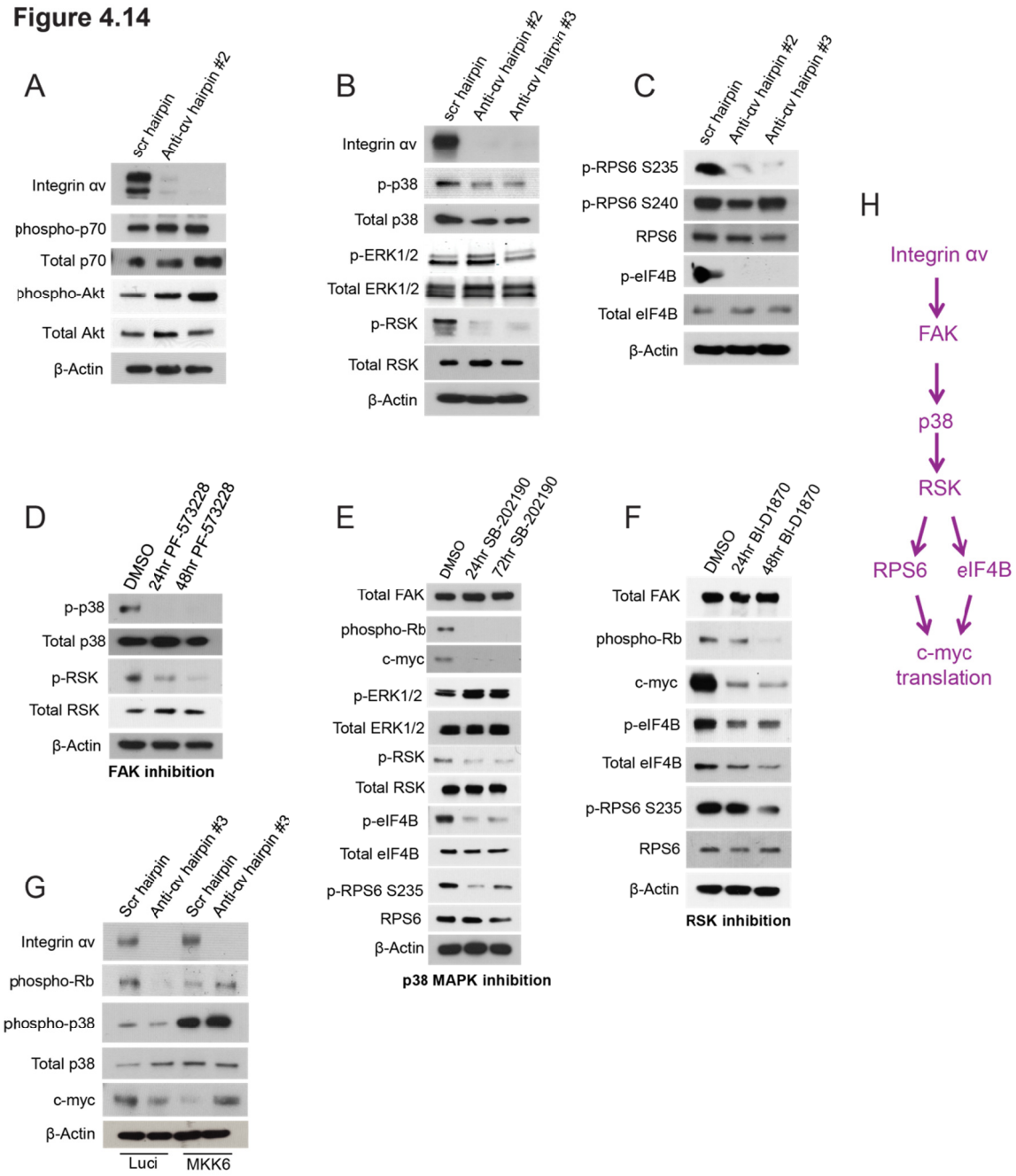

Figure 4.14: αv and FAK regulate c-myc translation through p38 and RSK signaling. **A.** Western blots showing Akt-mTOR signaling pathway changes upon integrin αv knock down with two independent hairpin in keratinocytes. **B,C.** Western blots showing p38/ERK/RSK (**B**) or RPS6/eIF4B (**C**) signaling pathway changes upon αv knock down with two independent hairpins in keratinocytes. **D.** Western blot showing signaling pathway changes upon treatment of

keratinocytes with DMSO or FAK inhibitor (1μM PF-573228) for 24 or 48 hours. **E.** Western blot showing changes in signaling pathways upon treatment of keratinocytes with DMSO or p38 MAPK inhibitor (10μM SB-202190) for 24 or 72 hours. **F.** Western blot showing changes in signaling pathways upon treatment of keratinocytes with DMSO or p90RSK inhibitor (1μM BI-D1870) for 24 or 48 hours. **G.** Western blot showing signaling pathway changes upon expression of MKK6(glu) in keratinocytes infected with indicated hairpins. **H.** Schematic of signaling pathway.

Figure 4.15

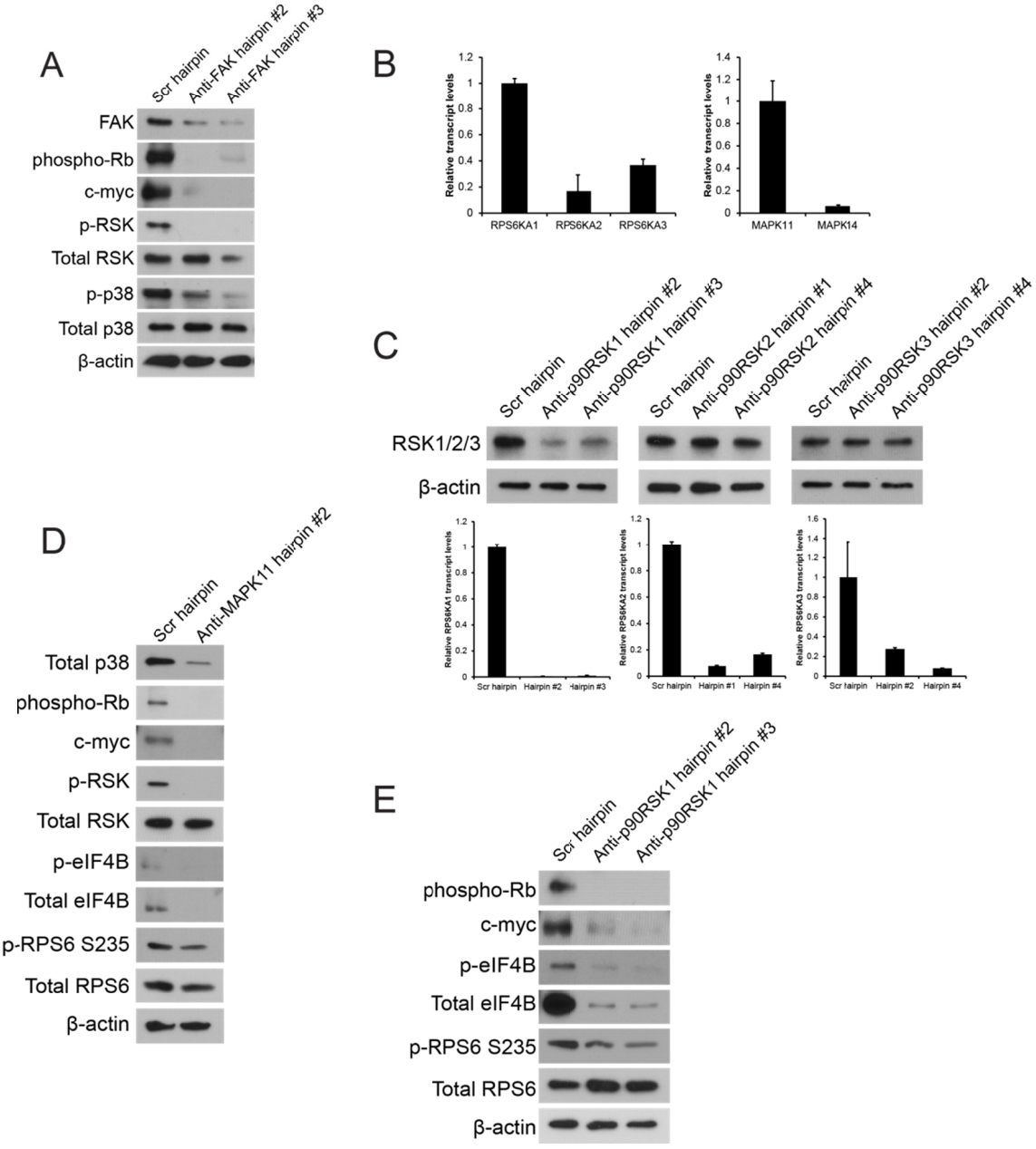

Figure 4.15: Validation of small molecule inhibitor data with shRNAs. **A.** Western blot showing signaling pathway changes upon FAK knock down with 2 independent hairpins. **B.** RNA levels for p90RSK isoforms (RPS6KA1, RPS6KA2, RPS6KA3) and p38 isoforms (MAPK11 and MAPK14) in human keratinocytes. N=3 biological replicates (mean ± SD). **C.** Western blot showing knock down efficiency for hairpins targeting RPS6KA1, RPS6KA2, RPS6KA3 at the RNA and protein

level. **D.** Western blot showing signaling pathway changes upon knock down of p38 (MAPK11). **E.** Western blot showing signaling pathway changes upon knock down of p90RSK1 with 2 independent hairpins.

Figure 4.16

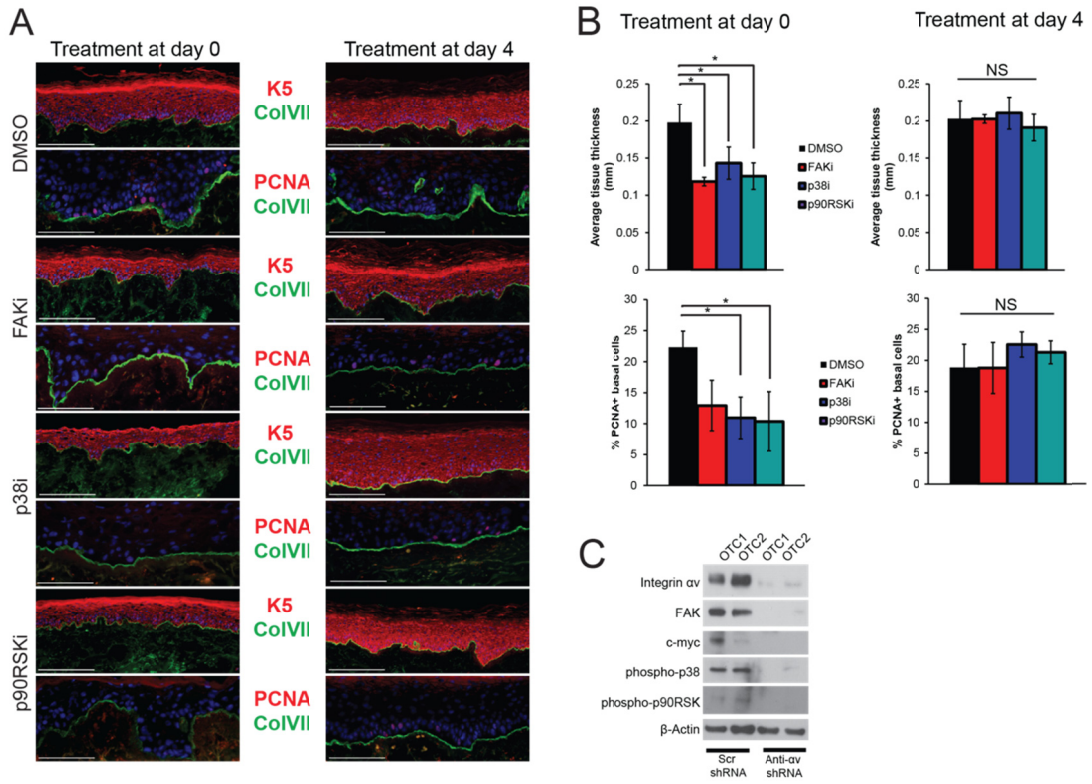

Figure 4.16: FAK, p38 and RSK are also necessary for organotypic tissue generation but not maintenance. **A.** Morphological analysis of organotypic tissue treated with the indicated inhibitors at the indicated time points. **B.** Quantification of tissue thickness measured in mm and PCNA+ basal cells from (F), (mean ± SD). N=3 independent organotypic tissues. P=0.00879 (upper left), P=0.423 (upper right), P=0.0157 (lower left), P=0.407 (lower right) using one-way ANOVA. **C.** Western blot from tissue lysates made from keratinocytes infected with the indicated shRNAs. Scale bar=200μm. *=p<0.05 using Tukey's HSD post-hoc test.

DISCUSSION

Here, we describe a focal adhesion (FA)-independent role for αv integrins and show that the lack of αv localization to FAs in keratinocytes is not due to lack of keratinocyte β3. Active, ligand-engaged integrins have been shown, in some instances, to localize outside of focal adhesions. Activated integrins can switch between immobile, focal adhesion-associated, states and freely diffusing states (Rossier et al., 2012). However, it is unclear whether these freely diffusing integrins can signal downstream. It was recently shown that ligand-engaged integrins can signal within endosomes to suppress anoikis (Alanko et al., 2015). We have shown for the first time that αv integrins are completely dissociated from mature focal adhesions in keratinocytes, that this integrin can signal outside of focal adhesions, and that this phenomenon is cell type-dependent. It is unclear, however, what the temporal dynamics of αv integrins in keratinocytes are. It is possible that they transiently associate with focal adhesions, or that they form nascent adhesions that never mature into visible focal adhesions. Examining this integrin over time using super-resolution microscopy may shed some light onto the dynamics of αv trafficking. It is also unclear why αv has different localization dependent on the cell type. Proteomic analyses of both focal adhesions and αv adhesions in different cell types may reveal specific mechanisms by which αv is excluded from focal adhesions in keratinocytes. This may additionally provide insight regarding how αv controls FAK expression levels without affecting the structural integrity of the β1-containing FAs. The fact that L230 blocking antibody treatment, which is reported to block αv interaction with one of its ligands Vitronectin, phenocopies αv knock down indicates that αv's functions in keratinocytes are likely ligand-dependent (Weinacker et al., 1994).

αv integrins have been shown previously to signal through Src-FAK, Ras-MEK-ERK, and PI3K-Akt pathways to promote proliferation and survival (Bianchi-Smiraglia et al., 2013; Hood, 2003; Janes and Watt, 2004). Specifically, in a squamous cell carcinoma cell line, αvβ6 was shown to suppress anoikis through increased PKB/Akt activation (Janes and Watt, 2004). However, in cultured primary human keratinocytes, we show that αv depletion does not alter

signaling through Src or ERK pathways, does not affect anoikis, and increases Akt activity. This is consistent with the mouse model of αv loss in the epidermis, in which elevated Akt activity is observed (Savar et al., 2014). This discrepancy in results indicates a clear context-dependent role for αv integrins; however, it is unclear what factors may affect the choice in signaling pathways.

We show instead that αv controls cap-dependent c-myc translation through control of a FAK→p38→p90RSK signaling pathway. We provide evidence that αv controls c-myc protein synthesis specifically, and that this is essential for αv's control of cell cycle. There are many additional changes in total protein levels in the cell upon αv loss that may also be the direct result of αv's translational control. We observe decreased FAK, c-jun, Skp2 and Rb protein levels upon αv knock down. This may be the result of signaling feedback, but could also be the direct result of translation defects. We know that FAK mRNA is unaltered in response to αv loss; however, due to FAK's long half-life (>20 hours), it is difficult to determine whether FAK is controlled by αv at the level of protein synthesis or protein degradation (Ochel et al., 1999).

We do show that αv's control of FAK expression is at least partially dependent on TGFβ signaling. The exact mechanism for this is unclear. Several reports have shown highly divergent mechanisms for TGFβ induced activation of FAK, including Src-dependent, adhesion-dependent and ECM remodeling-dependent mechanisms (Cicchini et al., 2008; Thannickal et al., 2003; Wang et al., 2004; Wendt and Schiemann, 2009). There could be TGFβ-dependent defects in the focal adhesions upon αv loss that prevent recruitment, stability, or activation of FAK at focal adhesions. We further show that αv's regulation of re-epithelialization in our organotypic model is partially dependent on TGFβ signaling. This is in contrast to the majority of the literature which shows that genetic ablation of TGFβ signaling pathway components results in accelerated wound re-epithelialization, potentially due to release of TGFβ's anti-proliferative effects (Amendt et al., 2002; Ashcroft et al., 1999; Chan et al., 2002; Falanga et al., 2004; Guasch et al., 2007; Werner and Grose, 2003). These differences may lie in the mechanism of TGFβ signaling inactivation. αv regulates the direct activation of latent TGFβ in the extracellular matrix. Upon genetic ablation of

TGFβ receptors or Smads, there is still TGFβ ligand present, which can induce non-canonical TGFβ signaling. This may be solely responsible for accelerated wound healing or tumorigenesis in the absence of canonical TGFβ signaling. There are a few reports describing a pro-proliferative role for TGFβ in wound healing in vivo. In a corneal wound model in vivo, ablation of TGFβRII delayed wound healing, as well as p38 MAPK activation (Terai et al., 2011). Consistent with this, TGFβ was shown to promote keratinocyte proliferation in an in vivo wound healing model through up-regulation of miR-132, indicating that TGFβ can have pleiotropic effects (Li et al., 2015b). We show that αv's regulation of TGFβ in keratinocytes is necessary for epidermal re-epithelialization.

The p38→p90RSK component of this signaling pathway is particularly novel since p90RSK was thought to be primarily activated by ERK signaling, not by p38 (Roux et al., 2007). P38 was shown to activate p90RSK in dendritic cells through intermediates MK2 and MK3 (Zaru et al., 2007; Zaru et al., 2015). We show that p38 blockade (through a small molecule inhibitor or shRNA) does not alter ERK phosphorylation, but decreases p90RSK phosphorylation. This indicates that this non-canonical p38→p90RSK pathway extends beyond dendritic cells to keratinocytes. It will be interesting to determine whether this also occurs through MK2 and MK3 intermediates. While p38 is not known to have a role in cutaneous wound healing, inhibition of p38 delays corneal wound healing (Sharma et al., 2003). P38β (the predominant p38 isoform in keratinocytes) knockout mice are viable and fertile, and cutaneous wound healing has not been tested in this model (Beardmore et al., 2005). No p90RSK1 knockout mouse has been made, and its role in wound healing is unknown.

The phenotypes that we observe upon αv loss are consistent with mouse models of epidermal c-myc loss. C-myc appears to control proliferation in mouse epidermis during development, but does not alter skin homeostasis when deleted in adult epidermis (Oskarsson et al., 2006; Zanet et al., 2005). The effects of c-myc depletion on wound healing in these mice has not been tested. In the intestinal epithelium, c-myc plays a similar role in crypt generation but not crypt homeostasis (Bettess et al., 2005). In contrast to our results, c-myc is shown to be up-

regulated at the epidermal wound edge in chronic wounds (Stojadinovic et al., 2005). The *in vivo* relevance of this observation, however, is unclear.

FAK deletion in the epidermis does not alter wound healing in mice (Essayem et al., 2006). However, these wounds were not stinted and thus the epidermal contribution of FAK to the specific process of re-epithelialization may have been masked by rapid wound contraction. FAK does seem to play a role in intestinal epithelial proliferation in response to injury (Owen et al., 2011). A thorough examination of the *in vivo* roles of these additional pathway elements—FAK, p38, p90RSK and c-myc—utilizing physiologically relevant wound healing models is warranted to determine whether all of these signaling pathways contribute equally to wound healing and whether they could be targeted pharmacologically to treat pathologic scarring and/or chronic wounds.

CHAPTER 5

Role of integrin αv in squamous cell carcinoma and potential therapeutic utility of blocking antibodies

Parts of this chapter have been previously published in:

Duperret EK, Dahal A, Ridky TW. Focal adhesion-independent integrin αv regulation of FAK and c-myc is necessary for 3D skin formation and tumor invasion. *J Cell Sci.* 2015; 128(21):3997-4013.

RESULTS

αvβ6 is up-regulated in squamous cell carcinomas and correlates with poor prognosis in Head and Neck Squamous Cell Carcinoma (HNSCC)

Because tissue generation and epidermal carcinoma are both associated with upregulated basal cell proliferation, we hypothesized that αv might be required during tumorigenesis. We examined αv expression and localization in human epidermal squamous cell carcinomas, and found that nearly every tumor cell displayed intense membrane-localized αv staining (Figure 5.1A). Various αv integrin binding partners have shown increased expression at the RNA and protein level in epithelial carcinomas (Bandyopadhyay and Raghavan, 2009; Reuter et al., 2009). Specifically, integrin β6 protein is increased in oral SCCs at the invasive edge (Hamidi et al., 2000; Jones et al., 1997). We examined the temporal changes in RNA levels for various integrin subunits in a previously published dataset from a human xenograft model of SCC, and found temporal up-regulation of integrin β6 RNA in both Ras and Raf driven tumors (Figure 5.1B) (Reuter et al., 2009). Integrin αv and its other β binding partners showed minimal change upon tumor induction (Figure 5.1B). To examine the potential clinical significance of integrin β6 in head and neck SCC (HNSCC), we analyzed 400 HNSCC cancer specimens from The Cancer Genome Atlas (TCGA). We found that increased β6 expression significantly

correlated with decreased overall survival for HNSCC patients (Figure 5.2A). 210 of these clinical samples also contained phospho-protein array data. To determine which signaling pathways might be associated with increased β6 RNA levels in HNSCC patients, we took an unbiased approach and examined levels of all 43 phospho-proteins in the dataset. Significant changes were seen in only 5 phospho-proteins when comparing patients with high versus low β6 RNA expression (Figure 5.2B). 4 of the 5 proteins identified are involved in protein translation (Figure 5.2B). Consistent with our previous data, we observed a positive correlation between RPS6 S235 phosphorylation, p38 T180 phosphorylation and integrin β6 RNA expression in HNSCC tumors (Figure 5.2C,D). There was also a specific positive correlation between RPS6 S235 but not S240 phosphorylation (Figure 5.2D). These data indicate that the integrin p38-dependent, αvβ6 translational effects we observed in our genetically-defined organotypic skin models are also reflected in spontaneous head and neck SCCs, and that this pathway likely contributes to enhanced tumor progression.

Integrins αvβ5 and αvβ6 are required for SCC tumor invasion at all stages of tumorigenesis

To determine whether αv or its binding partners, β5, β6 and β8, are required for tumor initiation, we knocked down each of these subunits in keratinocytes engineered to express a medically relevant oncogene pair including active Cdk4 (R24C), and HRas (G12V), which are sufficient to convert normal organotypic epidermis into SCC that invades through the basement membrane into dermis (Lazarov et al., 2002; Ridky et al., 2010). We found that knock down of αv, β5 or β6 in tissue prior to oncogene activation blocked tumor invasion, while β8 knock down had no major effect (Figure 5.3A,B). The requirement for β5 in tumor invasion was interesting, given that this subunit is not over-expressed at the RNA level in cutaneous SCCs.

To determine whether αv is also required for tumor invasion in already established organotypic tumors, we performed a doxycycline-inducible αv knock down time course (similar to that presented in Figure 3.7) in keratinocytes expressing Cdk4 (R24C) and H-Ras (G12V) (Figure

5.4A). Doxycycline-induction was sufficient to inhibit neoplastic invasion at every time point, including 2 days post-seeding, indicating that integrin αv is required for both neoplastic invasion initiation and progression (Figure 5.4B,C). These results suggest that integrins αvβ5 and αvβ6 may be useful therapeutic targets for SCC.

To identify potential therapeutic agents for blocking αvβ5 or αvβ6, we treated organotypic tissue made from keratinocytes expressing Cdk4 R24C and H-Ras G12V (an ER-HRas fusion responsive to tamoxifen administration) with various blocking antibodies. We tested L230, a pan-αv blocking antibody, 10D5, a β6-specific blocking antibody, and P1F6 and P5H9, both β5-specific blocking antibodies (Mitjans et al., 1995; Ramos et al., 2002; Thomas et al., 2002). We found that both L230 and 10D5 were highly effective in blocking tumor invasion and reducing organotypic tumor area (Figure 5.5A,B). P1F6 and P5H9 did not reduce either tumor area or tumor invasion (Figure 5.5A,B). Based on this data, it is clear that blocking antibodies targeting pan-αv integrins or specifically αvβ6 can be effective at reducing organotypic tumor burden. While both β5 blocking antibodies were not sufficient to block tumor invasion, we cannot conclude that β5 is a poor therapeutic target, since it is possible that these blocking antibodies have lower binding affinities or poor blocking function compared to the other antibodies tested.

FAK, p38 and p90RSK are similarly required for SCC tumor invasion

Next, we questioned whether the pathway elements that we found downstream of αv in normal tissue (FAK→p38→p90RSK) may also be therapeutic targets for SCC. Inhibition of each of these elements with small molecule inhibitors, at doses that did not affect normal tissue (Figure 4.16), significantly attenuated Ras-driven neoplastic invasion (Figure 5.6A,B).

L230 treatment reduces tumor burden *in vivo*

We next wondered whether αv was equally required for tumor formation *in vivo*. While both L230 (pan-αv) and 10D5 (αvβ6) were effective in organotypic culture, we chose to test L230 in an orthotopic xenograft model *in vivo*, because it is a human-specific antibody and allowed us

to specifically define the contribution of epidermal αv in tumor progression. For this study, we utilized skin grafts expressing Cdk4 R24C and a doxycycline-inducible TRIPZ-H-Ras G12V construct. When grafted onto mice, these tissues generate normal skin and can be induced to form tumors by with doxycycline administration. To test the effects of αv blockade in these inducible tumors, we began L230 treatment 1 day prior to oncogene activation, and harvested tumors at 2 weeks. Histological analysis of these tumors revealed that control, mouse IgG treated, tumors were all large and invasive (Figure 5.7). L230 treatment resulted in large reduction of tumor burden in 4/7 cases, and minimal reduction in 3/7 cases (Figure 5.7). This variability in response can potentially be attributed to differences in antibody delivery or binding *in vivo*. Quantification in tumor area and Ki67 staining shows a statistically significant reduction upon αv blockade (Figure 5.8A-C). The Ki67 marker used in this case is a human-specific antibody, and thus we can be certain that we are quantifying only human tissue. Phospho-ERK1/2 staining showed no difference (per tumor area) in positive area or staining intensity between control and L230-treated groups, indicating that the reduction in tumor burden was not likely due to lack of induction of the H-Ras G12V oncogene (Figure 5.8D,E). Overall, these data indicate that αv contributes to human cutaneous squamous cell carcinoma tumor formation and proliferation *in vivo*.

FIGURES

Figure 5.1

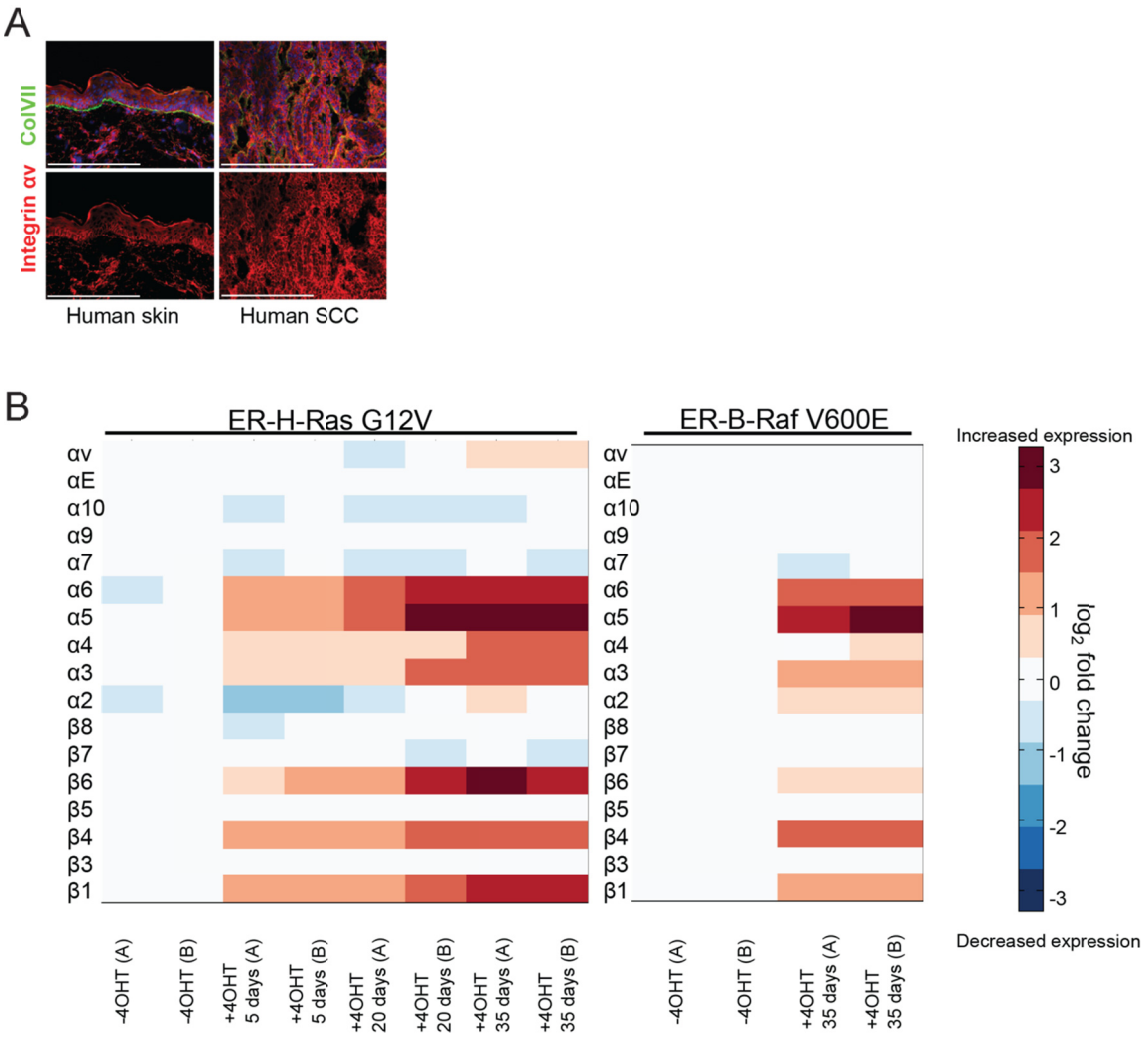

Figure 5.1: Integrin expression in human SCC. **A.** Immunofluorescence staining of integrin αv in normal human skin and human cutaneous SCC samples. **B.** Heat map showing integrin mRNA changes in two different inducible human squamous cell carcinoma models. Raw data from Reuter *et al.* were re-analyzed for this heat map (Reuter et al., 2009).

Figure 5.2

A

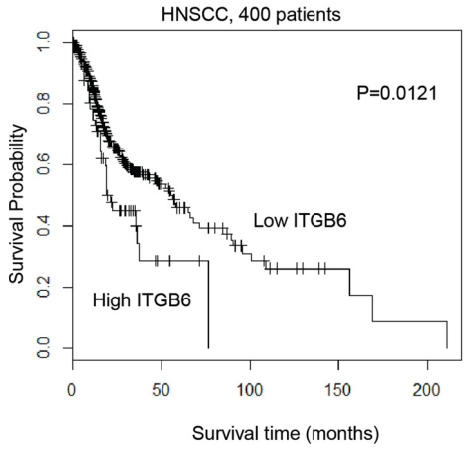

B

Phospho-protein	Avg. Protein Abundance (High β6)	Avg. Protein Abundance (Low β6)	P value
RPS6 S235	0.14	-0.62	0.002
EIF4EBP1 S65	0.56	0.32	0.004
p38 T180	0.004	-0.74	0.009
YBX1 S102	0.14	-0.44	0.042
Src Y527	0.25	-0.39	0.045

C

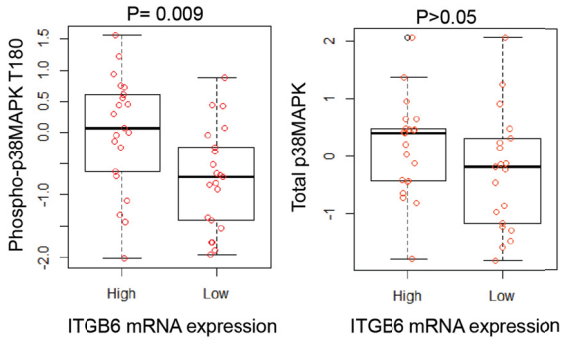

D

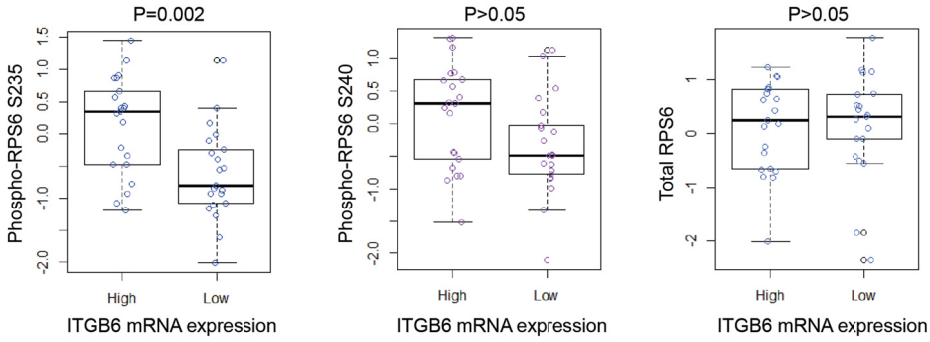

Figure 5.2: Integrin αvβ6 expression correlates with poor prognosis in HNSCC and is associated with p38 and RPS6 signaling. **A.** Kaplan-Meier analysis of HNSCC samples from TCGA showing overall survival over time for high and low integrin β6 expression (n=400). Kaplan-Meier analysis was done using R, and statistical significance was calculated using the log-rank test. **B.** Table showing significant changes in phospho-proteins for high and low integrin β6 expressing tumors (43 phospho-proteins included in the panel, n=210 patients). **C,D.** Boxplots showing changes in

phospho- and total- p38 MAPK (**C**) or phospho- and total RPS6 (**D**) protein levels in high and low β6-expressing tumors. Statistical analysis for C,D was calculated using student's t-test.

Figure 5.3

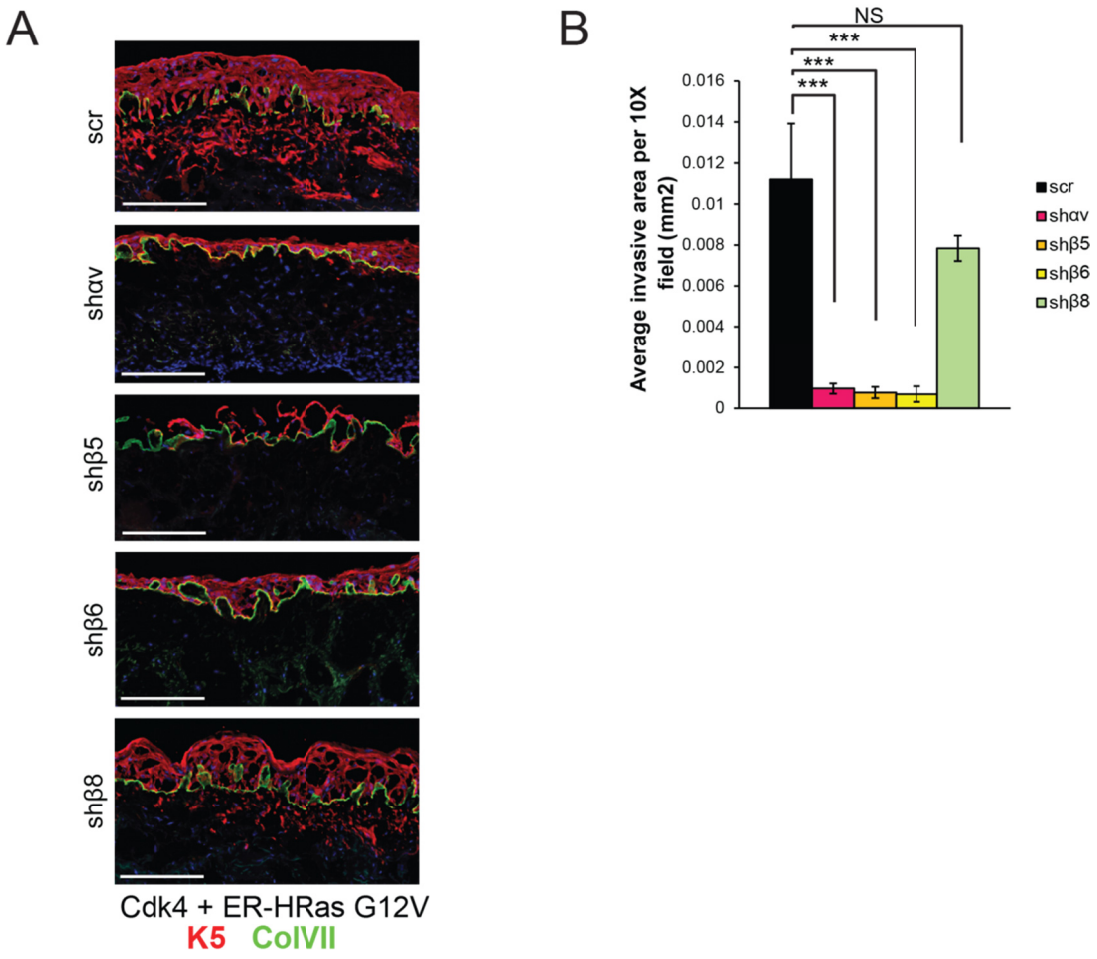

Figure 5.3: Integrin αv and its binding partners β5 and β6 are necessary for organotypic SCC invasion initiation. **A.** Morphologic analysis of organotypic tissue containing keratinocytes infected with Cdk4 R24C, ER-HRas G12V (treated with 100nM 4-OHT) and either a scramble hairpin or hairpins targeting integrins αv, β5, β6, β8. **B.** Quantification of invasive area from (**A**) measured in mm^2 (mean ± SD). N=3 organotypic tissues. Representative of 2 independent experiments. $P=8.55x10^{-6}$ using one-way ANOVA. Scale bar= 200μm. ***=p<0.0005 using Tukey's HSD post-hoc test.

Figure 5.4

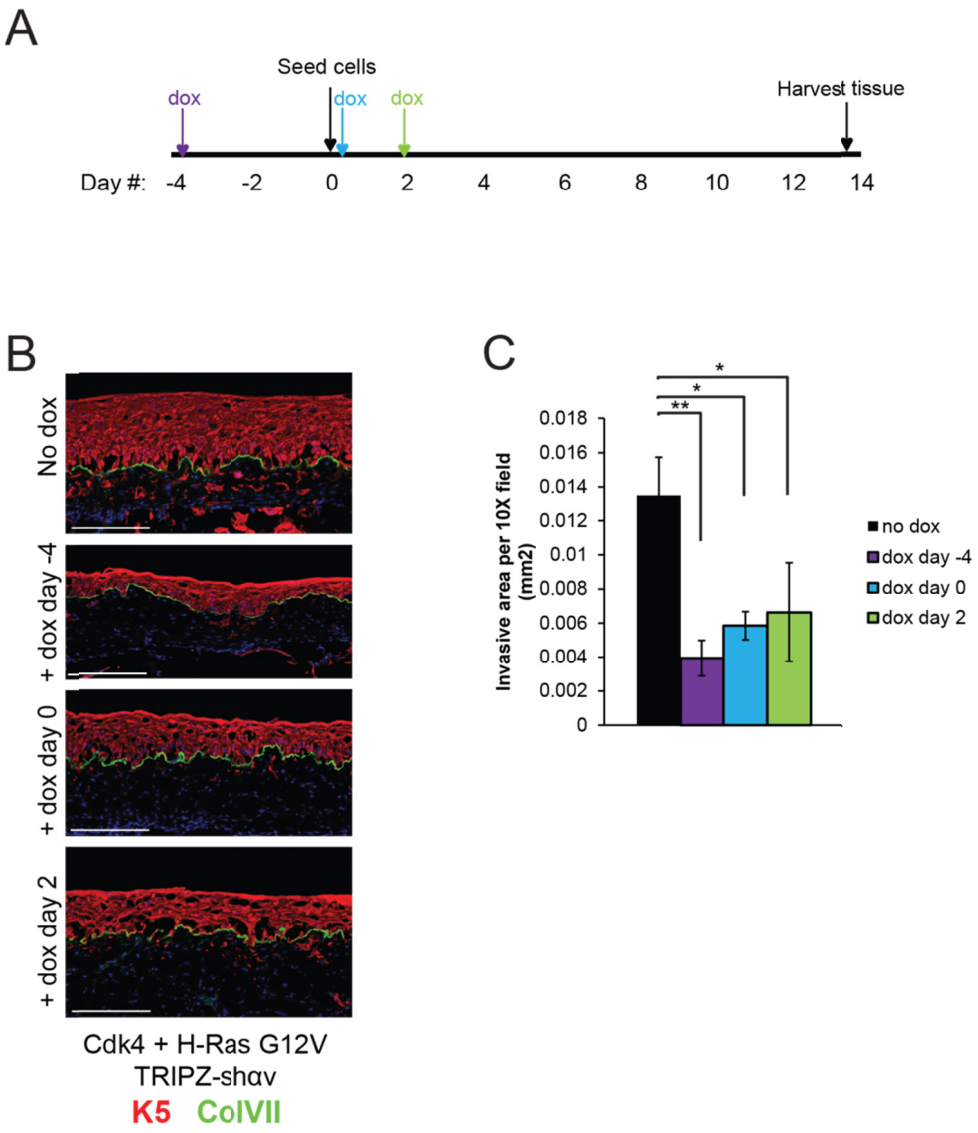

Figure 5.4: Integrin αv is necessary for organotypic SCC invasion initiation and progression. **A.** Experimental setup. Human keratinocytes infected with Cdk4 R24C, H-Ras G12V and TRIPZ-shαv and sorted with flow cytometry were induced with doxycycline at various time points in organotypic culture (indicated with arrows): 4 days prior to seeding, 2 days prior to seeding, day of seeding, 2 days post seeding. **B.** Representative images taken from 2 independent experiments for setup described in (**A**). **C.** Quantification of invasive area from (**B**) measured in

mm^2 (mean ± SD). Representative of 2 independent experiments. N=3 organotypic tissues. P=0.00155 using one-way ANOVA. Scale bar=200μm. *=P<0.05, **=P<0.005 using Tukey's HSD post-hoc test.

Figure 5.5

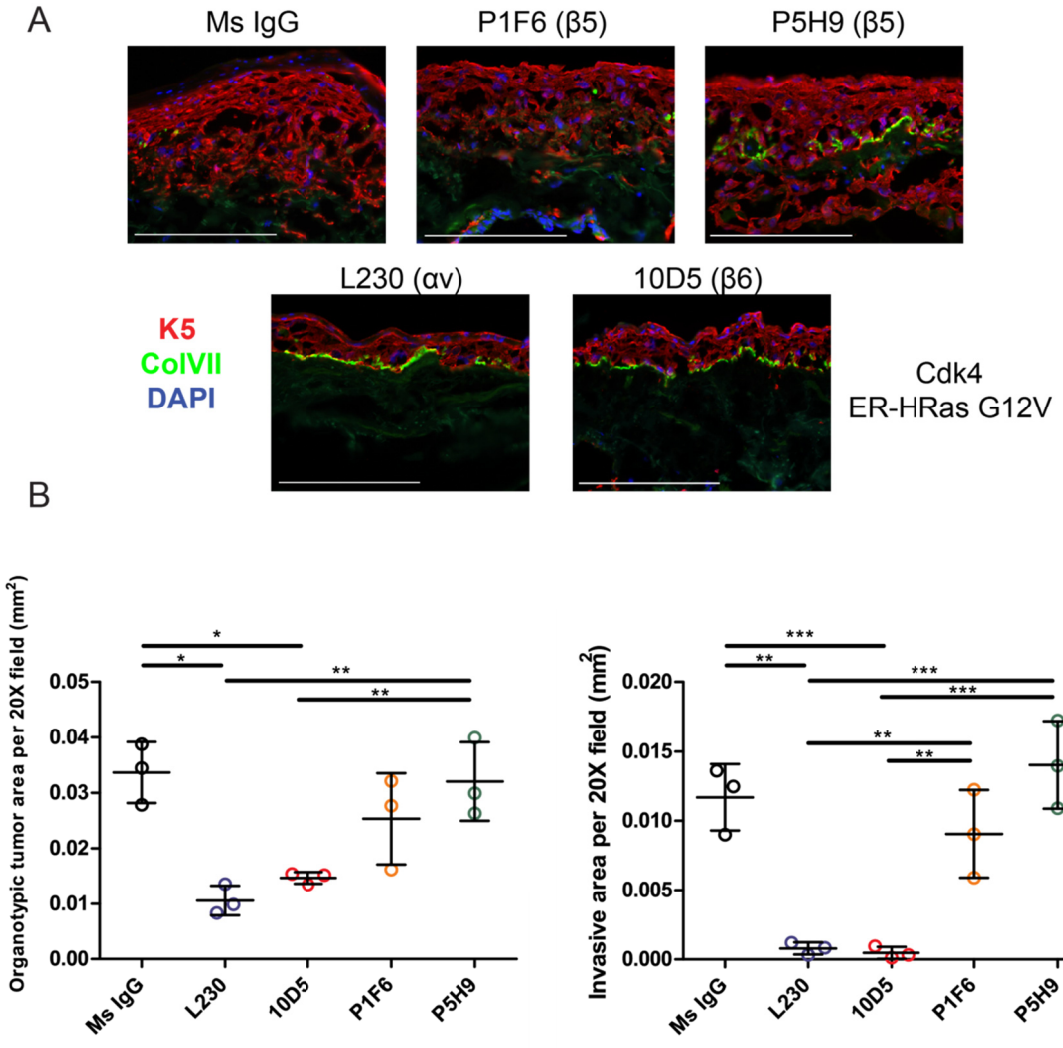

Figure 5.5: Blocking antibodies targeting all αv integrins (L230) or αvβ6 block organotypic tumor invasion. **A.** Morphologic analysis of organotypic tissue containing keratinocytes infected with Cdk4 R24C, ER-HRas G12V (treated with 100nM 4-OHT) and treated with 7μg/mL of the following antibodies: Mouse IgG (control), L230 (pan-αv), 10D5 (αvβ6), P1F6 (αvβ5) or P5H9 (αvβ5). **B.** Quantification of organotypic tumor area (total K5+ area, left) and invasive area (right) from (**A**) measured in mm^2 (mean ± SD). N=3 organotypic tissues. P=0.0015 (left) and P<0.0001

(right) using one-way ANOVA. Scale bar= 200μm. *=p<0.05, **=p<0.005, ***=p<0.0005 using Tukey's HSD post-hoc test.

Figure 5.6

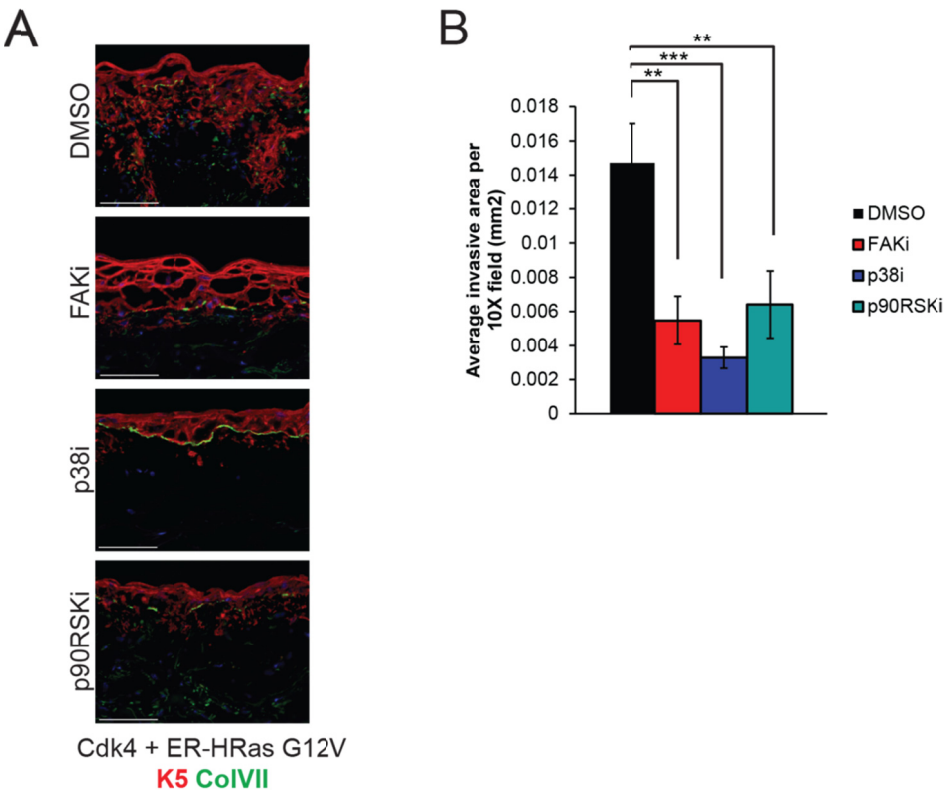

Figure 5.6: FAK, p38 and p90RSK are also necessary for organotypic SCC invasion. **A.** Keratinocytes were transduced with Cdk4 (R24C) and ER-H-Ras (G12V) and treated with the indicated inhibitors. The following concentrations of inhibitors were used: 1μM PF-573228 (FAKi), 10μM SB 202190 (p38i) and 1μM BI-D1870 (p90RSKi), with media replacement every day. Representative images are shown. **B.** Quantification of invasive area from (**A**) measured in mm^2 (mean ± SD). N=3 organotypic tissues. P=0.000607 using one-way ANOVA. Scale bar=100μm. **=p<0.005, ***=p<0.0005 using Tukey's HSD post-hoc test.

Figure 5.7

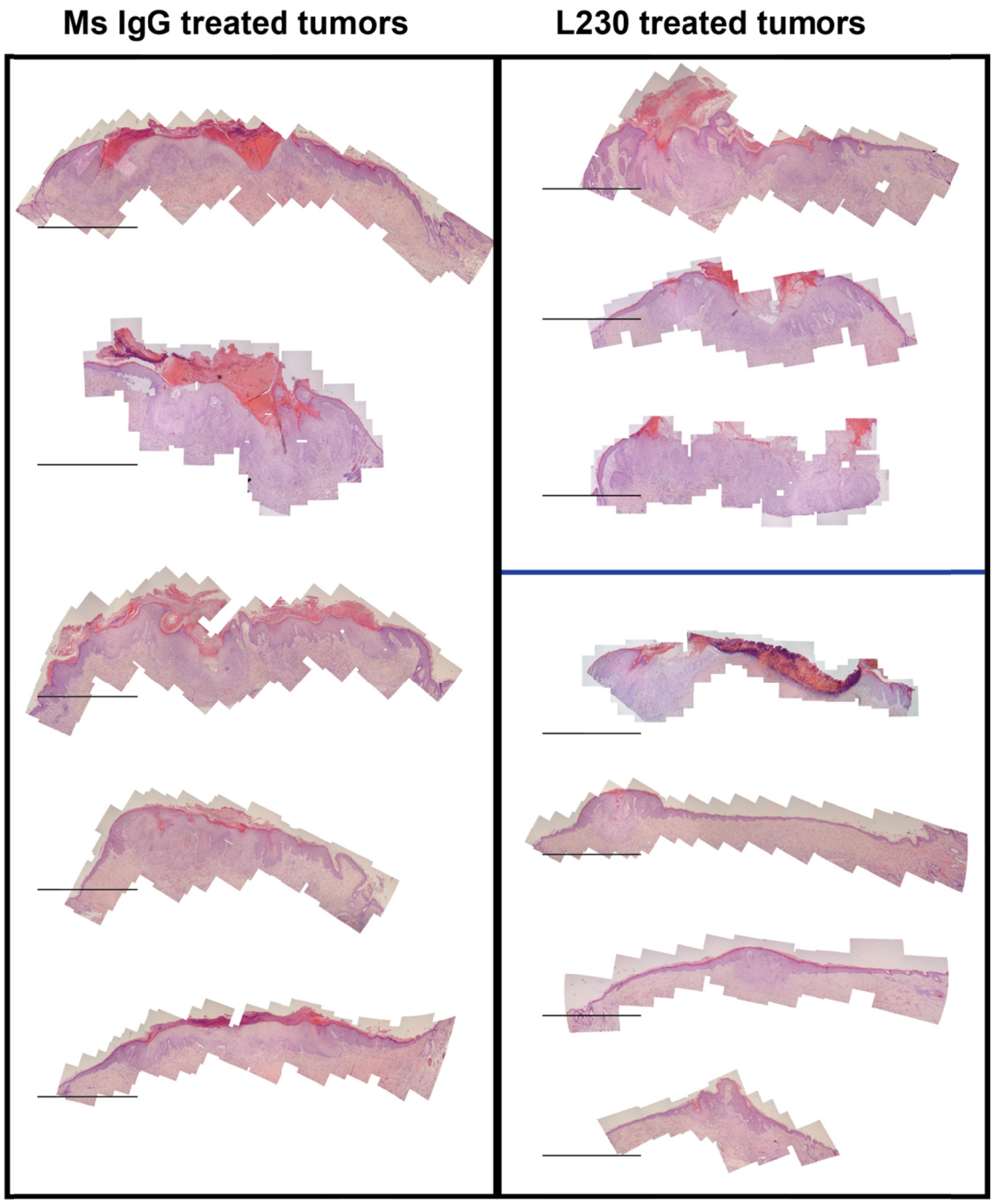

Figure 5.7: Integrin αv blocking antibody, L230, decreases SCC tumor size in an in vivo orthotopic inducible model. Human skin made from keratinocytes expressing Cdk4 R24C and a

doxycycline-inducible H-Ras G12V was grafted onto SCID mice. After complete healing of the skin graft (3 weeks after grafting), antibody treatment was started and mice were switched to doxycycline chow one day later. Mice were treated with 100μg of antibody every other day for 2 weeks, and the tumors were harvested. Shown are composite H&E images of whole tumor cross-sections from control (mouse IgG) treated mice and L230 treated mice. All images are to scale relative to one another. On the right side, the tumors with large reductions in area are shown on the bottom (4/7 tumors) and tumors that had minimal reduction are shown on the top (3/7 tumors). Scale bar=1mm.

Figure 5.8

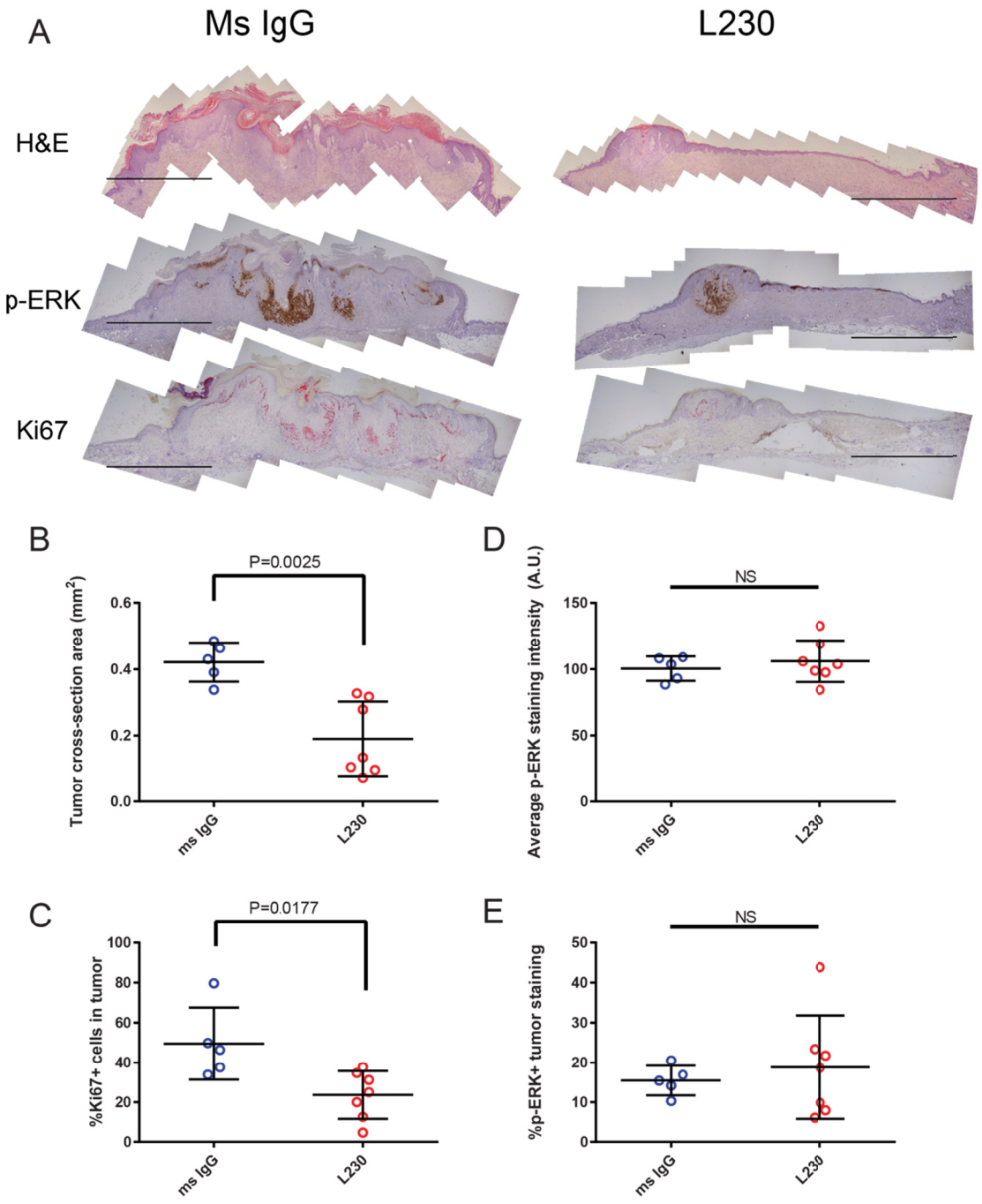

Figure 5.8: Integrin αv blocking antibody, L230, decreases tumor size and proliferation without altering ERK1/2 activity. **A.** Representative images of orthotopic human SCC tumors (control mouse IgG treated or L230 treated) stained with Ki67 (human-specific antibody) or phospho-

ERK1/2. The L230-treated tumor shown is a tumor that had reduced area (lower right quadrant of Figure 5.7). **B.** Quantification of tumor cross-section area from Figure 5.7 in mm^2. P=0.0025 using non-parametric Mann Whitney test. **C.** Quantification of %Ki67+ tumor cells within the tumor from tumors represented in Figure 5.7. P=0.0177 using Mann Whitney test. **D.** Average intensity of p-ERK1/2 staining in tumor sections from figure 5.7. NS= not statistically significant. A.U.= arbitrary units. **E.** Percentage of the tumor area (of tumors from Figure 5.7) that is p-ERK1/2-positive. NS= not statistically significant. Scale bar=1mm.

DISCUSSION

Here, we show that integrin αv heterodimers are necessary for tumor progression and invasion both in organotypic culture and in an inducible, orthotopic human xenograft SCC model *in vivo*. We also show that blocking antibodies targeting both pan-αv integrins (L230) and αvβ6 specifically (10D5) can block tumor invasion. The downstream signaling pathway controlled by αv in normal skin—FAK→p38→p90RSK—is also essential for tumor invasion, thus providing additional potential therapeutic targets for this disease.

While most cutaneous SCCs in immunocompetent individuals can be treated with local excisions or topical delivery of immunomodulatory and chemotherapy, there are frequently cases in which patients are not good surgical candidates. Additionally, immunosuppressed SCC patients often suffer from SCC metastasis and unfortunately have limited treatment options.

As mentioned in previous chapters, αv integrins have been shown to have tumor-suppressive roles in certain mouse models (McCarty et al., 2008; Savar et al., 2014; Xie et al., 2012). However, in many human cancers and human cancer models, αv appears to have a tumor-promoting role. αvβ6 is over-expressed in epidermal SCC, higher αvβ6 expression correlates with decreased survival in human cervical SCC, and αvβ6 promotes invasion in human oral SCC cell lines (Hazelbag et al., 2007; Hsu et al., 2011; Li et al., 2003; Li et al., 2013; Nystrom et al., 2006; Reuter et al., 2009; Van Aarsen et al., 2008; Xue et al., 2001). Also potentially complicating direct comparisons between mouse and human systems is the fact that in most mouse models, integrin expression is depleted during embryogenesis, rather than in adult tissue. Acute loss of integrins in adult mouse skin has been shown to have markedly different phenotypic effects compared to loss during development (Brakebusch et al., 2000; López-Rovira et al., 2005; Raghavan et al., 2000). Of course, if long-term blockade of αv leads to spontaneous tumor formation (as seen in the eyelid and conjunctiva upon genetic deletion of αv), this would certainly be cause for concern (McCarty et al., 2008). The long-term effects of αv blockade should certainly be examined more thoroughly before promoting use of αv blocking agents in the clinic.

The idea of targeting specific αv heterodimers as an anti-cancer strategy is intriguing, since these specific heterodimers appear to control both FAK and c-myc. FAK is known to promote tumor formation in mouse SCC models, and several small molecule FAK inhibitors are in early stage clinical trials (McLean et al., 2001; McLean et al., 2004; Sulzmaier et al., 2014). Targeting FAK indirectly through αv may lead to greater specificity than small molecule kinase inhibitors, and as a cell surface protein, αv may be vulnerable to blocking antibodies and peptide based agents. It will also be interesting to determine whether αv controls the FAK→p38→c-myc pathway in other epithelial malignancies dependent on myc signaling (Gabay et al., 2014). Targeting each heterodimer individually may lead to fewer side-effects than antagonism of the entire αv group, since the β subunits are not as ubiquitously expressed as αv, and their corresponding knockout mice have minimal phenotypes (Huang et al., 1996; Huang et al., 2000a).

While it is clear that αv integrins promote cutaneous SCC progression, the roles of αv integrins may differ in other tumor types. In pancreatic cancer, αvβ6 suppresses tumor formation likely through TGFβ signaling (Hezel et al., 2012). However, in breast cancer αvβ6 is necessary for invasion and metastasis, and up-regulation of mRNA for β6 is associated with poor survival in patients (Eberlein et al., 2013; Li et al., 2015a; Moore et al., 2014). β6 mRNA is also up-regulated in colon tumors and is associated with reduced survival (Bates et al., 2005). There is less known about the specific roles of β5 integrins in tumor progression. β5 knock down can reduce tumor volume in breast and ovarian cancer cell lines, and is associated with increased tumor stage in ovarian cancer (Bianchi-Smiraglia et al., 2013; Tancioni et al., 2014). However, there is little known about the role of αvβ5 in other malignancies. In our organotypic SCC model, β5 knock down decreases tumor invasion; however, it is unclear whether a blocking antibody targeting β5 may be effective in reducing tumor burden. Development of more effective blocking β5 antibodies may be necessary for preclinical testing.

In summary, we have shown that acute loss of αvβ5 and αvβ6 leads to loss of de novo epidermal tissue generation and tumor invasion, but not tissue maintenance; therefore these heterodimers may be useful targets for human epidermal cancer.

CHAPTER 6

Summary and Future Directions

Parts of this chapter have been previously published in:

Duperret EK, Dahal A, Ridky TW. Focal adhesion-independent integrin αv regulation of FAK and c-myc is necessary for 3D skin formation and tumor invasion. *J Cell Sci.* 2015; 128(21):3997-4013.

Major Conclusions

Here, we have utilized an shRNA screen in organotypic skin to identify the αv family of integrins as essential mediators of skin tissue generation. We have found that αv mediates its functions through binding partners β5 and β6, but not β1 or β8 (Figure 6.1). We show that integrin αv is dispensable for skin tissue maintenance in organotypic culture and *in vivo*, but is necessary for proliferation during human wound healing *in vivo*. αv plays a specific role in promoting cell cycle progression, but not adhesion, in keratinocytes. It promotes a signaling pathway involving TGFβ- and FAK- mediated control of protein translation. Specifically, αv controls c-myc translation through p38 and p90RSK signaling pathways (Figure 6.1). Surprisingly, αv mediates its signaling functions and control of FAK activation outside of classic focal adhesions. We find that the key downstream targets of αv—FAK, p38 and p90RSK—are similarly necessary for skin tissue generation, but dispensable for tissue maintenance. Because of αv's role in promoting hyperproliferation in human wounds, we wondered whether it may contribute to cutaneous squamous cell carcinoma. We found that αvβ6 is up-regulated in squamous cell carcinoma and correlates with poor prognosis in head and neck SCCs. αvβ5 and αvβ6 and downstream targets FAK, p38 and p90RSK are required for organotypic SCC invasion. Blockade of all αv heterodimers (using blocking antibody L230) or αvβ6 specifically (using blocking antibody 10D5) also halts organotypic SCC progression. Finally, treatment of an orthotopic human xenograft

model of cutaneous SCC with L230 reduces tumor burden *in vivo*. These results have provided novel functional and specific mechanistic insight into the roles of αv integrins in both skin tissue homeostasis and Squamous Cell Carcinoma.

Future Directions: Validation of additional RNAi screen targets

While we chose to focus on the αv class of integrins for this dissertation, our RNAi screen identified several additional β1-binding integrins that were necessary for skin tissue generation. Knock down of integrins α2, α4, α5 and α10 all led to remarkable fitness disadvantage in skin tissue. The results from α4 and α10 were surprising since they have not been reported to be expressed in skin tissues, while α2 and α5 have constitutive expression in the skin (Duperret and Ridky, 2013; Margadant et al., 2010). We verified that α4 and α10 are indeed expressed, albeit at low levels, in freshly isolated primary human keratinocytes (Figure 6.2A). To verify that the results for α4 knock down in our shRNA screen were not an off-target shRNA effect, we knocked down α4 with three independent shRNAs in cultured human keratinocytes (Figure 6.2B). Two of the hairpins effectively reduced α4 protein level in keratinocytes, and also resulted in decreased Rb phosphorylation, while the other hairpin (hairpin #2) had no effect on either α4 protein or Rb phosphorylation (Figure 6.2B). This indicates that α4 does play a role in controlling cell cycle progression in human keratinocytes.

The integrin α2 knockout mouse is viable, fertile and normal (Chen et al., 2002). There is no reported change in re-epithelialization during wound healing in this mouse; however, no skin-specific conditional knockout strain has been generated (Grenache et al., 2007; Zweers et al., 2007). The knockout mouse for integrin α10 is also viable and fertile, and wound healing has not been assessed in this mouse (Bengtsson et al., 2005). Knockout mice for integrins α4 and α5 exhibit embryonic lethality, and the corresponding skin-specific knockout mice have not been generated (Gurtner et al., 1995; Yang et al., 1993). Thus, this is a wide-open area for future research into the specific functions of these integrins in skin tissue homeostasis, skin tissue generation in the context of wound healing and tumorigenesis.

Utilizing similar approaches as those described in this dissertation, we can determine whether integrins α2, α4, α5 or α10 may be involved in re-epithelialization during wound healing by: 1) examining their expression and localization in human skin and human skin wounds, 2) determining their role in organotypic skin tissue through constitutive and inducible shRNA knock down approaches, and 3) Determining their functional relevance in *in vivo* epidermis and wound healing using function-blocking antibodies (which exist for all of these subunits with the exception of α10) (Byron et al., 2009). Additionally, we can define the roles for α2 and α10 in tumorigenesis by performing DMBA-TPA chemical carcinogen treatment on the backs of the corresponding knockout mice. This will help determine whether blockade of either of these subunits may potentially be therapeutically beneficial. In the case of the α2-null mouse, it has been shown that α2 deletion blocks tumor formation and metastasis in a K14-HPV background (Tran et al., 2011). It remains to be determined, however, whether this can be extended to other oncogenic driver mutations.

Future Directions: Determine how integrin αv controls FAK recruitment to focal adhesions

A major unanswered question from this work is: how does integrin αv control FAK activation and localization to focal adhesions? Integrin αv is not localized to focal adhesions, yet somehow alters focal adhesions indirectly. Within the focal adhesion, the known major FAK binding partners are Talin and Paxillin (Calderwood et al., 2013; Schaller, 2010). We demonstrated that Paxillin is present in focal adhesions upon αv knock down. Furthermore, Paxillin is dispensable for targeting of FAK to focal adhesions (Cooley et al., 2000). In mature adhesions, Talin has been suggested to recruit FAK (Chen et al., 1995; Frame et al., 2010; Lawson et al., 2012). TGFβ signaling is known to upregulate several integrin subunits and focal adhesion proteins (Margadant and Sonnenberg, 2010). There is also some evidence that TGFβ signaling can regulate Talin expression (Rafiei, 2007). We thus wondered if αv knock down would result in depletion of Talin protein from keratinocytes. Indeed, when we knocked down αv, Talin1 protein levels were reduced (Figure 6.3). This reduction in Talin1 protein expression could be

rescued by addition of TGFβ1 at doses ranging from 1pM-1nM (Figure 6.3). This indicates that αv controls Talin1 expression through TGFβ signaling.

The roles of Talin1 in maintaining focal adhesion structure and recruiting FAK to focal adhesions are somewhat controversial and cell-type dependent. In mammary epithelial cells, Talin knock down leads to efficient attachment to the ECM and integrin-dependent cell spreading; however, Vinculin, Paxillin, FAK and ILK are not recruited to adhesion sites (Rossier et al., 2012; Wang et al., 2011). In contrast, Talin 1/2 null mouse embryonic fibroblasts have normal Src family kinase activation, but no integrin linkage to the extracellular matrix, severe defects in cell spreading, adhesion and FAK signaling (Zhang et al., 2008). While Talin was originally thought to recruit FAK to focal adhesions, recent evidence supports a role for FAK in recruiting Talin to nascent adhesions (Chen et al., 1995; Frame et al., 2010; Lawson et al., 2012). Thus, it would be valuable to clarify the role of Talin in FAK recruitment to focal adhesions in human keratinocytes, and determine the relevance of αv's control of Talin1.

First, we should examine the expression and localization of both Talin isoforms, Talin1 and Talin2, in response to αv knock down. Talin1 and Talin2 can compensate for one another in culture; however, their localization is slightly different: Talin1 is localized only at focal adhesions, while Talin2 is additionally localized at fibrillar adhesions (larger adhesion complexes located closer to the body of the cell) (Praekelt et al., 2012). αv knock down did not completely abolish Talin1 expression (Figure 6.3), and thus it is possible that the stoichiometry of Talin1 protein within the adhesion is altered upon αv loss. Next, we should examine the effects of Talin1/2 knock down in keratinocytes, and determine whether that results in loss of FAK expression, activation, and/or localization to focal adhesions. Finally, if Talin disruption alters FAK activity, we should restore Talin expression in αv-deficient keratinocytes and determine whether that is sufficient to restore FAK function.

It is possible that Talin is not the only mediator of FAK activity in keratinocytes, and thus we should take a proteomics approach to determine what might be different about focal adhesions in the absence of αv, which will be detailed in the next section.

Future Directions: Utilize proteomics to determine how αv alters focal adhesions and identify novel binding partners for αv

A recent wave of advances in proteomics has allowed the identification of hundreds of focal adhesion-associated proteins (Ajeian et al., 2015; Byron et al., 2012; Byron et al., 2015; Horton et al., 2015; Humphries et al., 2009; Jones et al., 2015; Kuo et al., 2011; Robertson et al., 2015). Almost all of these efforts have focused on identifying the integrin adhesome for Fibronectin-binding integrins, primarily α4β1, α5β1 and αvβ3. Specific protocols exist for identifying adhesion complexes after plating cells for short time periods on specific extracellular matrix substrates (Jones et al., 2015). These protocols have been optimized for mesenchymal cell types, and may require optimization for rigid, keratin-rich keratinocytes (Jones et al., 2015). However, these focal adhesion isolation approaches, combined with mass spectrometry, can potentially identify key focal adhesion components that change upon αv depletion in keratinocytes.

While these approaches are effective at identifying components within adhesions, it will be more challenging to determine with what integrin αv directly interacts. Conventional immunoprecipitation approaches in our hands have been effective at determining with which β subunits integrin αv interacts (Figure 3.4). However, mass spectrometry of these immunoprecipitates has not consistently identified any additional binding partners across biological replicates. This is likely due to the harsh lysis conditions required for isolation of integrins from the membrane for the immunoprecipitation protocol. New approaches have been developed to biotin-label proteins in living cells (Lam et al., 2014; Rhee et al., 2013). APEX2, an engineered peroxidase, can be fused to a protein of interest, and in the presence of biotin-phenol and H_2O_2, APEX2 is able to oxidize biotin-phenol to create a radical that can covalently tag endogenous proteins proximal to APEX2 with biotin (Lam et al., 2014; Rhee et al., 2013). Biotinylated proteins can then be enriched using streptavidin beads for subsequent proteomic analysis. We can utilize this approach, by tagging αv integrin cytoplasmic tails, to identify interacting partners of αv without the need for immunoprecipitation approaches.

Future Directions: Determine the therapeutic potential for targeting FAK, p38 or p90RSK in cutaneous Squamous Cell Carcinoma

Currently, several small molecule inhibitors targeting FAK and various p38 isoforms are in clinical trials for cancer. Compounds have been developed that block FAK catalytic activity, either through ATP-competitive inhibition or targeting FAK scaffolding properties (Sulzmaier et al., 2014). Initial Phase I clinical trials of PF-562,271 (Pfizer) showed low toxicity and stable disease for a variety of different advanced solid tumors (Infante et al., 2012). Phase II trials are currently ongoing for additional compounds, including VS-6063 (Pfizer); however, no results are currently available from these trials (NCT01951690 and NCT02004028, clinicaltrials.gov). FAK mRNA is over-expressed in human head and neck squamous cell carcinoma, genetic ablation of FAK in *in vivo* cutaneous SCC models decreases tumor growth and invasion, FAK blockade has been shown to enhance radiosensitivity of SCC cancer cell lines, and treatment of mice with the FAK inhibitor PF-562,271 reduced subcutaneous SCC xenograft tumor size (Canel et al., 2006; Eke et al., 2012; Graham et al., 2011; McLean et al., 2001; McLean et al., 2004; Serrels et al., 2012). However, the mechanism of action of FAK blockade in SCC tumors remains largely unknown. Defining mechanisms of action for drugs is important, because it can define potential biomarkers for therapeutic efficacy, and potentially help identify new targets. In the case of FAK inhibition, reports have shown that FAK inhibition may be more effective in non-small cell lung cancers that have INK4a/Arf inactivation and that loss of the neurofibromatosis 2 tumor suppressor gene in mesothelioma sensitizes to FAK inhibition (Konstantinidou et al., 2013; Shah et al., 2014). Thus, future experiments in our laboratory could include evaluation of FAK inhibitors in our *in vivo* orthotopic cutaneous SCC model, and identification of specific downstream mechanisms of action. It will be interesting to determine whether FAK inhibition leads to c-myc loss in the context of tumorigenesis, and if this signaling pathway could be extended to other tumor types that may be addicted to myc signaling.

Similarly, p38 inhibitors have shown pre-clinical therapeutic utility for treatment of a variety of different malignancies (Igea and Nebreda, 2015). P38 isoforms are known to play a pro-

proliferative role within tumor cells, and to be highly activated by inflammatory cytokines in the tumor microenvironment. Because p38 regulates inflammatory signaling, caution must be taken when utilizing p38 inhibitors, since p38 has been shown to be essential for protection against colitis-associated colon cancer in the intestinal epithelium (Gupta et al., 2014). P38 inhibitors were initially developed for treatment of inflammatory diseases such as rheumatoid arthritis, but many showed initial toxicity and no therapeutic efficacy (Coulthard et al., 2009; Genovese, 2009). Currently, Phase I studies are ongoing to test several p38 inhibitors (LY2228820, LY3007113) in solid tumors and lymphomas (NCT02364206, NCT01463631, NCT01393990) (Campbell et al., 2014). Pre-clinical models have shown efficacy for p38 inhibition for the treatment of head and neck SCC in xenograft tumor models (Leelahavanichkul et al., 2014). Similar to the FAK inhibitor data, there is little known regarding the specific mechanism of action of these p38-targeting drugs in halting tumor growth.

P90RSK represents a new potential therapeutic target, as no p90RSK inhibitors are in clinical trials for cancer. Targeting the translation machinery is becoming a promising new therapeutic area for treatment of cancer, with targets including mTOR signaling pathway elements, components of the eukaryotic initiation factor complex, and MNK (Bhat et al., 2015; Grzmil and Hemmings, 2012). Several studies have reported pre-clinical efficacy for p90RSK inhibitors (Smith et al., 2005; Sulzmaier and Ramos, 2013). RSK2 was shown to be essential for head and neck SCC tumor growth and invasion *in vivo*. However, our studies show that RSK1 is the more important isoform for the cutaneous epithelium (Duperret et al., 2015). It would thus be useful to characterize the efficacy of the dual- RSK1/2 inhibitor BI-D1870 in treatment of cutaneous SCC in our *in vivo* orthotopic model (Sapkota et al., 2007). Toxicity, dose-escalation and efficacy studies may be required for this compound to bring it closer towards inclusion in clinical trials.

Future Directions: Extend our findings into an *in vivo* orthotopic melanoma model

Our laboratory recently showed that loss of the tumor suppressor locus CDKN2B, which encodes the p15 protein, is essential for development of radial-phase melanomas from benign nevi utilizing our human orthotopic xenograft model (McNeal et al., 2015). However, what regulates invasive behavior in this model is poorly understood. Others have shown that Akt activation (primarily through genetic loss of the PTEN tumor suppressor) can promote the transition between radial and vertical growth phase in melanoma (Govindarajan et al., 2007). We have confirmed that expression of a constitutively active AKT3 mutant (E17K) results in increased invasion of human melanomas generated using primary nevus melanocytes in our orthotopic xenograft model *in vivo* (Figure 6.4) (Davies et al., 2008). Integrins (in particular αvβ3) have also been implicated in the transition of melanoma from radial to vertical growth phase (Hsu et al., 1998; Petitclerc et al., 1999). We analyzed integrin subunit expression at the RNA level in primary melanocytes compared to a panel of melanoma cell lines and melanocytes transduced with oncogenes. This revealed that many integrin subunits are highly over-expressed in melanomas (some exhibit over 200-fold over-expression) (Figure 6.5). In particular, the α4, α6 and α7 subunits were highly over-expressed in all cases (Figure 6.5). There is very little known about the roles for these integrins in invasive melanoma. Thus, we can use the same shRNA screening approaches to define specific functional roles for various integrins in the context of radial and vertical growth phase melanoma. In summary, the toolkit and screening techniques that I have developed as a part of this dissertation can be utilized for many additional tumor types that may rely on integrins for malignant behavior.

FIGURES

Figure 6.1

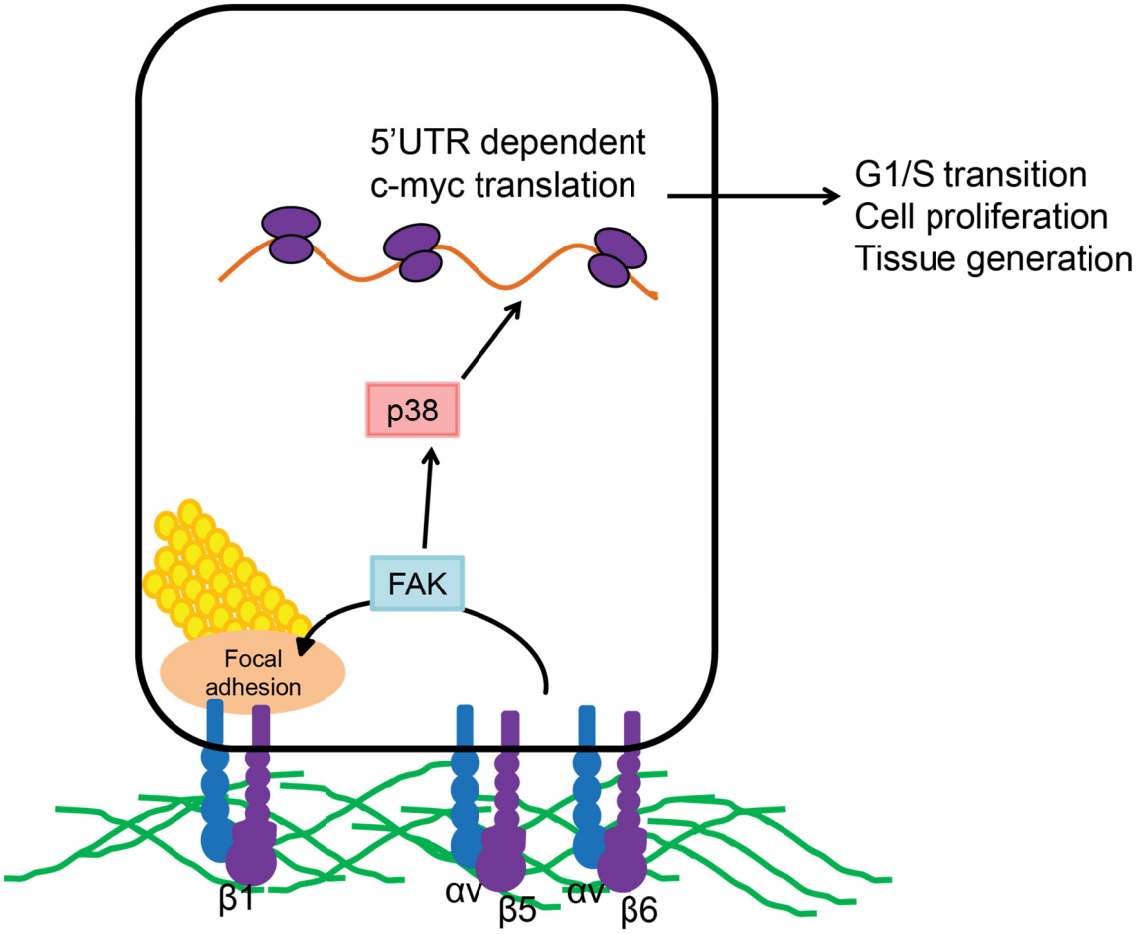

Figure 6.1: Diagram of signaling pathway described in this dissertation. Integrin αv dimerizes with β5 or β6 outside of focal adhesions to control FAK expression, activation and localization to focal adhesions. Downstream, FAK controls p38 phosphorylation to induce 5'UTR-dependent c-myc translation. This ultimately results in promotion of cell cycle progression, G1/S transition and skin tissue generation.

Figure 6.2

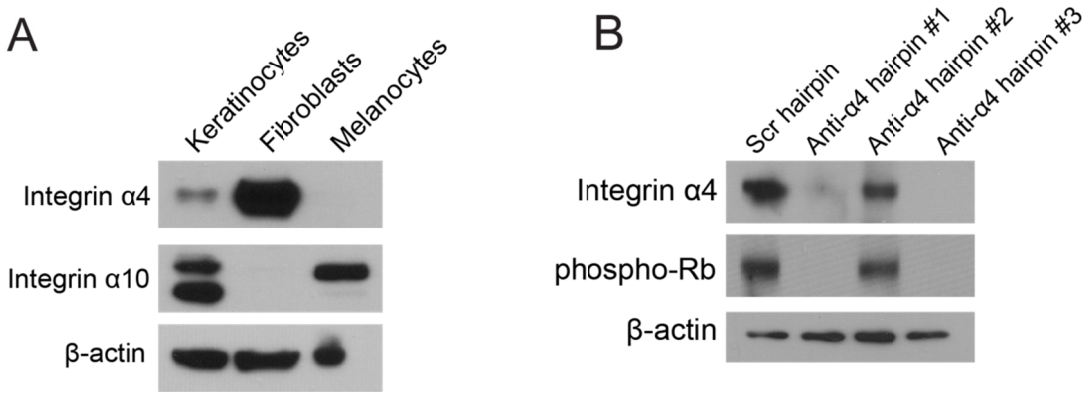

Figure 6.2: Integrin α4 and α10 expression in keratinocytes. **A.** Western blot of integrin α4 and α10 in human keratinocytes, melanocytes and fibroblasts. **B.** Western blot of keratinocytes infected with the indicated integrin α4 hairpins. Hairpin #3 was used for the shRNA screen in Chapter 3.

Figure 6.3

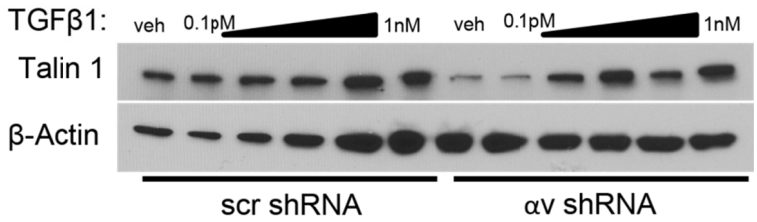

Figure 6.3: Integrin αv controls Talin1 expression through TGFβ signaling in keratinocytes. Western blot showing signaling pathway changes upon addition of varying doses of TGFβ1 in keratinocytes infected with indicated hairpins. TGFβ1 doses range from 0.1pM to 1nM, increasing by 10-fold.

Figure 6.4

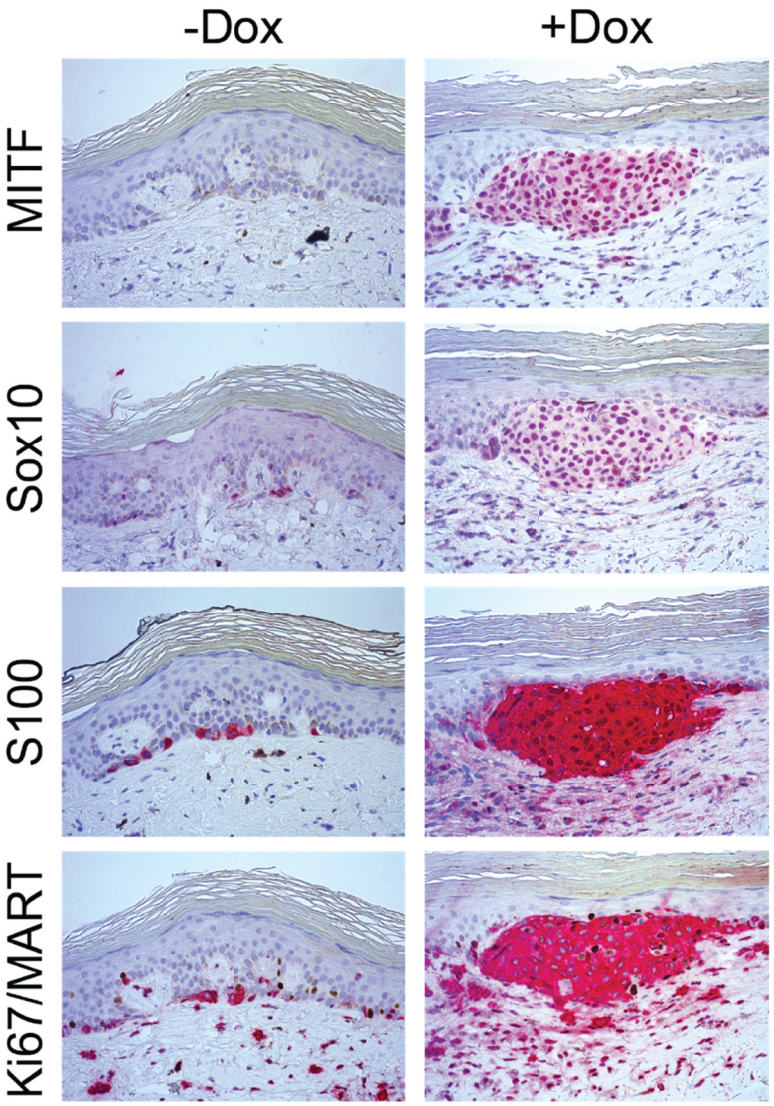

Figure 6.4: Akt promotes radial to vertical growth phase in melanoma. Nevus melanocytes were transduced with Cdk4 R24C, dnp53 (R248W), hTERT and diAKT3 (E17K) and xenografted onto SCID mice. A subset of the mice were switched to doxycycline chow, and 90 days after xenografting the tissue was harvested and stained for MITF, Sox10, S100 and Ki67/MART to analyze resulting melanomas.

Figure 6.5

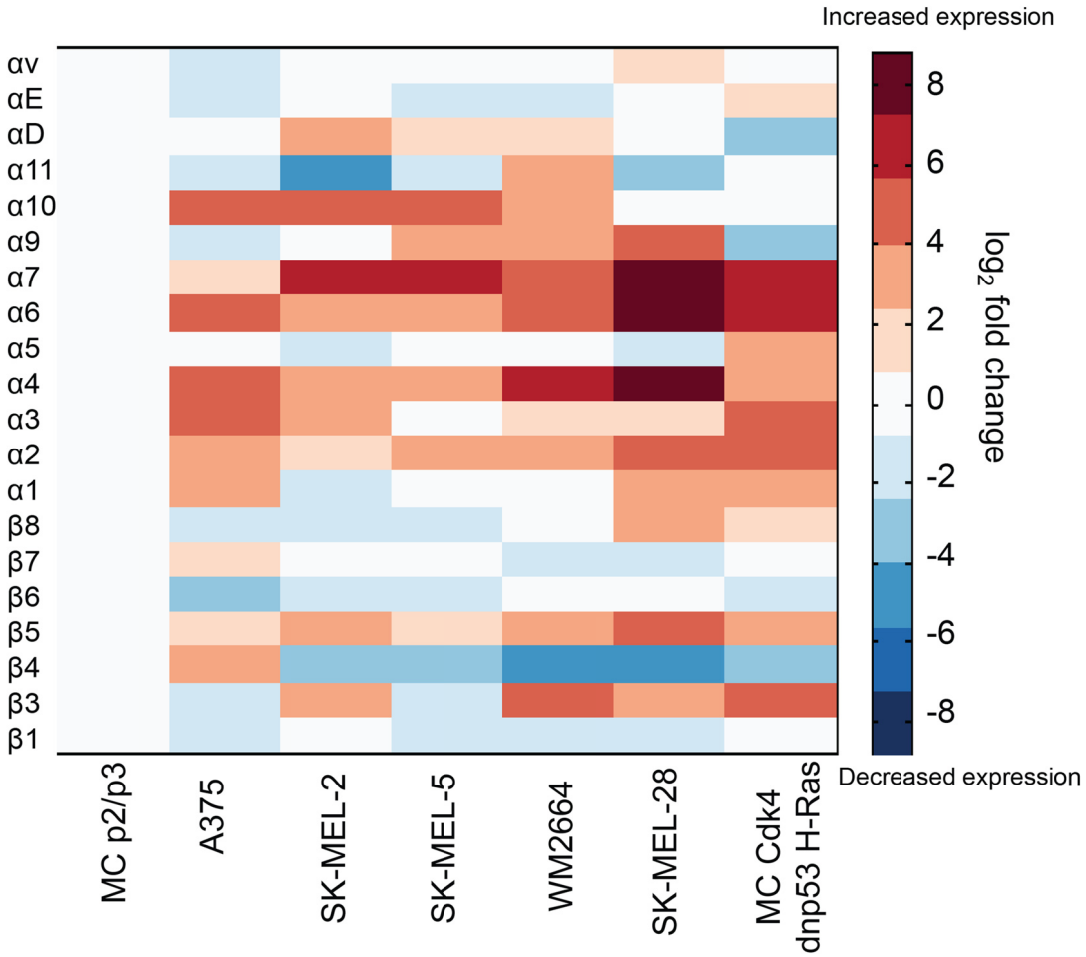

Figure 6.5: Integrin expression in melanocytes and melanoma cell lines.

Heat map showing integrin mRNA changes comparing primary early-passage (passage2 or passage 3) melanocytes to a panel of human melanoma cell lines and melanocytes transduced with oncogenes.

BIBLIOGRAPHY

Abel, E. L., Angel, J. M., Kiguchi, K. and DiGiovanni, J. (2009). Multi-stage chemical carcinogenesis in mouse skin: fundamentals and applications. *Nat. Protoc.* **4**, 1350–1362.

Acharya, M., Mukhopadhyay, S., Païdassi, H., Jamil, T., Chow, C., Kissler, S., Stuart, L. M., Hynes, R. O. and Lacy-Hulbert, A. (2010). αv Integrin expression by DCs is required for Th17 cell differentiation and development of experimental autoimmune encephalomyelitis in mice. *J. Clin. Invest.* **120**, 4445–4452.

Ajeian, J. N., Horton, E. R., Astudillo, P., Byron, A., Askari, J. A., Millon-Frémillon, A., Knight, D., Kimber, S. J., Humphries, M. J. and Humphries, J. D. (2015). Proteomic analysis of integrin-associated complexes from mesenchymal stem cells. *Proteomics. Clin. Appl.*

Alanko, J., Mai, A., Jacquemet, G., Schauer, K., Kaukonen, R., Saari, M., Goud, B. and Ivaska, J. (2015). Integrin endosomal signalling suppresses anoikis. *Nat. Cell Biol.*

AlDahlawi, S., Eslami, A., Häkkinen, L. and Larjava, H. S. (2006). The alphavbeta6 integrin plays a role in compromised epidermal wound healing. *Wound Repair Regen.* **14**, 289–297.

Alitalo, K., Kuismanen, E., Myllylä, R., Kiistala, U., Asko-Seljavaara, S. and Vaheri, A. (1982). Extracellular matrix proteins of human epidermal keratinocytes and feeder 3T3 cells. *J. Cell Biol.* **94**, 497–505.

Amendt, C., Mann, A., Schirmacher, P. and Blessing, M. (2002). Resistance of keratinocytes to TGFbeta-mediated growth restriction and apoptosis induction accelerates re-epithelialization in skin wounds. *J. Cell Sci.* **115**, 2189–2198.

Andreou, A. Z. and Klostermeier, D. (2014). eIF4B and eIF4G Jointly Stimulate eIF4A ATPase and Unwinding Activities by Modulation of the eIF4A Conformational Cycle. *J. Mol. Biol.* **426**, 51–61.

Annes, J. P., Munger, J. S. and Rifkin, D. B. (2003). Making sense of latent TGFbeta activation. *J. Cell Sci.* **116**, 217–224.

Anthis, N. J., Haling, J. R., Oxley, C. L., Memo, M., Wegener, K. L., Lim, C. J., Ginsberg, M. H. and Campbell, I. D. (2009). Beta integrin tyrosine phosphorylation is a conserved mechanism for regulating talin-induced integrin activation. *J. Biol. Chem.* **284**, 36700–36710.

Arwert, E. N., Hoste, E. and Watt, F. M. (2012). Epithelial stem cells, wound healing and cancer. *Nat. Rev. Cancer* **12**, 170–180.

Ashcroft, G. S., Yang, X., Glick, A. B., Weinstein, M., Letterio, J. L., Mizel, D. E., Anzano, M., Greenwell-Wild, T., Wahl, S. M., Deng, C., et al. (1999). Mice lacking Smad3 show accelerated wound healing and an impaired local inflammatory response. *Nat. Cell Biol.* **1**, 260–266.

Asthagiri, A. R., Nelson, C. M., Horwitz, A. F. and Lauffenburger, D. A. (1999). Quantitative relationship among integrin-ligand binding, adhesion, and signaling via focal adhesion kinase and extracellular signal-regulated kinase 2. *J. Biol. Chem.* **274**, 27119–27127.

Bader, B. L., Rayburn, H., Crowley, D., Hynes, R. O. and Hughes, H. (1998). Extensive Vasculogenesis, Angiogenesis and Organogenesis Precede Lethality in Mice Lacking All αv Integrins. *Cell* **95**, 507–519.

Bandyopadhyay, A. and Raghavan, S. (2009). Defining the role of integrin alphavbeta6 in cancer. *Curr. Drug Targets* **10**, 645–652.

Bao, W. and Strömblad, S. (2004). Integrin alphav-mediated inactivation of p53 controls a MEK1-dependent melanoma cell survival pathway in three-dimensional collagen. *J. Cell Biol.* **167**, 745–756.

Bates, R. C., Bellovin, D. I., Brown, C., Maynard, E., Wu, B., Kawakatsu, H., Sheppard, D., Oettgen, P. and Mercurio, A. M. (2005). Transcriptional activation of integrin beta6 during the epithelial-mesenchymal transition defines a novel prognostic indicator of aggressive colon carcinoma. *J. Clin. Invest.* **115**, 339–347.

Beardmore, V. A., Hinton, H. J., Eftychi, C., Apostolaki, M., Armaka, M., Darragh, J., McIlrath, J., Carr, J. M., Armit, L. J., Clacher, C., et al. (2005). Generation and Characterization of p38 (MAPK11) Gene-Targeted Mice. *Mol. Cell. Biol.* **25**, 10454–10464.

Bellam, N. and Pasche, B. (2010). Tgf-beta signaling alterations and colon cancer. *Cancer Treat. Res.* **155**, 85–103.

Bengtsson, T., Aszodi, A., Nicolae, C., Hunziker, E. B., Lundgren-Akerlund, E. and Fässler, R. (2005). Loss of alpha10beta1 integrin expression leads to moderate dysfunction of growth plate chondrocytes. *J. Cell Sci.* **118**, 929–936.

Bettess, M. D., Dubois, N., Murphy, M. J., Dubey, C., Roger, C., Robine, S. and Trumpp, A. (2005). c-Myc is required for the formation of intestinal crypts but dispensable for homeostasis of the adult intestinal epithelium. *Mol. Cell. Biol.* **25**, 7868–7878.

Bhat, M., Robichaud, N., Hulea, L., Sonenberg, N., Pelletier, J. and Topisirovic, I. (2015). Targeting the translation machinery in cancer. *Nat. Rev. Drug Discov.* **14**, 261–278.

Bianchi-Smiraglia, A., Paesante, S. and Bakin, A. V (2013). Integrin β5 contributes to the tumorigenic potential of breast cancer cells through the Src-FAK and MEK-ERK signaling pathways. *Oncogene* **32**, 3049–3058.

Bill, H. M., Knudsen, B., Moores, S. L., Muthuswamy, K., Rao, V. R., Brugge, J. S., Miranti, K., Muthuswamy, S. K. and Miranti, C. K. (2004). Epidermal Growth Factor Receptor-Dependent Regulation of Integrin-Mediated Signaling and Cell Cycle Entry in Epithelial Cells. *Mol. Cell. Biol.* **24**, 8586–8599.

Blanpain, C. and Fuchs, E. (2009). Epidermal homeostasis: a balancing act of stem cells in the skin. *Nat. Rev. Mol. Cell Biol.* **10**, 207–217.

Bornstein, S., White, R., Malkoski, S., Oka, M., Han, G., Cleaver, T., Reh, D., Andersen, P., Gross, N., Olson, S., et al. (2009). Smad4 loss in mice causes spontaneous head and neck cancer with increased genomic instability and inflammation. *J. Clin. Invest.* **119**, 3408–3419.

Boukamp, P. (2005). Non-melanoma skin cancer: what drives tumor development and progression? *Carcinogenesis* **26**, 1657–1667.

Brakebusch, C., Grose, R., Quondamatteo, F., Ramirez, a, Jorcano, J. L., Pirro, a, Svensson, M., Herken, R., Sasaki, T., Timpl, R., et al. (2000). Skin and hair follicle integrity is crucially dependent on beta 1 integrin expression on keratinocytes. *EMBO J.* **19**, 3990–4003.

Brantsch, K. D., Meisner, C., Schönfisch, B., Trilling, B., Wehner-Caroli, J., Röcken, M. and Breuninger, H. (2008). Analysis of risk factors determining prognosis of cutaneous squamous-cell carcinoma: a prospective study. *Lancet. Oncol.* **9**, 713–720.

Brooks, P. C., Clark, R. a and Cheresh, D. a (1994). Requirement of vascular integrin alpha v beta 3 for angiogenesis. *Science* **264**, 569–71.

Brooks, P. C., Strömblad, S., Sanders, L. C., von Schalscha, T. L., Aimes, R. T., Stetler-Stevenson, W. G., Quigley, J. P. and Cheresh, D. A. (1996). Localization of matrix metalloproteinase MMP-2 to the surface of invasive cells by interaction with integrin alpha v beta 3. *Cell* **85**, 683–693.

Byron, A., Humphries, J. D., Askari, J. A., Craig, S. E., Mould, A. P. and Humphries, M. J. (2009). Anti-integrin monoclonal antibodies. *J. Cell Sci.* **122**, 4009–4011.

Byron, A., Humphries, J. D., Craig, S. E., Knight, D. and Humphries, M. J. (2012). Proteomic analysis of α4β1 integrin adhesion complexes reveals α-subunit-dependent protein recruitment. *Proteomics* **12**, 2107–2114.

Byron, A., Askari, J. A., Humphries, J. D., Jacquemet, G., Koper, E. J., Warwood, S., Choi, C. K., Stroud, M. J., Chen, C. S., Knight, D., et al. (2015). A proteomic approach reveals integrin activation state-dependent control of microtubule cortical targeting. *Nat. Commun.* **6**, 6135.

Calderwood, D. A., Campbell, I. D. and Critchley, D. R. (2013). Talins and kindlins: partners in integrin-mediated adhesion. *Nat. Rev. Mol. Cell Biol.* **14**, 503–517.

Campbell, R. M., Anderson, B. D., Brooks, N. A., Brooks, H. B., Chan, E. M., De Dios, A., Gilmour, R., Graff, J. R., Jambrina, E., Mader, M., et al. (2014). Characterization of LY2228820 dimesylate, a potent and selective inhibitor of p38 MAPK with antitumor activity. *Mol. Cancer Ther.* **13**, 364–374.

Canel, M., Secades, P., Rodrigo, J.-P., Cabanillas, R., Herrero, A., Suarez, C. and Chiara, M.-D. (2006). Overexpression of focal adhesion kinase in head and neck squamous cell carcinoma is independent of fak gene copy number. *Clin. Cancer Res.* **12**, 3272–3279.

Cavani, A., Zambruno, G., Marconi, A., Manca, V., Marchetti, M. and Giannetti, A. (1993). Distinctive Integrin Expression in the Newly Forming Epidermis During Wound Healing in Humans. *J. Invest. Dermatol.* **101**, 600–604.

Chan, T., Ghahary, A., Demare, J., Yang, L., Iwashina, T., Scott, P. G. and Tredget, E. E. (2002). Development, characterization, and wound healing of the keratin 14 promoted transforming growth factor-beta1 transgenic mouse. *Wound Repair Regen.* **10**, 177–187.

Chen, H. C., Appeddu, P. A., Parsons, J. T., Hildebrand, J. D., Schaller, M. D. and Guan, J. L. (1995). Interaction of focal adhesion kinase with cytoskeletal protein talin. *J. Biol. Chem.* **270**, 16995–16999.

Chen, J., Diacovo, T. G., Grenache, D. G., Santoro, S. a. and Zutter, M. M. (2002). The α2 Integrin Subunit-Deficient Mouse. *Am. J. Pathol.* **161**, 337–344.

Chen, H., Zou, Z., Sarratt, K. L., Zhou, D., Zhang, M., Sebzda, E., Hammer, D. a and Kahn, M. L. (2006). In vivo beta1 integrin function requires phosphorylation-independent regulation by cytoplasmic tyrosines. *Genes Dev.* **20**, 927–932.

Cherpelis, B. S., Marcusen, C. and Lang, P. G. (2002). Prognostic factors for metastasis in squamous cell carcinoma of the skin. *Dermatol. Surg.* **28**, 268–273.

Chicurel, M. E., Singer, R. H., Meyer, C. J. and Ingber, D. E. (1998). Integrin binding and mechanical tension induce movement of mRNA and ribosomes to focal adhesions. *Nature* **392**, 730–733.

Chung, H., Suh, E.-K., Han, I.-O. and Oh, E.-S. (2011). Keratinocyte-derived laminin-332 promotes adhesion and migration in melanocytes and melanoma. *J. Biol. Chem.* **286**, 13438–13447.

Cicchini, C., Laudadio, I., Citarella, F., Corazzari, M., Steindler, C., Conigliaro, A., Fantoni, A., Amicone, L. and Tripodi, M. (2008). TGFbeta-induced EMT requires focal adhesion kinase (FAK) signaling. *Exp. Cell Res.* **314**, 143–152.

Clark, R. A., Ashcroft, G. S., Spencer, M. J., Larjava, H. and Ferguson, M. W. (1996). Re-epithelialization of normal human excisional wounds is associated with a switch from alpha v beta 5 to alpha v beta 6 integrins. *Br. J. Dermatol.* **135**, 46–51.

Conti, F. J. a, Rudling, R. J., Robson, A. and Hodivala-Dilke, K. M. (2003). Alpha3Beta1-Integrin Regulates Hair Follicle But Not Interfollicular Morphogenesis in Adult Epidermis. *J. Cell Sci.* **116**, 2737–2747.

Cooley, M. A., Broome, J. M., Ohngemach, C., Romer, L. H. and Schaller, M. D. (2000). Paxillin binding is not the sole determinant of focal adhesion localization or dominant-negative activity of focal adhesion kinase/focal adhesion kinase-related nonkinase. *Mol. Biol. Cell* **11**, 3247–3263.

Corsi, J.-M., Houbron, C., Billuart, P., Brunet, I., Bouvrée, K., Eichmann, A., Girault, J.-A. and Enslen, H. (2009). Autophosphorylation-independent and -dependent functions of focal adhesion kinase during development. *J. Biol. Chem.* **284**, 34769–34776.

Coulthard, L. R., White, D. E., Jones, D. L., McDermott, M. F. and Burchill, S. A. (2009). p38(MAPK): stress responses from molecular mechanisms to therapeutics. *Trends Mol. Med.* **15**, 369–379.

Cranmer, L. D., Engelhardt, C. and Morgan, S. S. (2010). Treatment of Unresectable and Metastatic Cutaneous Squamous Cell Carcinoma. *Oncologist* **15**, 1320–1328.

Cui, W., Fowlis, D. J., Bryson, S., Duffie, E., Ireland, H., Balmain, A. and Akhurst, R. J. (1996). TGFbeta1 inhibits the formation of benign skin tumors, but enhances progression to invasive spindle carcinomas in transgenic mice. *Cell* **86**, 531–542.

Czuchra, A., Meyer, H., Legate, K. R., Brakebusch, C. and Fässler, R. (2006). Genetic analysis of beta1 integrin “activation motifs” in mice. *J. Cell Biol.* **174**, 889–99.

Dajee, M., Lazarov, M., Zhang, J. Y., Cai, T., Green, C. L., Russell, A. J., Marinkovich, M. P., Tao, S., Lin, Q., Kubo, Y., et al. (2003). NF-kappaB blockade and oncogenic Ras trigger invasive human epidermal neoplasia. *Nature* **421**, 639–43.

Dang, C. V (1999). c-Myc target genes involved in cell growth, apoptosis, and metabolism. *Mol. Cell. Biol.* **19**, 1–11.

Dang, C. V (2012). MYC on the path to cancer. *Cell* **149**, 22–35.

Davies, M. A., Stemke-Hale, K., Tellez, C., Calderone, T. L., Deng, W., Prieto, V. G., Lazar, A. J. F., Gershenwald, J. E. and Mills, G. B. (2008). A novel AKT3 mutation in melanoma tumours and cell lines. *Br. J. Cancer* **99**, 1265–1268.

Degen, M., Barron, P., Natarajan, E., Widlund, H. R. and Rheinwald, J. G. (2013). RSK activation of translation factor eIF4B drives abnormal increases of laminin γ2 and MYC protein during neoplastic progression to squamous cell carcinoma. *PLoS One* **8**, e78979.

Desmoulière, A., Geinoz, A., Gabbiani, F. and Gabbiani, G. (1993). Transforming growth factor-beta 1 induces alpha-smooth muscle actin expression in granulation tissue myofibroblasts and in quiescent and growing cultured fibroblasts. *J. Cell Biol.* **122**, 103–111.

DiPersio, C. M., Hodivala-Dilke, K. M., Jaenisch, R., Kreidberg, J. A. and Hynes, R. O. (1997). α3β1 Integrin is required for normal development of the epidermal basement membrane. *J. Cell Biol.* **137**, 729–742.

DiPersio, C. M., van der Neut, R., Georges-Labouesse, E., Kreidberg, J. a, Sonnenberg, A. and Hynes, R. O. (2000). Alpha3Beta1 and Alpha6Beta4 Integrin Receptors for Laminin-5 Are Not Essential for Epidermal Morphogenesis and Homeostasis During Skin Development. *J. Cell Sci.* **113**, 3051–62.

Dowling, J., Yu, Q.-C. and Fuchs, E. (1996). β4 integrin is required for hemidesmosome formation, cell adhesion and cell survival. *J. Cell Biol.* **134**, 559–572.

Duperret, E. K. and Ridky, T. W. (2013). Focal adhesion complex proteins in epidermis and squamous cell carcinoma. *Cell Cycle* **12**, 3272–3285.

Duperret, E. K., Oh, S. J., McNeal, A., Prouty, S. M. and Ridky, T. W. (2014). Activating FGFR3 mutations cause mild hyperplasia in human skin, but are insufficient to drive benign or malignant skin tumors. *Cell Cycle* **13**, 1551–1559.

Duperret, E. K., Dahal, A. and Ridky, T. W. (2015). Focal adhesion-independent integrin αv regulation of FAK and c-myc is necessary for 3D skin formation and tumor invasion. *J. Cell Sci.* **128**, 3887–4013.

Eberlein, C., Kendrew, J., McDaid, K., Alfred, A., Kang, J. S., Jacobs, V. N., Ross, S. J., Rooney, C., Smith, N. R., Rinkenberger, J., et al. (2013). A human monoclonal antibody 264RAD targeting αvβ6 integrin reduces tumour growth and metastasis, and modulates key biomarkers in vivo. *Oncogene* **32**, 4406–4416.

Eilers, M. and Eisenman, R. N. (2008). Myc's broad reach. *Genes Dev.* **22**, 2755–2766.

Eke, I., Deuse, Y., Hehlgans, S., Gurtner, K., Krause, M., Baumann, M., Shevchenko, A., Sandfort, V. and Cordes, N. (2012). β 1 Integrin / FAK / cortactin signaling is essential for human head and neck cancer resistance to radiotherapy. **122**, 1529–1540.

Escámez, M. J., García, M., Larcher, F., Meana, A., Muñoz, E., Jorcano, J. L. and Del Río, M. (2004). An in vivo model of wound healing in genetically modified skin-humanized mice. *J. Invest. Dermatol.* **123**, 1182–1191.

Essayem, S., Kovacic-Milivojevic, B., Baumbusch, C., McDonagh, S., Dolganov, G., Howerton, K., Larocque, N., Mauro, T., Ramirez, A., Ramos, D. M., et al. (2006). Hair cycle and wound healing in mice with a keratinocyte-restricted deletion of FAK. *Oncogene* **25**, 1081–1089.

Falanga, V., Schrayer, D., Cha, J., Butmarc, J., Carson, P., Roberts, A. B. and Kim, S.-J. (2004). Full-thickness wounding of the mouse tail as a model for delayed wound healing: accelerated wound closure in Smad3 knock-out mice. *Wound Repair Regen.* **12**, 320–326.

Fassler, R. and Meyer, M. (1995). Consequences of lack of beta 1 integrin gene expression in mice. *Genes Dev.* **9**, 1896–1908.

Ferreira, M., Fujiwara, H., Morita, K. and Watt, F. M. (2009). An activating beta1 integrin mutation increases the conversion of benign to malignant skin tumors. *Cancer Res.* **69**, 1334–1342.

Fraley, S. I., Feng, Y., Krishnamurthy, R., Kim, D.-H., Celedon, A., Longmore, G. D. and Wirtz, D. (2010). A distinctive role for focal adhesion proteins in three-dimensional cell motility. *Nat. Cell Biol.* **12**, 598–604.

Frame, M. C., Patel, H., Serrels, B., Lietha, D. and Eck, M. J. (2010). The FERM domain: organizing the structure and function of FAK. *Nat. Rev. Mol. Cell Biol.* **11**, 802–814.

Fuchs, E. (2008). Skin stem cells: rising to the surface. *J. Cell Biol.* **180**, 273–284.

Furuta, Y., Ilic, D., Kanazawa, S., Takeda, N., Yamamoto, T. and Aizawa, S. (1995a). Mesodermal defect in late phase of gastrulation by a targeted mutation of focal adhesion kinase, FAK. *Oncogene* **11**, 1989–1995.

Furuta, Y., Kanazawa, S. and Takeda, N. (1995b). Reduced cell motility and enhanced focal adhesion contact formation in cells from FAK-deficient mice. *Nature* **377**, 539–544.

Gabay, M., Li, Y. and Felsher, D. W. (2014). MYC activation is a hallmark of cancer initiation and maintenance. *Cold Spring Harb. Perspect. Med.*

Galiano, R. D., Michaels, J., Dobryansky, M., Levine, J. P. and Gurtner, G. C. (2004). Quantitative and reproducible murine model of excisional wound healing. *Wound Repair Regen.* **12**, 485–92.

Gardner, H., Kreidberg, J., Koteliansky, V. and Jaenisch, R. (1996). Deletion of integrin alpha 1 by homologous recombination permits normal murine development but gives rise to a specific deficit in cell adhesion. *Dev. Biol.* **175**, 301–313.

Genovese, M. C. (2009). Inhibition of p38: has the fat lady sung? *Arthritis Rheum.* **60**, 317–320.

George, E., Georges-Labouesse, E. N., Patel-King, R. S., Rayburn, H. and Hynes, R. O. (1993). Defects in mesoderm, neural tube and vascular development in mouse embryos lacking fibronectin. *Development* **1091**, 1079–1091.

Georges-Labouesse, E., Messaddeq, N., Yehia, G., Cadalbert, L., Dierich, A. and Le Meur, M. (1996). Absence of integrin α6 leads to epidermolysis bullosa and neonatal death in mice. *Nat. Genet.* **13**, 370–373.

Gera, J. F., Mellinghoff, I. K., Shi, Y., Rettig, M. B., Tran, C., Hsu, J., Sawyers, C. L. and Lichtenstein, A. K. (2004). AKT activity determines sensitivity to mammalian target of rapamycin (mTOR) inhibitors by regulating cyclin D1 and c-myc expression. *J. Biol. Chem.* **279**, 2737–2746.

Glick, A. B. (2012). The Role of TGFβ Signaling in Squamous Cell Cancer: Lessons from Mouse Models. *J. Skin Cancer* **2012**, 249063.

Glick, A. B., Lee, M. M., Darwiche, N., Kulkarni, A. B., Karlsson, S. and Yuspa, S. H. (1994). Targeted deletion of the TGF-beta 1 gene causes rapid progression to squamous cell carcinoma. *Genes Dev.* **8**, 2429–2440.

Go, C., He, W., Zhong, L., Li, P., Huang, J., Brinkley, B. R. and Wang, X. J. (2000). Aberrant cell cycle progression contributes to the early-stage accelerated carcinogenesis in transgenic epidermis expressing the dominant negative TGFbetaRII. *Oncogene* **19**, 3623–3631.

Golubovskaya, V. M. and Cance, W. (2010). Focal Adhesion Kinase and p53 signal transduction pathways in cancer. *Front. Biosci.* 901–912.

Golubovskaya, V. M., Finch, R. and Cance, W. G. (2005). Direct interaction of the N-terminal domain of focal adhesion kinase with the N-terminal transactivation domain of p53. *J. Biol. Chem.* **280**, 25008–25021.

Gooyit, M., Peng, Z., Wolter, W. R., Pi, H., Ding, D., Hesek, D., Lee, M., Boggess, B., Champion, M. M., Suckow, M. A., et al. (2014). A Chemical Biological Strategy to Facilitate Diabetic Wound Healing. *ACS Chem. Biol.* **9**, 105–110.

Gordon, K. J. and Blobe, G. C. (2008). Role of transforming growth factor-beta superfamily signaling pathways in human disease. *Biochim. Biophys. Acta* **1782**, 197–228.

Goswami, R. K., Bajjuri, K. M., Forsyth, J. S., Das, S., Hassenpflug, W., Huang, Z.-Z., Lerner, R. A., Felding-Habermann, B. and Sinha, S. C. (2011). Chemically Programmed Antibodies Targeting Multiple Alpha(v) Integrins and Their Effects on Tumor-Related Functions in Vitro. *Bioconjug. Chem.* **22**, 1535–1544.

Govindarajan, B., Sligh, J. E., Vincent, B. J., Li, M., Canter, J. A., Nickoloff, B. J., Rodenburg, R. J., Smeitink, J. A., Oberley, L., Zhang, Y., et al. (2007). Overexpression of Akt converts radial growth melanoma to vertical growth melanoma. *J. Clin. Invest.* **117**, 719–729.

Graham, K., Moran-Jones, K., Sansom, O. J., Brunton, V. G. and Frame, M. C. (2011). FAK deletion promotes p53-mediated induction of p21, DNA-damage responses and radio-resistance in advanced squamous cancer cells. *PLoS One* **6**, e27806.

Grenache, D. G., Zhang, Z., Wells, L. E., Santoro, S. a, Davidson, J. M. and Zutter, M. M. (2007). Wound healing in the alpha2beta1 integrin-deficient mouse: altered keratinocyte biology and dysregulated matrix metalloproteinase expression. *J. Invest. Dermatol.* **127**, 455–466.

Grinnell, F. (1994). Fibroblasts, myofibroblasts, and wound contraction. *J. Cell Biol.* **124**, 401–4.

Grose, R., Hutter, C., Bloch, W., Thorey, I., Watt, F., Fassler, R., Brakebusch, C. and Werner, S. (2002). A crucial role of β1 integrins for keratinocyte migration in vitro and during cutaneous wound repair. *Development* **2315**, 2303–2315.

Grzmil, M. and Hemmings, B. A. (2012). Translation Regulation as a Therapeutic Target in Cancer. *Cancer Res.* **72**, 3891–3900.

Guasch, G., Schober, M., Pasolli, H. A., Conn, E. B., Polak, L. and Fuchs, E. (2007). Loss of TGFβ signaling destabilizes homeostasis and promotes squamous cell carcinomas in stratified epithelia. *Cancer Cell* **12**, 313–327.

Gupta, J., del Barco Barrantes, I., Igea, A., Sakellariou, S., Pateras, I. S., Gorgoulis, V. G. and Nebreda, A. R. (2014). Dual function of p38α MAPK in colon cancer: suppression of colitis-associated tumor initiation but requirement for cancer cell survival. *Cancer Cell* **25**, 484–500.

Gurtner, G. C., Davis, V., Li, H., McCoy, M. J., Sharpe, a and Cybulsky, M. I. (1995). Targeted disruption of the murine VCAM1 gene: essential role of VCAM-1 in chorioallantoic fusion and placentation. *Genes Dev.* **9**, 1–14.

Häkkinen, L., Koivisto, L., Gardner, H., Saarialho-Kere, U., Carroll, J. M., Lakso, M., Rauvala, H., Laato, M., Heino, J. and Larjava, H. (2004). Increased expression of beta6-integrin in skin leads to spontaneous development of chronic wounds. *Am. J. Pathol.* **164**, 229–242.

Hamidi, S., Salo, T., Kainulainen, T., Epstein, J., Lerner, K. and Larjava, H. (2000). Expression of alpha(v)beta6 integrin in oral leukoplakia. *Br. J. Cancer* **82**, 1433–1440.

Hamilton, H. K., Rose, A. E., Christos, P. J., Shapiro, R. L., Berman, R. S., Mazumdar, M., Ma, M. W., Krich, D., Liebes, L., Brooks, P. C., et al. (2010). Increased shedding of HU177 correlates with worse prognosis in primary melanoma. *J. Transl. Med.* **8**, 19.

Has, C., Spartà, G., Kiritsi, D., Weibel, L., Moeller, A., Vega-Warner, V., Waters, A., He, Y., Anikster, Y., Esser, P., et al. (2012). Integrin α3 mutations with kidney, lung, and skin disease. *N. Engl. J. Med.* **366**, 1508–1514.

Hazelbag, S., Kenter, G., Gorter, A., Dreef, E., Koopman, L., Violette, S., Weinreb, P. and Gleuren, G. (2007). Overexpression of the αvβ6 integrin in cervical squamous cell carcinoma is a prognostic factor for decreased survival. *J. Pathol.* **212**, 316–324.

Henderson, N. C., Arnold, T. D., Katamura, Y., Giacomini, M. M., Rodriguez, J. D., McCarty, J. H., Pellicoro, A., Raschperger, E., Betsholtz, C., Ruminski, P. G., et al. (2013). Targeting of αv integrin identifies a core molecular pathway that regulates fibrosis in several organs. *Nat. Med.* **19**, 1617–1624.

Hezel, A. F., Deshpande, V., Zimmerman, S. M., Contino, G., Alagesan, B., O'Dell, M. R., Rivera, L. B., Harper, J., Lonning, S., Brekken, R. A., et al. (2012). TGF-β and αvβ6 integrin act in a common pathway to suppress pancreatic cancer progression. *Cancer Res.* **72**, 4840–4845.

Hoffman, B. and Liebermann, D. A. (2008). Apoptotic signaling by c-MYC. *Oncogene* **27**, 6462–6472.

Honeycutt, K. A., Waikel, R. L., Koster, M. I., Wang, X.-J. and Roop, D. R. (2010). The effect of c-myc on stem cell fate influences skin tumor phenotype. *Mol. Carcinog.* **49**, 315–319.

Hood, J. D. (2003). Differential v integrin-mediated Ras-ERK signaling during two pathways of angiogenesis. *J. Cell Biol.* **162**, 933–943.

Horton, E. R., Byron, A., Askari, J. A., Ng, D. H. J., Millon-Frémillon, A., Robertson, J., Koper, E. J., Paul, N. R., Warwood, S., Knight, D., et al. (2015). Definition of a consensus integrin adhesome and its dynamics during adhesion complex assembly and disassembly. *Nat. Cell Biol.*

Hsu, M. Y., Shih, D. T., Meier, F. E., Van Belle, P., Hsu, J. Y., Elder, D. E., Buck, C. A. and Herlyn, M. (1998). Adenoviral gene transfer of beta3 integrin subunit induces conversion from radial to vertical growth phase in primary human melanoma. *Am. J. Pathol.* **153**, 1435–1442.

Hsu, A., Esmaeli, B., Hayek, B., Hossain, M. G., Shinder, R., Lazar, A. J. and McCarty, J. H. (2011). Analysis of αv integrin protein expression in human eyelid and periorbital squamous cell carcinomas. *J. Cutan. Pathol.* **38**, 570–575.

Hsu, Y.-C., Li, L. and Fuchs, E. (2014). Emerging interactions between skin stem cells and their niches. *Nat. Med.* **20**, 847–856.

Huang, X., Wu, J., Cass, D. and Erle, D. (1996). Inactivation of the integrin beta 6 subunit gene reveals a role of epithelial integrins in regulating inflammation in the lung and skin. *J. Cell Biol.* **133**, 921–928.

Huang, X., Griffiths, M., Wu, J., Farese, R. V and Sheppard, D. (2000a). Normal development, wound healing, and adenovirus susceptibility in beta5-deficient mice. *Mol. Cell. Biol.* **20**, 755–759.

Huang, X. Z., Wu, J. F., Ferrando, R., Lee, J. H., Wang, Y. L., Jr, V. F. and Sheppard, D. (2000b). Fatal Bilateral Chylothorax in Mice Lacking the Integrin α9 β1. *Mol. Cell. Biol.* **20**, 5208–5215.

Humphries, J. D., Byron, A. and Humphries, M. J. (2006). Integrin ligands at a glance. *J. Cell Sci.* **119**, 3901–3903.

Humphries, J. D., Byron, A., Bass, M. D., Craig, S. E., Pinney, J. W., Knight, D. and Humphries, M. J. (2009). Proteomic analysis of integrin-associated complexes identifies RCC2 as a dual regulator of Rac1 and Arf6. *Sci. Signal.* **2**, ra51.

Humphries, J. D., Paul, N. R., Humphries, M. J. and Morgan, M. R. (2015). Emerging properties of adhesion complexes: what are they and what do they do? *Trends Cell Biol.* **25**, 388–397.

Hynes, R. O. (2004). The emergence of integrins: a personal and historical perspective. *Matrix Biol.* **23**, 333–340.

Igea, A. and Nebreda, A. R. (2015). The Stress Kinase p38α as a Target for Cancer Therapy. *Cancer Res.* **75**, 3997–4002.

Infante, J. R., Camidge, D. R., Mileshkin, L. R., Chen, E. X., Hicks, R. J., Rischin, D., Fingert, H., Pierce, K. J., Xu, H., Roberts, W. G., et al. (2012). Safety, pharmacokinetic, and pharmacodynamic phase I dose-escalation trial of PF-00562271, an inhibitor of focal adhesion kinase, in advanced solid tumors. *J. Clin. Oncol.* **30**, 1527–1533.

Janes, S. M. and Watt, F. M. (2004). Switch from αvβ5 to αvβ6 integrin expression protects squamous cell carcinomas from anoikis. *J. Cell Biol.* **166**, 419–31.

Janes, S. M. and Watt, F. M. (2006). New roles for integrins in squamous-cell carcinoma. *Nat. Rev. Cancer* **6**, 175–183.

Jones, J., Watt, F. M. and Speight, P. M. (1997). Changes in the expression of alpha v integrins in oral squamous cell carcinomas. *J. Oral Pathol. Med.* **26**, 63–68.

Jones, M. C., Humphries, J. D., Byron, A., Millon-Frémillon, A., Robertson, J., Paul, N. R., Ng, D. H. J., Askari, J. A. and Humphries, M. J. (2015). Isolation of integrin-based adhesion complexes. *Curr. Protoc. Cell Biol.* **66**, 9.8.1–9.8.15.

Kanchanawong, P., Shtengel, G., Pasapera, A. M., Ramko, E. B., Davidson, M. W., Hess, H. F. and Waterman, C. M. (2010). Nanoscale architecture of integrin-based cell adhesions. *Nature* **468**, 580–584.

Karia, P. S., Han, J. and Schmults, C. D. (2013). Cutaneous squamous cell carcinoma: estimated incidence of disease, nodal metastasis, and deaths from disease in the United States, 2012. *J. Am. Acad. Dermatol.* **68**, 957–966.

Katz, Z. B., Wells, A. L., Park, H. Y., Wu, B., Shenoy, S. M. and Singer, R. H. (2012). β-Actin mRNA compartmentalization enhances focal adhesion stability and directs cell migration. *Genes Dev.* **26**, 1885–1890.

Khavari, P. A. (2006). Modelling cancer in human skin tissue. *Nat. Rev. Cancer* **6**, 270–280.

Komar, A. A. and Hatzoglou, M. (2011). Cellular IRES-mediated translation: the war of ITAFs in pathophysiological states. *Cell Cycle* **10**, 229–40.

Konstantinidou, G., Ramadori, G., Torti, F., Kangasniemi, K., Ramirez, R. E., Cai, Y., Behrens, C., Dellinger, M. T., Brekken, R. A., Wistuba, I. I., et al. (2013). RHOA-FAK is a required signaling axis for the maintenance of KRAS-driven lung adenocarcinomas. *Cancer Discov.* **3**, 444–457.

Koppel, A. C., Kiss, A., Hindes, A., Burns, C. J., Marmer, B. L., Goldberg, G., Blumenberg, M. and Efimova, T. (2014). Delayed skin wound repair in proline-rich protein tyrosine kinase 2 knockout mice. *Am. J. Physiol. Cell Physiol.* **306**, C899–909.

Koria, P., Yagi, H., Kitagawa, Y., Megeed, Z., Nahmias, Y., Sheridan, R. and Yarmush, M. L. (2011). Self-assembling elastin-like peptides growth factor chimeric nanoparticles for the treatment of chronic wounds. *Proc. Natl. Acad. Sci. U. S. A.* **108**, 1034–1039.

Kracklauer, M. P., Schmidt, C. and Sclabas, G. M. (2003). TGFbeta1 signaling via alphaVbeta6 integrin. *Mol. Cancer* **2**, 28.

Kreidberg, J. a, Donovan, M. J., Goldstein, S. L., Rennke, H., Shepherd, K., Jones, R. C. and Jaenisch, R. (1996). Alpha 3 beta 1 integrin has a crucial role in kidney and lung organogenesis. *Development* **122**, 3537–3547.

Kuo, J.-C., Han, X., Hsiao, C.-T., Yates, J. R. and Waterman, C. M. (2011). Analysis of the myosin-II-responsive focal adhesion proteome reveals a role for β-Pix in negative regulation of focal adhesion maturation. *Nat. Cell Biol.* **13**, 383–393.

Lacy-Hulbert, A., Smith, A. M., Tissire, H., Barry, M., Crowley, D., Bronson, R. T., Roes, J. T., Savill, J. S. and Hynes, R. O. (2007). Ulcerative colitis and autoimmunity induced by loss of myeloid v integrins. *Proc. Natl. Acad. Sci.* **104**, 15823–15828.

Lam, S. S., Martell, J. D., Kamer, K. J., Deerinck, T. J., Ellisman, M. H., Mootha, V. K. and Ting, A. Y. (2014). Directed evolution of APEX2 for electron microscopy and proximity labeling. *Nat. Methods* **12**, 51–54.

Laplante, M. and Sabatini, D. M. (2009). mTOR signaling at a glance. *J. Cell Sci.* **122**, 3589–3594.

Lawson, C., Lim, S.-T., Uryu, S., Chen, X. L., Calderwood, D. A. and Schlaepfer, D. D. (2012). FAK promotes recruitment of talin to nascent adhesions to control cell motility. *J. Cell Biol.* **196**, 223–232.

Lazarov, M., Kubo, Y., Cai, T., Dajee, M., Tarutani, M., Lin, Q., Fang, M., Tao, S., Green, C. L. and Khavari, P. A. (2002). CDK4 coexpression with Ras generates malignant human epidermal tumorigenesis. *Nat. Med.* **8**, 1105–1114.

Leelahavanichkul, K., Amornphimoltham, P., Molinolo, A. A., Basile, J. R., Koontongkaew, S. and Gutkind, J. S. (2014). A role for p38 MAPK in head and neck cancer cell growth and tumor-induced angiogenesis and lymphangiogenesis. *Mol. Oncol.* **8**, 105–118.

Li, X., Yang, Y., Hu, Y., Dang, D., Regezi, J., Schmidt, B. L., Atakilit, A., Chen, B., Ellis, D. and Ramos, D. M. (2003). Alphavbeta6-Fyn signaling promotes oral cancer progression. *J. Biol. Chem.* **278**, 41646–41653.

Li, H.-X., Zheng, J.-H., Fan, H.-X., Li, H.-P., Gao, Z.-X. and Chen, D. (2013). Expression of αvβ6 integrin and collagen fibre in oral squamous cell carcinoma: association with clinical outcomes and prognostic implications. *J. Oral Pathol. Med.* **42**, 547–556.

Li, Y., Drabsch, Y., Pujuguet, P., Ren, J., van Laar, T., Zhang, L., van Dam, H., Clément-Lacroix, P. and Ten Dijke, P. (2015a). Genetic depletion and pharmacological targeting of αv integrin in breast cancer cells impairs metastasis in zebrafish and mouse xenograft models. *Breast Cancer Res.* **17**, 28.

Li, D., Wang, A., Liu, X., Meisgen, F., Grünler, J., Botusan, I. R., Narayanan, S., Erikci, E., Li, X., Blomqvist, L., et al. (2015b). MicroRNA-132 enhances transition from inflammation to proliferation during wound healing. *J. Clin. Invest.* **125**, 3008–3026.

Lim, S.-T., Chen, X. L., Lim, Y., Hanson, D. a, Vo, T.-T., Howerton, K., Larocque, N., Fisher, S. J., Schlaepfer, D. D. and Ilic, D. (2008). Nuclear FAK promotes cell proliferation and survival through FERM-enhanced p53 degradation. *Mol. Cell* **29**, 9–22.

Lo, S. H. (2006). Focal adhesions: what's new inside. *Dev. Biol.* **294**, 280–291.

Logullo, A. F., Nonogaki, S., Miguel, R. E., Kowalski, L. P., Nishimoto, I. N., Pasini, F. S., Federico, M. H. H., Brentani, R. R. and Brentani, M. M. (2003). Transforming growth factor beta1 (TGFbeta1) expression in head and neck squamous cell carcinoma patients as related to prognosis. *J. Oral Pathol. Med.* **32**, 139–145.

Longmate, W. M. and Dipersio, C. M. (2014). Integrin Regulation of Epidermal Functions in Wounds. *Adv. wound care* **3**, 229–246.

López-Lastra, M., Rivas, A. and Barría, M. I. (2005). Protein synthesis in eukaryotes: the growing biological relevance of cap-independent translation initiation. *Biol. Res.* **38**, 121–146.

Lopez-Pajares, V., Yan, K., Zarnegar, B., Jameson, K. and Khavari, P. (2012). Genetic pathways in disorders of epidermal differentiation. *Trends Genet.* **29**, 31–40.

López-Rovira, T., Silva-Vargas, V. and Watt, F. M. (2005). Different consequences of beta1 integrin deletion in neonatal and adult mouse epidermis reveal a context-dependent role of integrins in regulating proliferation, differentiation, and intercellular communication. *J. Invest. Dermatol.* **125**, 1215–1227.

Mamuya, F. A. and Duncan, M. K. (2013). αV Integrins and TGF-β Induced EMT; a Circle of Regulation. *J Cell Mol Med* **16**, 445–455.

Margadant, C. and Sonnenberg, A. (2010). Integrin-TGF-beta crosstalk in fibrosis, cancer and wound healing. *EMBO Rep.* **11**, 97–105.

Margadant, C., Raymond, K., Kreft, M., Sachs, N., Janssen, H. and Sonnenberg, A. (2009). Integrin alpha3beta1 inhibits directional migration and wound re-epithelialization in the skin. *J. Cell Sci.* **122**, 278–288.

Margadant, C., Charafeddine, R. A. and Sonnenberg, A. (2010). Unique and redundant functions of integrins in the epidermis. *FASEB J.* **24**, 4133–4152.

Marinkovich, M. P. (2007). Tumour microenvironment: laminin 332 in squamous-cell carcinoma. *Nat. Rev. Cancer* **7**, 370–380.

Markowitz, S., Wang, J., Myeroff, L., Parsons, R., Sun, L., Lutterbaugh, J., Fan, R. S., Zborowska, E., Kinzler, K. W. and Vogelstein, B. (1995). Inactivation of the type II TGF-beta receptor in colon cancer cells with microsatellite instability. *Science* **268**, 1336–1338.

Marques da Costa, R., Jesus, F. M., Aniceto, C. and Mendes, M. (1997). Double-blind randomized placebo-controlled trial of the use of granulocyte-macrophage colony-stimulating factor in chronic leg ulcers. *Am. J. Surg.* **173**, 165–168.

Massagué, J. (2008). TGFbeta in Cancer. *Cell* **134**, 215–230.

Maubec, E., Petrow, P., Scheer-Senyarich, I., Duvillard, P., Lacroix, L., Gelly, J., Certain, A., Duval, X., Crickx, B., Buffard, V., et al. (2011). Phase II Study of Cetuximab As First-Line Single-Drug Therapy in Patients With Unresectable Squamous Cell Carcinoma of the Skin. *J. Clin. Oncol.* **29**, 3419–3426.

Mayer, U., Saher, G., Fassler, R., Bornemann, A., Echtermeyer, F., von der Mark, H., Miosge, N., Poschl, E. and von der Mark, K. (1997). Abence of integrin α7 causes a novel form of muscular dystrophy. *Nature* **17**, 318–323.

McCarty, J. H., Monahan-Earley, R. A., Brown, L. F., Keller, M., Gerhardt, H., Rubin, K., Shani, M., Dvorak, H. F., Wolburg, H., Bader, B. L., et al. (2002). Defective associations between blood vessels and brain parenchyma lead to cerebral hemorrhage in mice lacking alphav integrins. *Mol. Cell. Biol.* **22**, 7667–7677.

McCarty, J. H., Lacy-Hulbert, A., Charest, A., Bronson, R. T., Crowley, D., Housman, D., Savill, J., Roes, J. and Hynes, R. O. (2005). Selective ablation of alphav integrins in the central nervous system leads to cerebral hemorrhage, seizures, axonal degeneration and premature death. *Development* **132**, 165–176.

McCarty, J. H., Barry, M., Crowley, D., Bronson, R. T., Lacy-Hulbert, A. and Hynes, R. O. (2008). Genetic ablation of alphav integrins in epithelial cells of the eyelid skin and conjunctiva leads to squamous cell carcinoma. *Am. J. Pathol.* **172**, 1740–1747.

McLean, G., Brown, K., Arbuckle, M., Wyke, A., Pikkarainen, T., Ruoslahti, E. and Frame, M. (2001). Decreased focal adhesion kinase suppresses papilloma formation during experimental mouse skin carcinogenesis. *Cancer Res.* **61**, 8385–8389.

McLean, G. W., Komiyama, N. H., Serrels, B., Asano, H., Reynolds, L., Conti, F., Hodivala-Dilke, K., Metzger, D., Chambon, P., Grant, S. G. N., et al. (2004). Specific deletion of focal adhesion kinase suppresses tumor formation and blocks malignant progression. *Genes Dev.* **18**, 2998–3003.

McNeal, A. S., Liu, K., Nakhate, V., Natale, C. A., Duperret, E. K., Capell, B. C., Dentchev, T., Berger, S. L., Herlyn, M., Seykora, J. T., et al. (2015). CDKN2B Loss Promotes Progression from Benign Melanocytic Nevus to Melanoma. *Cancer Discov.* **5**, 1072–1085.

Merrick, W. C. (2004). Cap-dependent and cap-independent translation in eukaryotic systems. *Gene* **332**, 1–11.

Meves, A., Geiger, T., Zanivan, S., DiGiovanni, J., Mann, M. and Fässler, R. (2011). Beta1 integrin cytoplasmic tyrosines promote skin tumorigenesis independent of their phosphorylation. *Proc. Natl. Acad. Sci. U. S. A.* **108**, 15213–8.

Meves, A., Stremmel, C., Thomas Böttcher, R. and Fässler, R. (2013). β1 integrins with individually disrupted cytoplasmic NPxY motifs are embryonic lethal but partially active in epidermis. *J. Invest. Dermatol.*

Meyer, N. and Penn, L. Z. (2008). Reflecting on 25 years with MYC. *Nat. Rev. Cancer* **8**, 976–990.

Mitjans, F., Sander, D., Adán, J., Sutter, A., Martinez, J. M., Jäggle, C. S., Moyano, J. M., Kreysch, H. G., Piulats, J. and Goodman, S. L. (1995). An anti-alpha v-integrin antibody that blocks integrin function inhibits the development of a human melanoma in nude mice. *J. Cell Sci.* **108**, 2825–2838.

Mitra, S. K., Hanson, D. A. and Schlaepfer, D. D. (2005). Focal adhesion kinase: in command and control of cell motility. *Nat. Rev. Mol. Cell Biol.* **6**, 56–68.

Moore, K. M., Thomas, G. J., Duffy, S. W., Warwick, J., Gabe, R., Chou, P., Ellis, I. O., Green, A. R., Haider, S., Brouilette, K., et al. (2014). Therapeutic targeting of integrin αvβ6 in breast cancer. *J. Natl. Cancer Inst.*

Mordasky Markell, L., Pérez-Lorenzo, R., Masiuk, K. E., Kennett, M. J. and Glick, A. B. (2010). Use of a TGFbeta type I receptor inhibitor in mouse skin carcinogenesis reveals a dual role for TGFbeta signaling in tumor promotion and progression. *Carcinogenesis* **31**, 2127–2135.

Moreno-Layseca, P. and Streuli, C. H. (2014). Signalling pathways linking integrins with cell cycle progression. *Matrix Biol.* **34**, 144–153.

Mullamitha, S. a, Ton, N. C., Parker, G. J. M., Jackson, A., Julyan, P. J., Roberts, C., Buonaccorsi, G. a, Watson, Y., Davies, K., Cheung, S., et al. (2007). Phase I evaluation of a fully human anti-alphav integrin monoclonal antibody (CNTO 95) in patients with advanced solid tumors. *Clin. Cancer Res.* **13**, 2128–2135.

Müller, U., Wang, D., Denda, S., Meneses, J. J., Pedersen, R. a and Reichardt, L. F. (1997). Integrin alpha8beta1 is critically important for epithelial-mesenchymal interactions during kidney morphogenesis. *Cell* **88**, 603–13.

Mustoe, T. (2004). Understanding chronic wounds: a unifying hypothesis on their pathogenesis and implications for therapy. *Am. J. Surg.* **187**, S65–S70.

Neurath, M. F. (2014). New targets for mucosal healing and therapy in inflammatory bowel diseases. *Mucosal Immunol.* **7**, 6–19.

Ng, B., Zakrzewski, J., Warycha, M., Christos, P. J., Bajorin, D. F., Shapiro, R. L., Berman, R. S., Pavlick, A. C., Polsky, D., Mazumdar, M., et al. (2008). Shedding of distinct cryptic collagen epitope (HU177) in sera of melanoma patients. *Clin. Cancer Res.* **14**, 6253–8.

Niculescu, C., Ganguli-Indra, G., Pfister, V., Dupé, V., Messaddeq, N., De Arcangelis, A. and Georges-Labouesse, E. (2011). Conditional ablation of integrin alpha-6 in mouse epidermis leads to skin fragility and inflammation. *Eur. J. Cell Biol.* **90**, 270–277.

Nystrom, M. L., McCulloch, D., Weinreb, P. H., Violette, S. M., Speight, P. M., Marshall, J. F., Hart, I. R. and Thomas, G. J. (2006). Cyclooxygenase-2 inhibition suppresses alphavbeta6 integrin-dependent oral squamous carcinoma invasion. *Cancer Res.* **66**, 10833–10842.

O'Day, S., Pavlick, A., Loquai, C., Lawson, D., Gutzmer, R., Richards, J., Schadendorf, D., Thompson, J. a, Gonzalez, R., Trefzer, U., et al. (2011). A randomised, phase II study of intetumumab, an anti-αv-integrin mAb, alone and with dacarbazine in stage IV melanoma. *Br. J. Cancer* **105**, 346–352.

Ochel, H. J., Schulte, T. W., Nguyen, P., Trepel, J. and Neckers, L. (1999). The benzoquinone ansamycin geldanamycin stimulates proteolytic degradation of focal adhesion kinase. *Mol. Genet. Metab.* **66**, 24–30.

Oktay, M., Wary, K. K., Dans, M., Birge, R. B. and Giancotti, F. G. (1999). Integrin-mediated activation of focal adhesion kinase is required for signaling to Jun NH2-terminal kinase and progression through the G1 phase of the cell cycle. *J. Cell Biol.* **145**, 1461–1469.

Oskarsson, T., Essers, M. A. G., Dubois, N., Offner, S., Dubey, C., Roger, C., Metzger, D., Chambon, P., Hummler, E., Beard, P., et al. (2006). Skin epidermis lacking the c-Myc gene is resistant to Ras-driven tumorigenesis but can reacquire sensitivity upon additional loss of the p21Cip1 gene. *Genes Dev.* **20**, 2024–2029.

Owen, K. a, Abshire, M. Y., Tilghman, R. W., Casanova, J. E. and Bouton, A. H. (2011). FAK regulates intestinal epithelial cell survival and proliferation during mucosal wound healing. *PLoS One* **6**, e23123.

Parsons, J. T. (2003). Focal adhesion kinase: the first ten years. *J. Cell Sci.* **116**, 1409–1416.

Pelengaris, S., Littlewood, T., Khan, M., Elia, G. and Evan, G. (1999). Reversible Activation of c-Myc in Skin. *Mol. Cell* **3**, 565–577.

Pende, M., Um, S. H., Mieulet, V., Sticker, M., Goss, V. L., Mestan, J., Mueller, M., Fumagalli, S., Kozma, S. C. and Thomas, G. (2004). S6K1(-/-)/S6K2(-/-) mice exhibit perinatal lethality and rapamycin-sensitive 5'-terminal oligopyrimidine mRNA translation and reveal a mitogen-activated protein kinase-dependent S6 kinase pathway. *Mol. Cell. Biol.* **24**, 3112–3124.

Penn, J. W., Grobbelaar, A. O. and Rolfe, K. J. (2012). The role of the TGF-β family in wound healing, burns and scarring: a review. *Int. J. Burns Trauma* **2**, 18–28.

Pérez-Lorenzo, R., Markell, L. M., Hogan, K. A., Yuspa, S. H. and Glick, A. B. (2010). Transforming growth factor beta1 enhances tumor promotion in mouse skin carcinogenesis. *Carcinogenesis* **31**, 1116–1123.

Petitclerc, E., Strömblad, S., Schalscha, T. L. Von, Survival, T. C., Stro, S., Mitjans, F., Piulats, J., Montgomery, A. M. P., Cheresh, D. A. and Brooks, P. C. (1999). Integrin alphavbeta3 Promotes M21 Melanoma Growth in Human Skin by Regulating Tumor Cell. *Cancer Res.* **59**, 2724–2730.

Popova, S. N., Barczyk, M., Tiger, C.-F., Beertsen, W., Zigrino, P., Aszodi, A., Miosge, N., Forsberg, E. and Gullberg, D. (2007). Alpha11 beta1 integrin-dependent regulation of periodontal ligament function in the erupting mouse incisor. *Mol. Cell. Biol.* **27**, 4306–4316.

Praekelt, U., Kopp, P. M., Rehm, K., Linder, S., Bate, N., Patel, B., Debrand, E., Manso, A. M., Ross, R. S., Conti, F., et al. (2012). New isoform-specific monoclonal antibodies reveal different sub-cellular localisations for talin1 and talin2. *Eur. J. Cell Biol.* **91**, 180–191.

Preneau, S., Rio, E., Brocard, A., Peuvrel, L., Nguyen, J.-M., Quéreux, G. and Dreno, B. (2014). Efficacy of cetuximab in the treatment of squamous cell carcinoma. *J. Dermatolog. Treat.* **25**, 424–427.

Provenzano, P. P. and Keely, P. J. (2011). Mechanical signaling through the cytoskeleton regulates cell proliferation by coordinated focal adhesion and Rho GTPase signaling. *J. Cell Sci.* **124**, 1195–1205.

Rafiei, S. (2007). Talin : a novel inducible antagonist of transforming growth factor-beta 1 (TGF-[beta]1) signal transduction.

Raghavan, S., Bauer, C., Mundschau, G., Li, Q. and Fuchs, E. (2000). Conditional ablation of β1 integrin in skin: Severe defects in epidermal proliferation, basement membrane formation, and hair follicle invagination. *J. Cell Biol.* **150**, 1149–1160.

Ramos, D. M., But, M., Regezi, J., Schmidt, B. L., Atakilit, A., Dang, D., Ellis, D., Jordan, R. and Li, X. (2002). Expression of integrin beta 6 enhances invasive behavior in oral squamous cell carcinoma. *Matrix Biol.* **21**, 297–307.

Ratushny, V., Gober, M. D., Hick, R., Ridky, T. W. and Seykora, J. T. (2012). Review series From keratinocyte to cancer : the pathogenesis and modeling of cutaneous squamous cell carcinoma. *J. Clin. Invest.* **122**, 464–472.

Raymond, K., Kreft, M., Janssen, H., Calafat, J. and Sonnenberg, A. (2005). Keratinocytes display normal proliferation, survival and differentiation in conditional beta4-integrin knockout mice. *J. Cell Sci.* **118**, 1045–1060.

Reinke, J. M. and Sorg, H. (2012). Wound repair and regeneration. *Eur. Surg. Res.* **49**, 35–43.

Reiske, H. R., Kao, S. C., Cary, L. A., Guan, J. L., Lai, J. F. and Chen, H. C. (1999). Requirement of phosphatidylinositol 3-kinase in focal adhesion kinase-promoted cell migration. *J. Biol. Chem.* **274**, 12361–12366.

Reuter, J. A., Ortiz-Urda, S., Kretz, M., Garcia, J., Scholl, F. A., Pasmooij, A. M. G., Cassarino, D., Chang, H. Y. and Khavari, P. A. (2009). Modeling inducible human tissue neoplasia identifies an extracellular matrix interaction network involved in cancer progression. *Cancer Cell* **15**, 477–488.

Reynolds, L. E., Conti, F. J., Lucas, M., Grose, R., Robinson, S., Stone, M., Saunders, G., Dickson, C., Hynes, R. O., Lacy-Hulbert, A., et al. (2005). Accelerated re-epithelialization in beta3-integrin-deficient- mice is associated with enhanced TGF-beta1 signaling. *Nat. Med.* **11**, 167–174.

Reynolds, A. R., Hart, I. R., Watson, A. R., Welti, J. C., Silva, R. G., Robinson, S. D., Da Violante, G., Gourlaouen, M., Salih, M., Jones, M. C., et al. (2009). Stimulation of tumor growth and angiogenesis by low concentrations of RGD-mimetic integrin inhibitors. *Nat. Med.* **15**, 392–400.

Rhee, H.-W., Zou, P., Udeshi, N. D., Martell, J. D., Mootha, V. K., Carr, S. A. and Ting, A. Y. (2013). Proteomic mapping of mitochondria in living cells via spatially restricted enzymatic tagging. *Science* **339**, 1328–1331.

Ricono, J. M., Huang, M., Barnes, L. A., Lau, S. K., Weis, S. M., Schlaepfer, D. D., Hanks, S. K. and Cheresh, D. A. (2009). Specific cross-talk between epidermal growth factor receptor and integrin alphavbeta5 promotes carcinoma cell invasion and metastasis. *Cancer Res.* **69**, 1383–1391.

Ridgway, R. a, Serrels, B., Mason, S., Kinnaird, A., Muir, M., Patel, H., Muller, W. J., Sansom, O. J. and Brunton, V. G. (2012). Focal adhesion kinase is required for β-catenin-induced mobilization of epidermal stem cells. *Carcinogenesis* **33**, 2369–2376.

Ridky, T. W., Chow, J. M., Wong, D. J. and Khavari, P. A. (2010). Invasive three-dimensional organotypic neoplasia from multiple normal human epithelia. *Nat. Med.* **16**, 1450–1455.

Robertson, J., Jacquemet, G., Byron, A., Jones, M. C., Warwood, S., Selley, J. N., Knight, D., Humphries, J. D. and Humphries, M. J. (2015). Defining the phospho-adhesome through the phosphoproteomic analysis of integrin signalling. *Nat. Commun.* **6**, 6265.

Robinson, D. W., Cormier, J. N., Zhao, N., Uhlar, C. M., Revicki, D. a and Cella, D. (2012). Health-related quality of life among patients with metastatic melanoma: results from an international phase 2 multicenter study. *Melanoma Res.* **22**, 54–62.

Rogers, H. W., Weinstock, M. A., Harris, A. R., Hinckley, M. R., Feldman, S. R., Fleischer, A. B. and Coldiron, B. M. (2010). Incidence estimate of nonmelanoma skin cancer in the United States, 2006. *Arch. Dermatol.* **146**, 283–287.

Rolli, M., Fransvea, E., Pilch, J., Saven, A. and Felding-Habermann, B. (2003). Activated integrin alphavbeta3 cooperates with metalloproteinase MMP-9 in regulating migration of metastatic breast cancer cells. *Proc. Natl. Acad. Sci. U. S. A.* **100**, 9482–9487.

Rossier, O., Octeau, V., Sibarita, J.-B., Leduc, C., Tessier, B., Nair, D., Gatterdam, V., Destaing, O., Albigès-Rizo, C., Tampé, R., et al. (2012). Integrins β1 and β3 exhibit distinct dynamic nanoscale organizations inside focal adhesions. *Nat. Cell Biol.* **14**, 1057–1067.

Roth, J. M., Caunt, M., Cretu, A., Akalu, A., Policarpio, D., Li, X., Gagne, P., Formenti, S. and Brooks, P. C. (2006). Inhibition of experimental metastasis by targeting the HUIV26 cryptic epitope in collagen. *Am. J. Pathol.* **168**, 1576–1586.

Roux, P. P., Shahbazian, D., Vu, H., Holz, M. K., Cohen, M. S., Taunton, J., Sonenberg, N. and Blenis, J. (2007). RAS/ERK signaling promotes site-specific ribosomal protein S6 phosphorylation via RSK and stimulates cap-dependent translation. *J. Biol. Chem.* **282**, 14056–14064.

Sachs, N., Secades, P., van Hulst, L., Kreft, M., Song, J.-Y. and Sonnenberg, A. (2012). Loss of integrin alpha3 prevents skin tumor formation by promoting epidermal turnover and depletion of slow-cycling cells. *Proc. Natl. Acad. Sci. U. S. A.* **109**, 21468–21473.

Sakai, T., Jove, R., Fässler, R. and Mosher, D. F. (2001). Role of the cytoplasmic tyrosines of beta 1A integrins in transformation by v-src. *Proc. Natl. Acad. Sci. U. S. A.* **98**, 3808–3813.

Sapkota, G. P., Cummings, L., Newell, F. S., Armstrong, C., Bain, J., Frodin, M., Grauert, M., Hoffmann, M., Schnapp, G., Steegmaier, M., et al. (2007). BI-D1870 is a specific inhibitor of the p90 RSK (ribosomal S6 kinase) isoforms in vitro and in vivo. *Biochem. J.* **401**, 29–38.

Savar, A., Acin, S., Gonzalez, C. L., El-Sawy, T., Mejia, O., Li, Z., Esmaeli, B., Lacy-Hulbert, A., El-Naggar, A. K., McCarty, J. H., et al. (2014). Loss of epithelial p53 and αv integrin cooperate through Akt to induce squamous cell carcinoma yet prevent remodeling of the tumor microenvironment. *Oncogene* **34**, 516–524.

Scaringi, C., Minniti, G., Caporello, P. and Enrici, R. M. (2012). Integrin inhibitor cilengitide for the treatment of glioblastoma: a brief overview of current clinical results. *Anticancer Res.* **32**, 4213–4223.

Schäfer, M. and Werner, S. (2008). Cancer as an overhealing wound: an old hypothesis revisited. *Nat. Rev. Mol. Cell Biol.* **9**, 628–638.

Schaller, M. D. (2010). Cellular functions of FAK kinases: insight into molecular mechanisms and novel functions. *J. Cell Sci.* **123**, 1007–1113.

Schiller, H. B., Hermann, M.-R., Polleux, J., Vignaud, T., Zanivan, S., Friedel, C. C., Sun, Z., Raducanu, A., Gottschalk, K.-E., Théry, M., et al. (2013). β1- and αv-class integrins cooperate to regulate myosin II during rigidity sensing of fibronectin-based microenvironments. *Nat. Cell Biol.* **15**, 625–636.

Schindler, E. M., Baumgartner, M., Gribben, E. M., Li, L. and Efimova, T. (2007). The role of proline-rich protein tyrosine kinase 2 in differentiation-dependent signaling in human epidermal keratinocytes. *J. Invest. Dermatol.* **127**, 1094–1106.

Schober, M., Raghavan, S., Nikolova, M., Polak, L., Pasolli, H. A., Beggs, H. E., Reichardt, L. F. and Fuchs, E. (2007). Focal adhesion kinase modulates tension signaling to control actin and focal adhesion dynamics. *J. Cell Biol.* **176**, 667–680.

Schwartz, M. a and Assoian, R. K. (2001). Integrins and cell proliferation: regulation of cyclin-dependent kinases via cytoplasmic signaling pathways. *J. Cell Sci.* **114**, 2553–2560.

Sen, C. K., Gordillo, G. M., Roy, S., Kirsner, R., Lambert, L., Hunt, T. K., Gottrup, F., Gurtner, G. C. and Longaker, M. T. (2009). Human skin wounds: a major and snowballing threat to public health and the economy. *Wound Repair Regen.* **17**, 763–771.

Serrels, A., McLeod, K., Canel, M., Kinnaird, A., Graham, K., Frame, M. C. and Brunton, V. G. (2012). The role of focal adhesion kinase catalytic activity on the proliferation and migration of squamous cell carcinoma cells. *Int. J. Cancer* **131**, 287–297.

Shah, N. R., Tancioni, I., Ward, K. K., Lawson, C., Chen, X. L., Jean, C., Sulzmaier, F. J., Uryu, S., Miller, N. L. G., Connolly, D. C., et al. (2014). Analyses of merlin/NF2 connection to FAK inhibitor responsiveness in serous ovarian cancer. *Gynecol. Oncol.* **134**, 104–111.

Shan, B. and Chang, C. (1994). The transcription factor E2F-1 mediates the autoregulation of RB gene expression. *Mol. Cell. Biol.* **14**, 299–309.

Shanmugasundaram, K., Block, K., Nayak, B. K., Livi, C. B., Venkatachalam, M. A. and Sudarshan, S. (2013). PI3K regulation of the SKP-2/p27 axis through mTORC2. *Oncogene* **32**, 2027–2036.

Sharma, G.-D., He, J. and Bazan, H. E. P. (2003). p38 and ERK1/2 Coordinate Cellular Migration and Proliferation in Epithelial Wound Healing: EVIDENCE OF CROSS-TALK ACTIVATION BETWEEN MAP KINASE CASCADES. *J. Biol. Chem.* **278**, 21989–21997.

Shaw, T. J. and Martin, P. (2009). Wound repair at a glance. *J. Cell Sci.* **122**, 3209–3213.

Shen, Y., Guo, Y., Mikus, P., Sulniute, R., Wilczynska, M., Ny, T. and Li, J. (2012). Plasminogen is a key proinflammatory regulator that accelerates the healing of acute and diabetic wounds. *Blood* **119**, 5879–5887.

Shi, Y., Sharma, A., Wu, H., Lichtenstein, A. and Gera, J. (2005). Cyclin D1 and c-myc internal ribosome entry site (IRES)-dependent translation is regulated by AKT activity and enhanced by rapamycin through a p38 MAPK- and ERK-dependent pathway. *J. Biol. Chem.* **280**, 10964–10973.

Silvera, D., Formenti, S. C. and Schneider, R. J. (2010). Translational control in cancer. *Nat. Rev. Cancer* **10**, 254–266.

Singer, A. J. and Clark, R. A. (1999). Cutaneous wound healing. *N. Engl. J. Med.* **341**, 738–746.

Singh, P., Chen, C., Pal-Ghosh, S., Stepp, M. A., Sheppard, D. and Van De Water, L. (2009). Loss of integrin alpha9beta1 results in defects in proliferation, causing poor re-epithelialization during cutaneous wound healing. *J. Invest. Dermatol.* **129**, 217–228.

Smith, J. A., Poteet-Smith, C. E., Xu, Y., Errington, T. M., Hecht, S. M. and Lannigan, D. A. (2005). Identification of the first specific inhibitor of p90 ribosomal S6 kinase (RSK) reveals an unexpected role for RSK in cancer cell proliferation. *Cancer Res.* **65**, 1027–1034.

Stephens, L. E., Sutherland, a E., Klimanskaya, I. V, Andrieux, a, Meneses, J., Pedersen, R. a and Damsky, C. H. (1995). Deletion of beta 1 integrins in mice results in inner cell mass failure and peri-implantation lethality. *Genes Dev.* **9**, 1883–1895.

Stojadinovic, O., Brem, H., Vouthounis, C., Lee, B., Fallon, J., Stallcup, M., Merchant, A., Galiano, R. D. and Tomic-Canic, M. (2005). Molecular pathogenesis of chronic wounds: the role of beta-catenin and c-myc in the inhibition of epithelialization and wound healing. *Am. J. Pathol.* **167**, 59–69.

Stoneley, M., Chappell, S. A., Jopling, C. L., Dickens, M., MacFarlane, M. and Willis, A. E. (2000). c-Myc protein synthesis is initiated from the internal ribosome entry segment during apoptosis. *Mol. Cell. Biol.* **20**, 1162–1169.

Subkhankulova, T., Mitchell, S. A. and Willis, A. E. (2001). Internal ribosome entry segment-mediated initiation of c-Myc protein synthesis following genotoxic stress. *Biochem. J.* **359**, 183–192.

Sulzmaier, F. J. and Ramos, J. W. (2013). RSK isoforms in cancer cell invasion and metastasis. *Cancer Res.* **73**, 6099–6105.

Sulzmaier, F. J., Jean, C. and Schlaepfer, D. D. (2014). FAK in cancer: mechanistic findings and clinical applications. *Nat. Rev. Cancer* **14**, 598–610.

Tancioni, I., Uryu, S., Sulzmaier, F. J., Shah, N. R., Lawson, C., Miller, N. L. G., Jean, C., Chen, X. L., Ward, K. K. and Schlaepfer, D. D. (2014). FAK Inhibition disrupts a β5 integrin signaling axis controlling anchorage-independent ovarian carcinoma growth. *Mol. Cancer Ther.* **13**, 2050–2061.

Tang, X., Zhu, Y., Han, L., Kim, A. L., Kopelovich, L., Bickers, D. R. and Athar, M. (2007). CP-31398 restores mutant p53 tumor suppressor function and inhibits UVB-induced skin carcinogenesis in mice. *J. Clin. Invest.* **117**, 3753–3764.

Terai, K., Call, M. K., Liu, H., Saika, S., Liu, C.-Y., Hayashi, Y., Chikama, T., Zhang, J., Terai, N., Kao, C. W.-C., et al. (2011). Crosstalk between TGF-beta and MAPK signaling during corneal wound healing. *Invest. Ophthalmol. Vis. Sci.* **52**, 8208–8215.

Thannickal, V. J., Lee, D. Y., White, E. S., Cui, Z., Larios, J. M., Chacon, R., Horowitz, J. C., Day, R. M. and Thomas, P. E. (2003). Myofibroblast differentiation by transforming growth factor-beta1 is dependent on cell adhesion and integrin signaling via focal adhesion kinase. *J. Biol. Chem.* **278**, 12384–12389.

Thomas, G. J., Hart, I. R., Speight, P. M. and Marshall, J. F. (2002). Binding of TGF-beta1 latency-associated peptide (LAP) to alpha(v)beta6 integrin modulates behaviour of squamous carcinoma cells. *Br. J. Cancer* **87**, 859–867.

Tran, M., Rousselle, P., Nokelainen, P., Tallapragada, S., Nguyen, N. T., Fincher, E. F. and Marinkovich, M. P. (2008). Targeting a tumor-specific laminin domain critical for human carcinogenesis. *Cancer Res.* **68**, 2885–2894.

Tran, T., Barlow, B., O'Rear, L., Jarvis, B., Li, Z., Dickeson, K., Dupont, W. and Zutter, M. (2011). Loss of the α2β1 integrin alters human papilloma virus-induced squamous carcinoma progression in vivo and in vitro. *PLoS One* **6**, e26858.

Trent, J. T. and Kirsner, R. S. (2003). Wounds and malignancy. *Adv. Skin Wound Care* **16**, 31–34.

Trikha, M., Zhou, Z., Nemeth, J. a, Chen, Q., Sharp, C., Emmell, E., Giles-Komar, J. and Nakada, M. T. (2004). CNTO 95, a fully human monoclonal antibody that inhibits alphav integrins, has antitumor and antiangiogenic activity in vivo. *Int. J. cancer* **110**, 326–335.

Truong, A.-T. N., Kowal-Vern, A., Latenser, B. A., Wiley, D. E. and Walter, R. J. (2005). Comparison of dermal substitutes in wound healing utilizing a nude mouse model. *J. Burns Wounds* **4**, e4.

Van Aarsen, L. a K., Leone, D. R., Ho, S., Dolinski, B. M., McCoon, P. E., LePage, D. J., Kelly, R., Heaney, G., Rayhorn, P., Reid, C., et al. (2008). Antibody-mediated blockade of integrin alpha v beta 6 inhibits tumor progression in vivo by a transforming growth factor-beta-regulated mechanism. *Cancer Res.* **68**, 561–570.

Vermorken, J. B., Guigay, J., Mesia, R., Trigo, J. M., Keilholz, U., Kerber, A., Bethe, U., Picard, M. and Brummendorf, T. H. (2011). Phase I/II trial of cilengitide with cetuximab, cisplatin and 5-fluorouracil in recurrent and/or metastatic squamous cell cancer of the head and neck: findings of the phase I part. *Br. J. Cancer* **104**, 1691–1696.

Vicente-Manzanares, M. and Horwitz, A. R. (2011). Adhesion dynamics at a glance. *J. Cell Sci.* **124**, 3923–3927.

Wang, X. and Proud, C. G. (2006). The mTOR pathway in the control of protein synthesis. *Physiology (Bethesda).* **21**, 362–369.

Wang, X. J., Greenhalgh, D. A., Bickenbach, J. R., Jiang, A., Bundman, D. S., Krieg, T., Derynck, R. and Roop, D. R. (1997). Expression of a dominant-negative type II transforming growth factor beta (TGF-beta) receptor in the epidermis of transgenic mice blocks TGF-beta-mediated growth inhibition. *Proc. Natl. Acad. Sci. U. S. A.* **94**, 2386–2391.

Wang, H., Radjendirane, V., Wary, K. K. and Chakrabarty, S. (2004). Transforming growth factor beta regulates cell-cell adhesion through extracellular matrix remodeling and activation of focal adhesion kinase in human colon carcinoma Moser cells. *Oncogene* **23**, 5558–5561.

Wang, P., Ballestrem, C. and Streuli, C. H. (2011). The C terminus of talin links integrins to cell cycle progression. *J. Cell Biol.* **195**, 499–513.

Wang, X., Ge, J., Tredget, E. E. and Wu, Y. (2013). The mouse excisional wound splinting model, including applications for stem cell transplantation. *Nat. Protoc.* **8**, 302–309.

Watt, F. M. and Fujiwara, H. (2011). Cell-extracellular matrix interactions in normal and diseased skin. *Cold Spring Harb. Perspect. Biol.*

Weinacker, A., Chen, A., Agrez, M., Cone, R. I., Nishimura, S., Wayner, E., Pytela, R. and Sheppard, D. (1994). Role of the integrin alpha v beta 6 in cell attachment to fibronectin. Heterologous expression of intact and secreted forms of the receptor. *J. Biol. Chem.* **269**, 6940–6948.

Weis, S. M. and Cheresh, D. a (2011). αv Integrins in Angiogenesis and Cancer. *Cold Spring Harb. Perspect. Med.* **1**, a006478.

Wendt, M. K. and Schiemann, W. P. (2009). Therapeutic targeting of the focal adhesion complex prevents oncogenic TGF-beta signaling and metastasis. *Breast Cancer Res.* **11**, R68.

Wennerberg, K. and Armulik, A. (2000). The cytoplasmic tyrosines of integrin subunit β1 are involved in focal adhesion kinase activation. *Mol. Cell. Biol.* **20**, 5758–5765.

Werner, S. and Grose, R. (2003). Regulation of wound healing by growth factors and cytokines. *Physiol. Rev.* **83**, 835–870.

Werner, A., Willem, M., Jones, L. L., Kreutzberg, G. W., Mayer, U. and Raivich, G. (2000). Impaired Axonal Regeneration in alpha7 Integrin-Deficient Mice. *J. Neurosci.* **20**, 1822–1830.

Wong, V. W., Sorkin, M., Glotzbach, J. P., Longaker, M. T. and Gurtner, G. C. (2011). Surgical Approaches to Create Murine Models of Human Wound Healing. *J. Biomed. Biotechnol.* **2011**, 1–8.

Xie, W., Bharathy, S., Kim, D., Haffty, B. G., Rimm, D. L. and Reiss, M. (2003). Frequent alterations of Smad signaling in human head and neck squamous cell carcinomas: a tissue microarray analysis. *Oncol. Res.* **14**, 61–73.

Xie, Y., McElwee, K. J., Owen, G. R., Häkkinen, L. and Larjava, H. S. (2012). Integrin β6-deficient mice show enhanced keratinocyte proliferation and retarded hair follicle regression after depilation. *J. Invest. Dermatol.* **132**, 547–555.

Xu, J., Rodriguez, D., Petitclerc, E., Kim, J. J., Hangai, M., Moon, Y. S., Davis, G. E., Brooks, P. C. and Yuen, S. M. (2001). Proteolytic exposure of a cryptic site within collagen type IV is required for angiogenesis and tumor growth in vivo. *J. Cell Biol.* **154**, 1069–1079.

Xue, H., Atakilit, A., Zhu, W., Li, X., Ramos, D. M. and Pytela, R. (2001). Role of the alpha(v)beta6 integrin in human oral squamous cell carcinoma growth in vivo and in vitro. *Biochem. Biophys. Res. Commun.* **288**, 610–618.

Yang, J. T., Rayburn, H. and Hynes, R. O. (1993). Embryonic mesodermal defects in alpha5 integrin-deficient mice. *Development* **1105**, 1093–1105.

Yeo, M. G., Partridge, M. A., Ezratty, E. J., Shen, Q., Gundersen, G. G. and Marcantonio, E. E. (2006). Src SH2 arginine 175 is required for cell motility: specific focal adhesion kinase targeting and focal adhesion assembly function. *Mol. Cell. Biol.* **26**, 4399–4409.

Zamir, E. and Geiger, B. (2001). Molecular complexity and dynamics of cell-matrix adhesions. *J. Cell Sci.* **114**, 3583–3590.

Zanet, J., Pibre, S., Jacquet, C., Ramirez, A., de Alborán, I. M. and Gandarillas, A. (2005). Endogenous Myc controls mammalian epidermal cell size, hyperproliferation, endoreplication and stem cell amplification. *J. Cell Sci.* **118**, 1693–1704.

Zaru, R., Ronkina, N., Gaestel, M., Arthur, J. S. C. and Watts, C. (2007). The MAPK-activated kinase Rsk controls an acute Toll-like receptor signaling response in dendritic cells and is activated through two distinct pathways. *Nat. Immunol.* **8**, 1227–35.

Zaru, R., Edgar, A. J., Hanauer, A. and Watts, C. (2015). Structural and functional basis for p38-MK2-activated Rsk signaling in toll-like receptor-stimulated dendritic cells. *Mol. Cell. Biol.* **35**, 132–140.

Zhang, Y. E. (2009). Non-Smad pathways in TGF-beta signaling. *Cell Res.* **19**, 128–139.

Zhang, X., Jiang, G., Cai, Y., Monkley, S. J., Critchley, D. R. and Sheetz, M. P. (2008). Talin depletion reveals independence of initial cell spreading from integrin activation and traction. *Nat. Cell Biol.* **10**, 1062–1068.

Zhao, J., Pestell, R. and Guan, J. L. (2001). Transcriptional activation of cyclin D1 promoter by FAK contributes to cell cycle progression. *Mol. Biol. Cell* **12**, 4066–4077.

Zhu, J., Motejlek, K., Wang, D., Zang, K., Schmidt, A. and Reichardt, L. F. (2002). Beta8 Integrins Are Required for Vascular Morphogenesis in Mouse Embryos. *Development* **129**, 2891–2903.

Zweers, M. C., Davidson, J. M., Pozzi, A., Hallinger, R., Janz, K., Quondamatteo, F., Leutgeb, B., Krieg, T. and Eckes, B. (2007). Integrin alpha2beta1 is required for regulation of murine wound angiogenesis but is dispensable for reepithelialization. *J. Invest. Dermatol.* **127**, 467–478.